SPATIOTEMPORAL DYNAMICS AND REGULATION OF CYCLIC NUCLEOTIDES AND THEIR EFFECTORS IN LIVING CELLS

by
Kirill Gorshkov

A dissertation submitted to Johns Hopkins University in conformity with the requirements for the degree of Doctor of Philosophy

Baltimore, Maryland
September 2016

Abstract

Cellular signaling is a tightly regulated process which defines how cells interact with their environment and maintain homeostasis. It is also the mechanism by which they change. Neuronal development is one such process that depends on the concerted activities of many molecular signaling pathways to proceed through highly typified stages. A neuron's morphology is a perfect example of spatially distinct compartments which change over time. The spatial and temporal regulation of signaling pathways within the dendrites, soma, and axon during development require second messengers and kinases for proper establishment of neuronal morphology. The second messenger 3'-5'-cyclic adenosine monophosphate (cAMP) and kinase cAMP-dependent protein kinase (PKA) are considered critical axon determinants; meaning without them the axon does not form. At the second messenger level, cAMP is generated by adenylyl cyclase and degraded by phosphodiesterases in the cellular milieu to balance the cAMP concentration in specific signaling microdomains. When activated by cAMP, PKA phosphorylates its substrates which can be both upstream and downstream of itself. But the cAMP/PKA signaling pathway components are not randomly strewn throughout the cell. Instead, they are bound and tightly regulated within a signaling platform called the A-kinase anchoring protein (AKAP) signalosome. AKAPs bring PKA into close proximity to its substrates, source of cAMP, and scaffold other signaling partners to produce profound effects on a neuron's fate. To understand how cAMP and PKA control neuronal polarization in living neurons, we utilized fluorescence resonance energy transfer (FRET)-based biosensors shed light on their activities in different regions and at different stages of development.

This dissertation is composed of four chapters: an introduction, the major project, a minor project, and concluding remarks. The first chapter introduces major concepts and information regarding cyclic nucleotide signaling, cyclic nucleotide effectors, signal compartmentalization and methods used to visualize molecular activity in living cells. The second chapter contains the bulk of the thesis work in which we investigated the role of spatiotemporally compartmentalized cAMP and PKA signaling in developing neurons. Here, we used the FRET-based cAMP reporter ICUE3 and PKA reporter AKAR4 to study how their molecular activities differ between the spatially distinct soma, dendrites, and axons of developing hippocampal neurons. In this study we have demonstrated how gradients of cAMP and PKA in the axon are regulated by phosphodiesterase activity and scaffolding by AKAPs. We also show the functional significance of AKAP anchoring in neuronal development by analyzing axon outgrowth. Lastly, we link the functional outcomes to the gradients of molecular activity and developed a conceptual model for our observations. In the third chapter, we describe and characterize a new suite of targeted cGMP biosensors to help further the understanding of cGMP compartmentalization. In the fourth and last chapter, we provide a review of the thesis work and provide some perspective on future directions.

As a whole, the studies presented here demonstrate how cAMP, PKA, and cGMP signaling within the spatially distinct compartments of living cells is regulated. The gradients alluded to in the literature over the years are now revealed using the spotlight of genetically encoded FRET-based biosensors. Furthermore, we present the field of neurodevelopment with a new target of study, the AKAPs, which we show have significant implication in the growth and differentiation of hippocampal neurons.

Thesis Advisor: Dr. Jin Zhang

Second Thesis Reader: Dr. Ron Schnaar

Acknowledgements

Graduate school has been the experience of a lifetime. Full of challenges, I have grown tremendously in my scientific prowess, increased my network of mentors, and defined my personal character. My family, including my parents, sister, and wife, have sacrificed much for me to finish the Ph.D., and for that I am grateful. This degree would not have been possible if it were not for the patience of my friends and family. I will remember the past five years for the rest of my life, as it has shaped my thinking and goals, and has led me towards an extremely bright future.

My first acknowledgement goes to Dr. Jin Zhang. An excellent mentor who allowed me to pursue my passion for neuroscience research, she welcomed me to the lab and paired me with Dr. Sohum Mehta, from who I learned the basics of cloning. Dr. Zhang supported me in funding my graduate career with a fellowship from the National Science Foundation, and it was her guidance that made us successful in our funding application. The past four years have certainly been challenging, but you stood by me as a great mentor and did not give up on training me to excel and fulfill my potential as a scientist.

Our lab has a great group of people without whom this work would not be possible. Countless lab meetings, subgroup meetings, and personal discussions have shaped this work to make it what it is today. Thanks to all who I have interacted with as a graduate student in this lab. Our lab environment was fun with adventures in Baltimore and outings in California which really provided an outlet for the stresses of graduate school life. For the second chapter, thanks to Eric Greenwald for help with discussions and critical thinking about the data which ultimately helped with a submission of a first-

author manuscript. A special thanks goes to Sohum, who was my rotation advisor, co-author for my paper, and a great scientific mentor during my time in the Zhang lab. Thanks to Chris Booth for being like a brother to me during my short stay in California. The move from Baltimore was difficult but with your and Kellsi's support I made it through. Thanks also to Xin Zhou for our late night discussions and her never-ending optimism. I cannot finish this paragraph without also thanking Dr. Charlene Depry who is one of the kindest and happy people I have ever met. Because of you, I met my wife Ashley, and there are not enough words in the world to express my gratitude for your support even years after you have left the lab.

Dr. Alex Kolodkin and Dr. Randal Hand welcomed Jin and I to discuss my project and it turned into a once in a lifetime training opportunity in neurobiology. With Alex's support and Randal's teaching, I learned about in-utero electroporation, ex-vivo slice culture, and confocal microscopy. Your time was pressed and yet, you patiently explained the reasoning behind everything and were a fantastic teacher. Together we generated beautiful high resolution brain slice images inspired me to keep going and digging deeper. These moments were truly awe-inspiring. Syed Khalid and Edric Tam are also previous members of the Kolodkin lab who participated in this work and were a pleasure to work with.

Thanks to the Hopkins Department of Pharmacology academic office for their commitment to students like me over the past five years. I fully appreciate and recognize all the ways that you have helped me and my peers get through graduate school. From the orientation day, to setting up seminars, to planning our events, and handling our finances, these behind the scenes activities have made the last five years really great. Thank you

for always making me feel welcome. Without your support, graduate school would be much more difficult, and there would be a lot less happy faces walking around 3rd floor WBSB. I appreciate your positive outlook and kindness towards me as I've made my way from joining the department to moving to UCSD, and finally giving my thesis presentation. I'll remember you guys as a critical part of my success here at Hopkins.

To my wife, Ashley, your patience cannot be repaid in a whole lifetime. Over the first two years of our relationship, you had to deal with late nights in lab, constant work at home, and quite a bit of complaining. Then you had to deal with the lab move, which was not easy for anyone. We got engaged, and I immediately left for a 3-month internship in Indianapolis followed by a 6-month move to San Diego. True love held us together and it was well worth the wait because now we are married, and I am coming home to you with a doctorate from one of the most prestigious and rigorous scientific institutions in the world. You motivated me to finish what I started, and your endless compassion helped me get to this day. I am so proud to be your husband. I cannot wait to start our life together and do amazing things.

My sister Victoria has also been a critical part of this journey as an ever curious girl to whom I could practice talking about my work, teaching what it means to be a student, and guiding her choices with my own experience. I thank you for inspiring me to be the best brother and man I could be. Your presence was felt during my time away, and I'm very proud of where you have taken yourself and who you have become.

Lastly, and most importantly, thank you to the two people who made me who I am, my parents. When I was a child you stressed how important education is be able to live the good life. Well now I have finished my formal education and there are no higher

degrees left in this path towards understanding the world around us. You risked everything by coming to America, leaving your whole family behind to make a better life for us. I hope I have made you proud and made this long journey worthwhile. I will remember your sacrifice forever. Thanks for sending food and care packages, and caring about whether or not I am sleeping and eating. I know it is what parents do, but sometimes I do forget, and they are much needed reminders. You drove with me to Baltimore in the summer of 2011. Now in the summer of 2016, five years later, I am finished with this stage of my life. As I find my way in this world of science, you will always be my cornerstone of support and a sounding board for my life goals.

Table of Contents

List of Figures

Chapter 3

Appendix

Chapter 1

Introduction

Parts of this chapter were adapted from previously published articles:

Gorshkov K, Zhang J, (2014) Monitoring Cyclic Nucleotides Using Genetically Encoded Fluorescent Reporter. In Cyclic Nucleotide Signaling. Taylor Francis Group

Gorshkov K, Zhang J, (2014) Dynamics of cyclic nucleotide signaling in neurons. Frontiers in Cellular Neuroscience. 4;8:395**.**

Cyclic Nucleotide Signaling: An Overview

The simplest unit of life is the cell. In complex multicellular organisms, many cells are organized together, as they are in specialized tissues, in order to keep the organism alive and functioning. A key component to life is the ability for cells and tissues to respond to changes in the external environment. Through a series of biochemical events called signal transduction pathways, or signaling cascades, cells transmit signals from a stimulus and convert it to a specific cellular response. Many signal transduction cascades are facilitated by cell surface receptor activation, which converts a signal into the production of many second messenger molecules. The second messengers then activate many downstream target effector molecules to continue the signaling cascade. In this way, signals are transduced and amplified by the activation of cellular machinery. An ancient and ubiquitous second messenger signaling pathway is comprised of the cyclic nucleotides cyclic 3', 5' adenosine monophosphate (cAMP) and cyclic 3', 5' guanosine monophosphate (cGMP) found in both prokaryotic and eukaryotic cells. Cyclic nucleotides are key players in important cellular functions like including homeostasis, cell division, and cell differentiation. The cyclic nucleotides act by binding and activating various targets that are immediately downstream of the second messenger. The major targets for cAMP, protein kinase A (PKA) and exchange protein directly activated by cAMP (Epac), mediate critical physiological functions like cardiac cell contractility, insulin secretion, nerve cell action potentials, and nerve cell axon growth. cGMP activates protein kinase G (PKG) to mediate smooth muscle relaxation, phototransduction in the retina, and nerve cell dendrite growth. This following sections and chapters of this thesis will focus on the role and regulation of cyclic nucleotides and their effectors with emphasis on their activity in the developing nervous system.

Indeed, the role of cAMP and cGMP in the nervous system is wide and varied. Importantly, the foundation for proper nervous system function is the proper formation of structures in both the central and peripheral nervous system. When a nerve stem cell makes the transition from a pre-mitotic to a post-mitotic cell, neuronal differentiation is initiated. Given that cyclic nucleotide signaling plays a critical part in neuronal differentiation, it is important to understand the molecular mechanisms regulating the dynamics of cyclic nucleotides at the single cell level.

An overview of cAMP and cGMP signaling

cAMP and cGMP are ubiquitous second messengers present in most cell types. Within the brain, cyclic nucleotides transduce neuromodulatory signals into functional outputs for individual neurons leading to changes in neural networks themselves or their function. The importance of cyclic nucleotide signaling pathways is well appreciated in the field of clinical neuroscience and psychiatry, with many drugs targeting the G-protein coupled receptors (GPCRs) to modulate neuronal activity[2, 3]. The effects of cAMP and cGMP signaling range from regulating neuronal differentiation and growth to axonal guidance and modulation of neuronal excitability. To accomplish this, cyclic nucleotides are coupled to many downstream effectors[4]. cAMP, the prototypical cyclic nucleotide, transduces G-protein signals to activate PKA and Epac. cGMP, on the other hand, relays signals from nitric oxide to activate PKG. Phosphodiesterase (PDE), the enzyme that degrades cyclic nucleotides, can also be an effector with its activity modulated by cyclic nucleotide binding to regulatory domains forming feedback loops[5]. Both cyclic nucleotides also activate cyclic nucleotide gated ion channels[6].

cAMP signaling

cAMP was discovered by Nobel Prize winner (1971) Earl Sutherland and T. W. Rall in the 1950's while studying the effect of epinephrine and other molecules on liver extracts[7]. The canonical cAMP signaling pathway relies on the activation of a transmembrane Gαs-coupled GPCR by binding of an extracellular agonist such as a hormone or a neurotransmitter (Fig. 1.1a)[8]. A change in conformation of the receptor leads to the release of the bound Gαs subunit from Gβγ on the intracellular side of the plasma membrane. Gαs binds to transmembrane adenylyl cyclase (tmAC), the enzyme responsible for converting ATP to cAMP[9, 10]. At the AC activation step, the signal is amplified through the generation of many cAMP molecules. Activation of soluble adenylyl cyclases (sAC), a diffusible protein found in discrete subcellular compartments, by bicarbonate and calcium is another route of cAMP generation[11, 12]. cAMP produced by either tmAC or sAC can bind to various effectors that include PKA, Epac, and ion channels to continue the signaling cascade[13]. PDEs degrade cAMP via a hydrolysis reaction and lower its concentration in the cell.

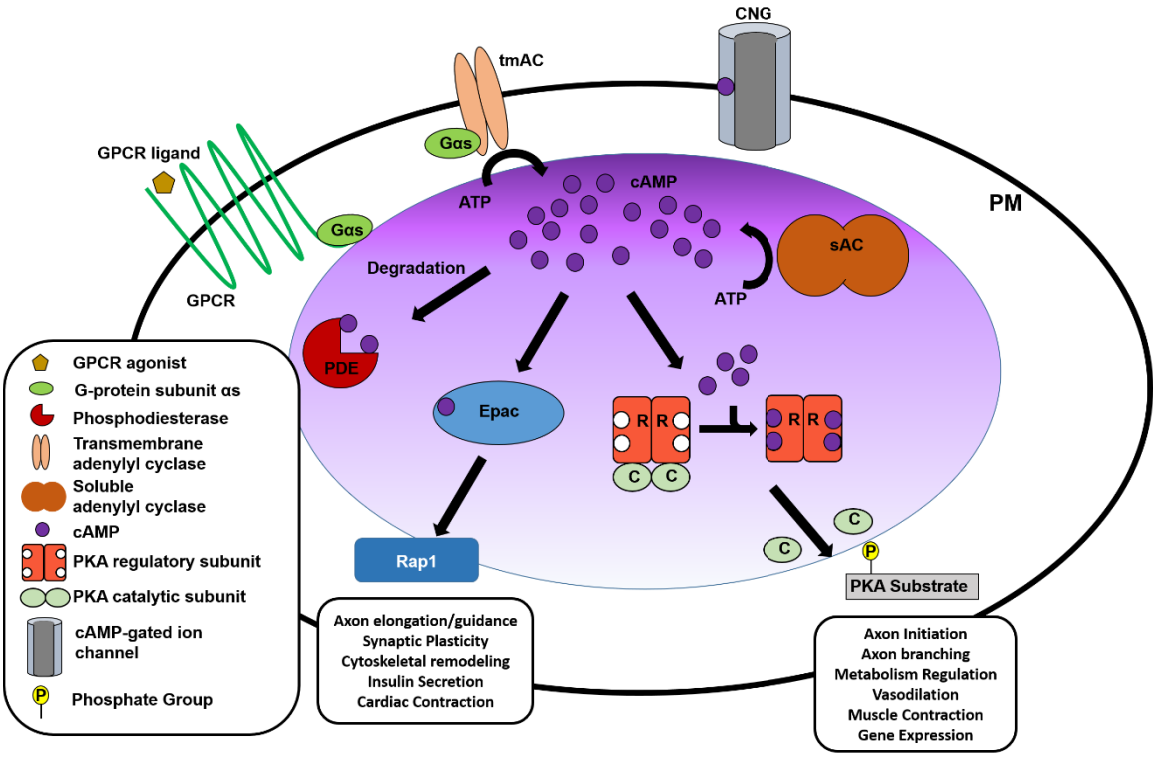

Figure 1.1a The cAMP/PKA Signaling Pathway
When a Gαs-protein coupled receptor is stimulated by an agonist, the cAMP signaling cascade is initiated. The bound Gαs dissociates and stimulates the tmAC to produce cAMP from ATP at the membrane. Alternatively, sAC, which is found in various locations in the cell, can be stimulated by bicarbonate or calcium to produce cAMP from ATP. cAMP can activate its various effectors including PKA, Epac, and cyclic nucleotide-gated ion channels. PDEs degrade cAMP and lower its concentration in the cell. Therefore, the concentration of free cAMP is a result of AC activity, PDE activity, and protein binding. Gradients of cAMP are formed as cAMP concentrations are controlled by PDEs and diffuses from the source of production.

PKA activation and signaling

PKA, the prototypical serine/threonine kinase, was the first kinase to be discovered in the second half the 20th century and serves as a model for kinase structure and modeling[14, 15]. PKA can be found in the form of a holoenzyme consisting of dimerized regulatory (R) subunits and two catalytic (C) subunits. PKA can be classified into two types depending on the regulatory subunit dimer. Type I PKA consists of RI subunits, while type

II PKA uses RII subunits. Four R subunit isoforms (RIα, RIβ, RIIα, & RIIβ) and three C subunit isoforms (Cα, Cβ, and Cγ) have been discovered with each isoform having specific biological functions and cellular expression profiles[16, 17]. The regulatory subunits contain a cyclic nucleotide binding domain (CNBD), which is a common feature of cyclic nucleotide effectors. Prior to binding cAMP, the regulatory subunits tightly bind and inhibit the catalytic subunits. Each regulatory subunit can cooperatively bind two molecules of cAMP with low nanomolar affinity, inducing a conformational change that releases the catalytic subunits to phosphorylate many PKA substrates on serine and threonine residues[15, 16]. For optimal catalytic activity, PKA requires phosphorylation of the active site residue Thr197 by the phosphoinositide dependent kinase (PDK1) or PDK1-like kinase[18-20]. PKA specificity is achieved by active site recognition of substrates that share a phosphorylation consensus motif (R-R-X-S/T-Φ, where Φ represents a hydrophobic residue), as well as the spatiotemporal compartmentalization of the kinase and its upstream modulators[34]. PKA activity is antagonized by phosphatases that dephosphorylate PKA substrates[21]. With the help of spatiotemporal compartmentalization, PKA converts the cAMP signal into many different functional outputs that are important for critical biological functions such as the metabolism of glycogen[22, 23], lipids[24], and steroids[25], gene regulation[26, 27], cell growth[28], proliferation[29], and differentiation[30, 31], synaptic plasticity[32-34], and ion channel conductivity[35].

Epac activation and signaling

The second major effector of cAMP is known as Epac was discovered by de Rooij *et al.* in 1998 whose effects are independent of PKA activity [36]. Its important discovery

explained why certain effects of cAMP could not be attributed to PKA or cyclic nucleotide-gated ion channels[37]. The Epac family is comprised of two identified isoforms, Epac1 and Epac2, which are guanine nucleotide exchange (GEF) factors that exchange GDP for GTP on the GTPase Rap1[38]. While Epac1 and Epac2 are variably expressed in different tissues and have differing roles, they do have a common structure that includes a regulatory CNBD and catalytic domain[39]. Epac1 contains a single cAMP binding site, while Epac2 contains two[40, 41]. Prior to activation, the catalytic domain is sterically hindered by the regulatory in auto-inhibitory fashion. Once cAMP is bound, the Epac undergoes a conformational change reorienting the enzyme into an active conformation. The net effect of cAMP signaling therefore includes the activation of PKA, Epac, and other effectors that may act independently[42], synergistically[43], or opposite[44] of each other to carry out and amplify the cAMP signal. Prior to the discovery of Epac, it was thought that the sole enzymatic effector of cAMP in neurons was PKA. Several years of research has now revealed that Epac1 plays a role in axon guidance[45] and is critical for the formation of axons in developing neurons[46-48].

cGMP signaling

The story of cGMP began with its synthesis in 1961 by Smith, Drummon, and Khorana[49], and it was later discovered in rat urine in 1963 [50]. The cGMP signaling pathway is initiated when nitric oxide synthase (NOS) is activated by calcium-calmodulin and converts the amino acid L-arginine to nitric oxide (NO)[51, 52] (Fig. 1.1b). NO transduces the signal to soluble guanylyl cyclase (sGC), which produces cGMP from GTP[53]. The particulate guanylyl cyclase is activated by natriuretic peptides (NP) and directly converts

GTP to cGMP[54]. These two routes of cGMP production can both activate the downstream effectors PKG, phosphodiesterases, and ion channels to produce different functional outputs for cGMP signaling[55]. It is important to note that cAMP and cGMP can antagonize each other by participating in mutual inhibition through the activation of each other's phosphodiesterases[56].

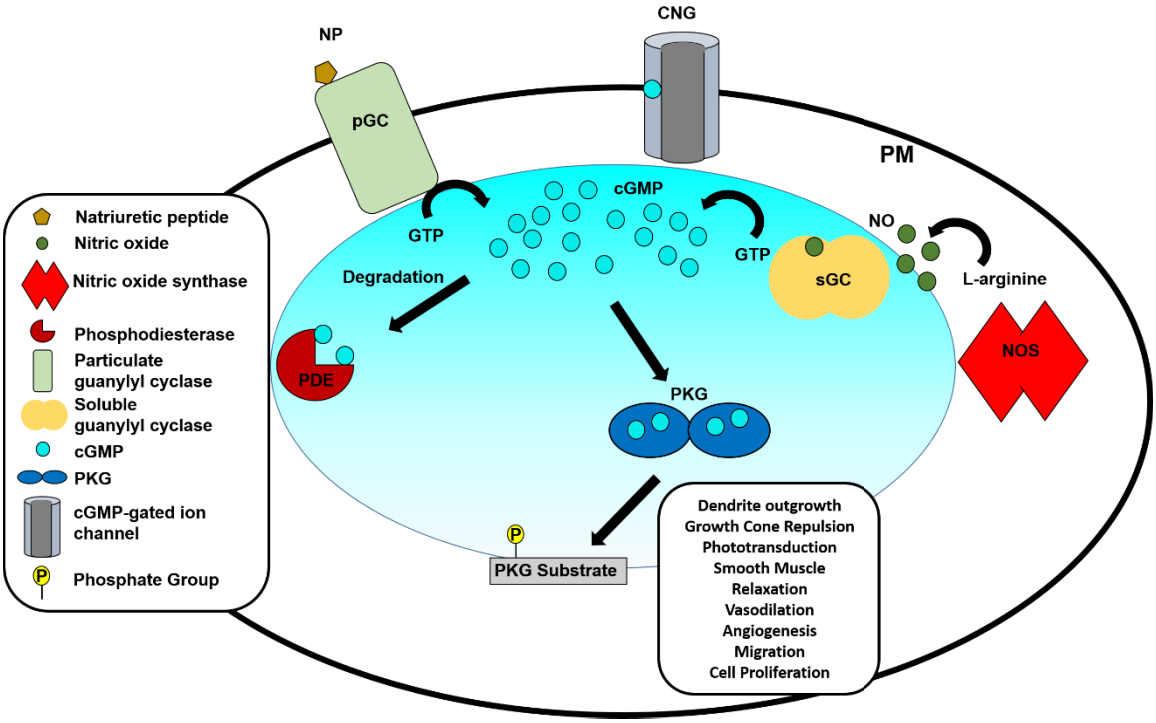

Figure 1.1b The cGMP/PKG Signaling Pathway
cGMP signaling is initiated by the stimulation of pGCs by natriuretic peptides or the stimulation of sGCs by nitric oxide synthase. Both pGC and sGC convert GTP to cGMP. cGMP can diffuse from the source of production to activate its various effectors including PKG and cyclic nucleotide-gated ion channels. PDEs degrade cGMP and lower its concentration in the cell. Gradients are cGMP are generated by this PDE activity and diffusion.

Spatiotemporal Compartmentalization of Cyclic Nucleotide Signaling

The idea of compartmentalized signaling is an essential component to the cyclic nucleotide signaling model. To elicit their diverse functional effects in a highly specific manner, cAMP and cGMP signaling is spatially compartmentalized and temporally regulated[57]. The levels of cyclic nucleotides and the activities of downstream effectors are not uniform throughout the cell, but instead form specific nanodomains or microdomains inside the cell. The spatial compartmentation is partially achieved by strict regulation of cyclic nucleotide production and degradation. At the level of production, ACs and GCs are found at different locations within the cell, and are activated by different mechanisms. PDEs have been shown to function as cAMP and cGMP sinks to help maintain these microdomains[58, 59]. The tight spatiotemporal regulation of cAMP is achieved with the help of the A-kinase anchoring protein[60], which assembles signaling complexes consisting of members of the cAMP/PKA signaling pathway like ACs, PDEs, PKA and its substrate, and other effectors. These signalosomes, which can be found throughout various compartments including the plasma membrane, the cytosol and the nucleus, have been shown to play important roles in achieving functional specificity of the cAMP/PKA pathway. In addition to biochemical regulation, the structural properties of cells can also affect the signaling dynamics of second messengers [61, 62]

Adenylyl and Guanylyl Cyclases

Mammalian cAMP production mediated by Gαs activation can occur through any one of the nine separate genes for tmAC designated producing the AC proteins designated as ACI through ACIX[63]. Differential tissue expression and modulation of the AC isoforms confers another level cAMP compartmentalization. For example, ACI is the only tmAC

specifically expressed in a neuro-specific fashion[64]. On one hand, both ACI and ACIII are maximally stimulated by coincidental binding of Gαs and Ca^{2+}-calmodulin, which links cAMP to voltage dependent changes in neuronal signaling. On the other hand, ACV and ACVI are inhibited by Ca^{2+} and are the major AC isoforms expressed in mammalian cardiac tissue for regulating cardiac contraction[65]. As already mentioned, sAC, activated by bicarbonate and calcium, is other source of cAMP in the cell and can be found in the bulk cytosol as well as in discrete locations like the nucleus.

The localization of sGC in neurons is one way that mediators of neuronal polarization can fulfill their functions. Often times, the localization of a downstream signaling component can spatially define the cellular response to an upstream signaling component. Such is the case with sGC and Sema3A in cortical neurons. Research on the role of Sema3a in neuronal polarity identified concentrated localizations of sGC in apical dendrites both *in vitro* and *in vivo*[66]. They further showed that sGC is not responsible for mediating the growth responses of Sema3a but rather orienting the growth of apical dendrites through its asymmetric localization in developing cortical neurons.

Phosphodiesterases

Both cAMP and cGMP are spatiotemporally regulated by the enzymatic activity of PDEs. PDEs shut down signaling by binding the cyclic nucleotides and carrying out a hydrolysis reaction of the phosphodiester bond to generate a nucleoside monophosphate. By degrading cyclic nucleotides, PDEs control the location, magnitude, and duration of cyclic nucleotide signaling in the cell[67, 68]. Without this regulation, cyclic nucleotides would lack signaling specificity; relying on simple diffusion rates and binding affinity to

activate various effectors. There are 11 PDE families that have varying affinities for the cyclic nucleotides. PDE1-3, PDE10, and PDE11 degrade both cAMP and cGMP. PDE4, PDE7, and PDE8 specifically degrade cAMP, whereas PDE5, PDE6, and PDE9 specifically degrade cGMP. Each PDE family has multiple isozymes with varying tissue and cell-type expression and intracellular localization. PDEs themselves are spatially controlled by scaffolding proteins described in the next section. Tissue expression and intracellular localization confers specificity to PDE function leading to different biological outcomes. For example, PDE3 and PDE4 within subcellular microdomains of the sarcoplasmic reticulum have been implicated in cardiomyocyte function[69]. Studies in neurons identified PDE4D as a major regulator of cAMP gradients during the process of neuronal polarization[70]. The localization of PDEs helps generate different "pools" of cAMP to activate different effectors further enhancing signaling specificity. PDE signaling dynamics are made more complex by the presence of post-translational modifications like phosphorylation and ubiquitinylation, protein-protein interactions, and binding of other molecules like calcium[71, 72]. Finally, it is important to note that as with many of the cAMP signaling enzymes, more than one isoform of PDEs are often found in different cell types, adding to the complexity of cAMP and cGMP signal regulation.

A-kinase anchoring proteins

One way to achieve compartmentalization of a signaling pathway is to spatially restrict protein localization and generate signaling microdomains. The cAMP/PKA signaling pathway is under the spatiotemporal regulation of the A-kinase anchoring protein (AKAP) family of scaffolding proteins of which there are more than 50 members. AKAPs

are characterized by three defining features[73]. First, they all bind PKA regulatory subunits. Second, they bind PKA substrates as well as other components involved in shaping the signaling response downstream of cAMP. Third, AKAPs themselves contain targeting motifs to localize to different subcellular compartments.

To spatially restrict PKA activity, AKAPs bind to PKA R subunit dimers in their hydrophobic pocket called the dimerization domain (D/D) using an α-helical stretch of 14 to 18 amino acids[74]. The RII-specific AKAPs are most abundant in cells, but AKAPs can bind either type I or type II PKA holoenzymes or both. The identity of the hydrophobic amino acids within the α-helix confer varying degrees of affinity for the RII subunit within the low nanomolar range. The RI subunit has a high nanomolar to low micromolar affinity for AKAPs that can be attributed to an N-terminal 12 amino acid shift in the D/D, which may hinder RI-AKAP interactions[75]. The lower affinity may also be explained by the compact structure PKA RI dimers, while PKA RII dimers are more extended [76].

In addition to PKA, the AKAPs also tether many other proteins including ACs[77], PDEs[78], phosphatases[79], other kinases like PKC or ERK[80], Epac[81], ion channels[82], and cytoskeletal elements[83] using similar α-helical binding domains. AKAPs regulate the specificity of PKA phosphorylation by bringing PKA substrates into close proximity to the kinase. By binding ACs and PDEs, AKAPs also control the temporal dynamics of compartmentalized cAMP production and degradation.

Further compartmentalization is achieved by the localization of AKAPs discrete subcellular compartments with the help of special targeting motifs[84, 85]. AKAPs can be found in multiple locations throughout the cell including the plasma membrane, organelle membranes, attached to cytoskeletal elements like actin or microtubules, and the nucleus.

For example, myristolation and palmitoylation of a specific motif can tether AKAPs to the plasma membrane.

The diversity of AKAP proteins and the multiple modes of cAMP/PKA regulation they confer creates a complex signaling environment. Tools to interrogate the biological relevance of PKA-AKAP anchoring have been developed using small peptides derived from endogenous AKAP sequences. One such tool is called st-Ht31, a stearated peptide derived from AKAP-Lbc with very high affinity for PKA RII[86] (Fig. 1.2). st-Ht31 is an anchoring disruptor and delocalizes PKA RII from all AKAPs. Other PKA anchoring disruptors derived from various AKAPs and PKA anchoring consensus sequences have been developed to study the biological function of AKAP anchoring with greater precision[87].

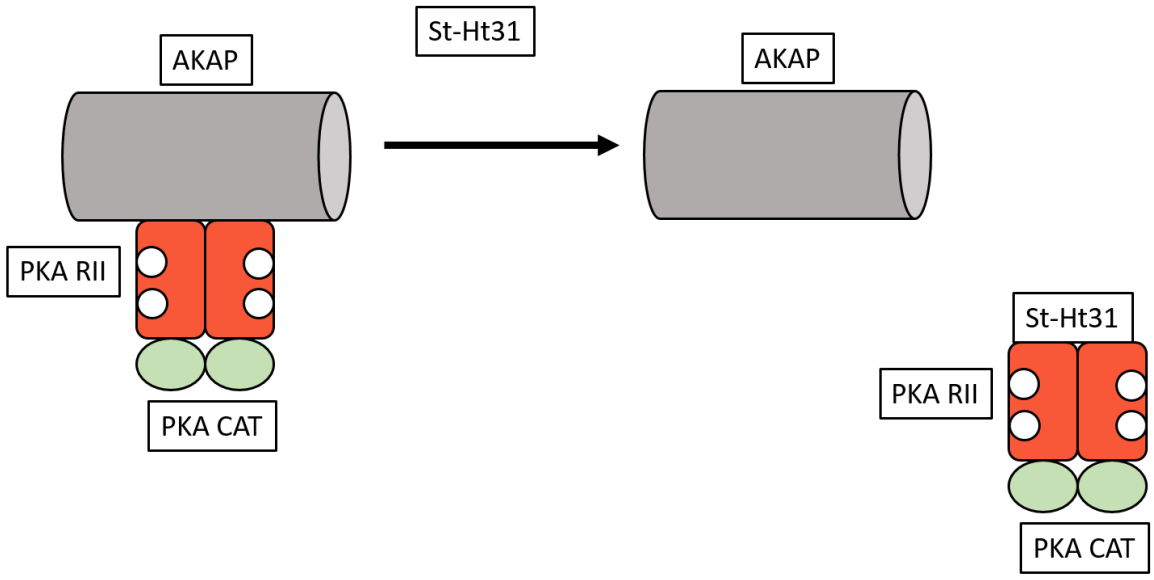

Figure 1.2 st-Ht31 disrupts AKAP anchoring of PKA
AKAP anchors PKA by binding the R subunits of the PKA holoenzyme. When st-Ht31 is added, the stearate peptide competes for the PKA RII subunits and binds them with high affinity.

Cyclic Nucleotide Signaling in Neuronal Polarization

The study of neuronal polarization began 40 years ago in the 1970s and 1980s when observations of differences between dendrites and axons were first made by pioneering neurodevelopment scientists like Gary Banker and others[88]. The axons and dendrites are spatially distinct neuronal compartments that allow neurons to communicate with one another. Neuronal stimulation induces the generation of an action potential that travels down the axon to synapses between that axon and dendrites of another cell. But before mature neurons are electrically active in such a way, they must first establish their identity through polarization. This process is fundamental to the growth of the central nervous system and the generation of the complex neural circuitry. *In vitro* cultures of hippocampal neurons were studied to understand how these cells achieve their elaborate forms. Researchers were able to show that there are breaks in the uniform symmetry of dissociated neurons, followed by extension of small filopodia, rapid growth of the future axon, and further elaboration of the future dendrites[89-92]. Since that time, many different signaling mechanisms have been found to affect the polarization and differentiation of neurons both *in vitro* and *in vivo.* Not surprisingly, cAMP and cGMP play essential roles for axon and dendrite development, respectively.

cAMP/PKA and Epac in neuronal morphogenesis

Neurotrophins are molecules that promote the growth and development of neurons. Typically released into the extracellular space, they bind to neurotrophin receptors and initiate signal transduction cascades that positively affect neuronal function. Brain-derived neurotrophic factor (BDNF) and nerve growth factor (NGF) are two of the many

neurotrophic factors that have been discovered. As mentioned in preceding sections, cAMP activates PKA and Epac to control cellular responses. Over the past decade, cAMP activation of both PKA and Epac engage signaling mechanisms that can control axon initiation and outgrowth. During the polarization process, research has found that cAMP stimulated PKA leads to the phosphorylation of Liver Kinase B1 and its accumulation in a single undifferentiated neurite to designate it as the future axon[93, 94]. BDNF and cAMP/PKA have been shown to participate in a localized positive feedback loop at axon growth cones to promote axon elongation[95]. Other work has shown that cAMP participates in long-range signal inhibition, where cAMP elevation in one neurite can decrease cAMP in the other neurites providing a mechanism for the generation of a single axon and multiple dendrites[70].

Recent years have produced new insights into axon growth signaling mechanisms, and Epac is now fully appreciated as a player in axon growth and guidance decisions that are distinct from those of PKA[96]. For example, using Epac specific cAMP-analogs, research found that PC12 cells undergo the switch from proliferation to differentiation and neurite outgrowth using cAMP activation of Epac[46]. The direct target of Epac GEF activity is the GTPase Rap1, a molecule whose localization to the tip of a growing neurite results in axon specification. In one study, pharmacological inhibition or knockdown of Epac1 reduced the growth of hippocampal neurons *in vitro*[47]. Another study used a photoactivatable adenylyl cyclase (PAC) to optically control cAMP levels and found Epac regulated axon elongation with higher concentrations of cAMP, while PKA regulated axon branching with lower concentrations of cAMP[97]. These results reveal the complexity of the

cAMP signaling network and indicate that the spatiotemporal regulation of cAMP plays important roles in axonal morphogenesis.

cGMP in dendrite specification

While cAMP is important for axon growth, cGMP influences the development of dendrites by mediating the signal from Semaphorin3A (Sema3a). Semaphorins are a highly varied family of secreted and membrane-bound signaling molecules critical for nervous system development[98]. Sema3a is recognized as a chemorepellent axon guidance molecule[99] and a chemoattractant for dendrites[66]. By coupling to the neuropilin receptor, Sema3a decreases cAMP, increases cGMP, and promotes dendrite formation in developing neurons. Although the exact mechanism has not been identified, sGC activation has been seen in *Xenopus* neurons treated with Sema3a. Another mechanism by which cGMP induces dendrite specification was found in *Xenopus* spinal commissural interneurons. Voltage gated calcium Cav2.3 channels localized to and specified future dendrites when cells were treated with Sema3a, which elevated cGMP[100]. This study linked cGMP/PKG to Cav2.3 expression and localization, and the specification of dendrites both *in vitro* and *in vivo*. These and other data demonstrate Sema3a mediated cGMP signaling pathways help to establish dendrite identity in developing neuronal systems.

Methods to Study Signal Transduction Pathways

Relatively recent advances in fluorescent biosensor technology allow researchers to track the dynamics of cyclic nucleotides and their effectors in living neurons and brain tissue. Indeed, several genetically encoded fluorescent biosensors for monitoring cyclic

nucleotide dynamics have been developed with advances in molecular and cell biology. These sensors have been implemented living cells, including neurons, for the purpose of understanding how cyclic nucleotides impact neuronal function and development.

An overview of fluorescence

Fluorescence microscopy is a cornerstone of modern biological investigation from the nanoscale to the whole organism level. Fluorescent protein (FP) technology revolutionized the field of cell and developmental biology by providing a genetically encodable fluorescent tag. Prior to the cloning of A. *victoria* GFP, cellular imaging required the preparation and microinjection of macromolecules conjugated with fluorescent dyes. Genetic encodability relieved researchers from the cumbersome protocols of labeling macromolecules by letting the cells do the work. Given the fact that the FP primary amino acid sequence contains all the information needed for fluorescence, there is tremendous versatility in the use of FPs to precisely monitor the signaling dynamics of living cells. In addition, the ability to add a specific subcellular localization sequence to a fusion construct increases the spatial resolution to "sub-microscopic" levels.[101] Extensive studies involving fluorescent fusion proteins have proven that FPs do not, in most cases, affect a protein's function or movement.

Fluorescent proteins, including green fluorescent protein from *A. victoria* (GFP) and dsRed, have chromophores buried within their tertiary structures that can absorb and emit light.[102] The chromophore is produced autocatalytically in an aerobic environment through a process known as maturation. Generally, an 11-stranded β-barrel makes up the tertiary structure that protects the chromophore from the solvent. The specific microenvironment of each chromophore is shaped by the surrounding amino acids and

contributes to the different spectral properties exhibited by different fluorophores.

There are dozens of enhanced FPs to choose from with different properties including the excitation and emission spectra, fluorescence lifetime, extinction coefficient, quantum yield, photostability and maturation speed.[103] The seven major variants of FPs are divided by their emission maxima as follows: blue (BFP 440-470 nm), cyan (CFP; 471-500 nm), green (GFP; 501-520 nm), yellow (YFP; 521-550 nm), orange (OFP; 551-575 nm), red (RFP; 576-610 nm), and far-red RFP (FRFP; 611-660 nm). It is important to choose the appropriate fluorescent protein for your desired application.

Genetically encodable fluorescent protein based biosensors

Genetically encoded fluorescent biosensors allow for the continuous monitoring of free cyclic nucleotide concentrations with high spatiotemporal resolution. These biosensors are engineered based on a general design: a sensing unit to detect the change in free cyclic nucleotide concentration and a reporting unit to convert the biochemical change into a fluorescent readout. The sensing unit for cyclic nucleotides biosensors is one or more cyclic nucleotide binding domains (CNBD). The reporting unit can be made up of two fluorescent proteins flanking the sensing unit as is the typical arrangement for fluorescence resonance energy transfer (FRET)-based biosensors. In FRET, energy is transferred non-radiatively, from an excited donor molecule to an acceptor molecule. For a fixed FRET donor-acceptor pair, the efficiency of FRET is dependent on the distance and orientation of the two fluorophores. In a FRET-based biosensor, cyclic nucleotide binding induces conformational changes of the CNBD sensing unit acting as a molecular switch to change the physical separation or orientation between the fluorescent protein pair resulting in a

change in FRET (Fig. 1.3A). In intensity-based biosensors, on the other hand, the reporting unit can be a single fluorescent protein. In this case, conformational changes in the sensing unit are translated into changes in fluorescence intensity (Fig. 1.3B). Different sensors vary in their CNBD sensing units and fluorescent protein reporting units. For a thorough overview of fluorescence and fluorescent proteins used in many different types of biosensors, please refer to the reviews by Sample et al. and Newman et al. [103, 104].

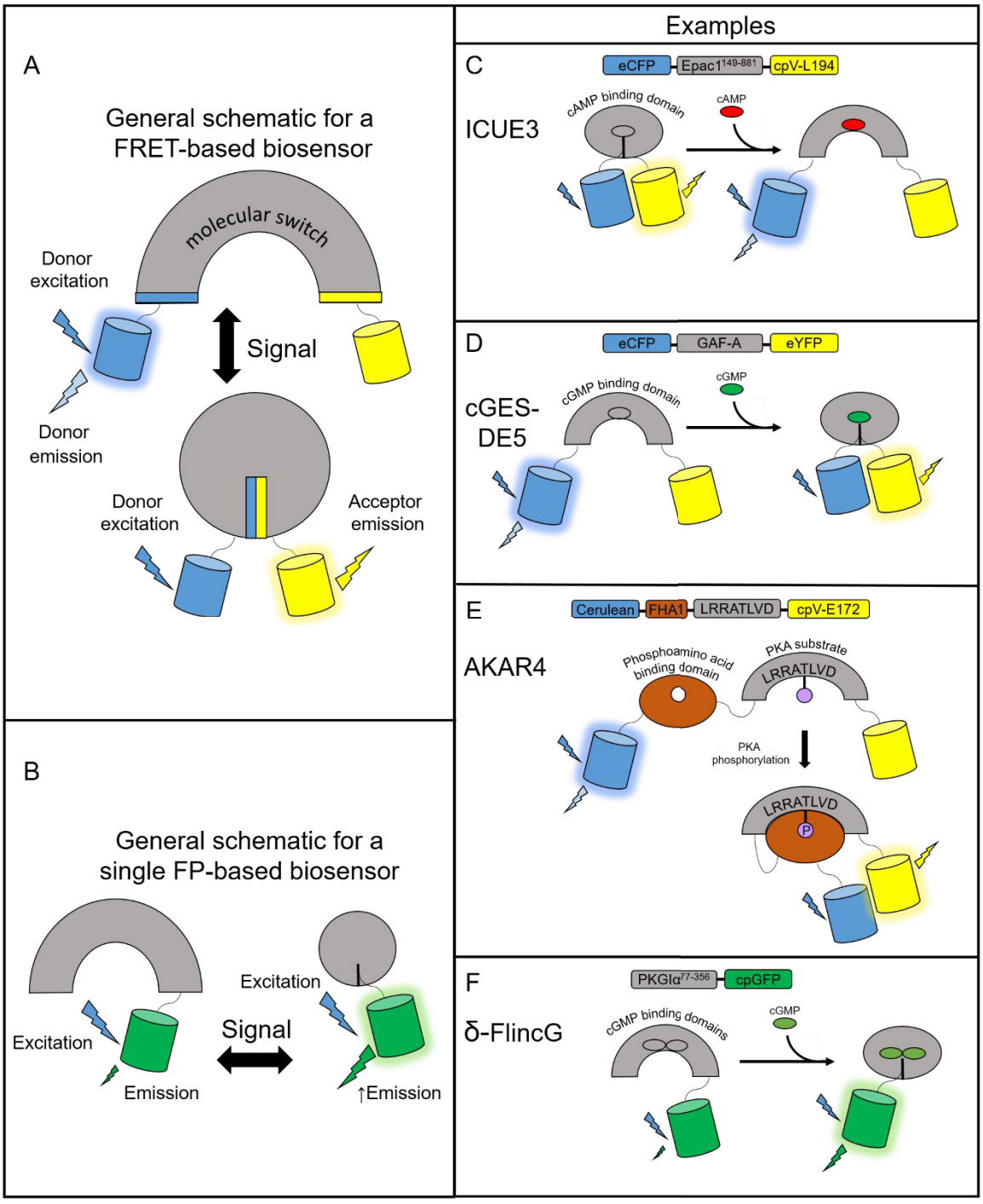

Figure 1.3. Designs of genetically encodable biosensors. (A) General design of a FRET-based biosensor consisting of a sensing unit that acts as a molecular switch to change the distance or orientation of the fluorescent protein reporting unit. In a low FRET situation, the donor fluorescent protein is excited and emits light at its own wavelength. In the high FRET situation, donor excitation allows for resonance energy transfer to the acceptor fluorescent protein that emits light at its own wavelength. **(B)** General design of a single

fluorescent protein-based biosensor. The sensing unit transduces a signal via a conformational change to the linked fluorescent protein reporting unit that undergoes its own conformational change and modulates fluorescence intensity. A circularly permuted GFP is often used to enhance the change in fluorescence. **(C)** ICUE3 consists of an Epac1$^{149\text{-}881}$ sensing unit flanked by an ECFP donor and a cpV-L194 acceptor reporting unit. Upon binding cAMP, the sensor switches from a high FRET to a low FRET conformation. **(D)** cGES-DE5 consists of a GAF-A sensing unit derived from PDE5A flanked by an ECFP donor and EYFP acceptor reporting unit. Upon binding cGMP, the sensor switches from a low FRET to a high FRET conformation. **(E)** AKAR4 contains a sensing unit consisting of a FHA1 phosphoamino acid binding domain and a substrate peptide. The reporting unit is comprised of a Cerulean donor and cpV-E172 acceptor reporting unit. When PKA activity is high, the substrate peptide is phosphorylated and binds the FHA1 domain to induce FRET. **(F)** δ-FlincG utilizes a PKG1α$^{77\text{-}356}$ sensing unit linked to a single cpGFP reporting unit. Upon binding cGMP, the fluorescence intensity of cpGFP increases.

A history of the Indicator of cAMP Using Epac

For the purposes of tracking cAMP, researchers have been developing molecular biosensors for the past several decades. For example, bimolecular PKA subunit-based probes, unimolecular Epac1 and Epac2-camps based on Epac CNBDs, and HCN2-camps based on the cAMP gated potassium channel HCN2, are different cAMP sensors that have been developed. Here, we would like to focus on a series of Epac based reporters called ICUE (**I**ndicator of **c**AMP **U**sing **E**pac) that have been developed as powerful and versatile cAMP sensors for live-cell imaging. First in the series, ICUE1 contained full-length Epac1 sandwiched between ECFP and the YFP variant Citrine[105]. Like Epac1-camps and Epac2-camps, ICUE also responds to cAMP with a decrease in the yellow to cyan emission ratio. ICUE2, an improved version of ICUE1, has an EC_{50} of ~12.5 μM and contains a N-terminally truncated Epac1 protein (Epac1$^{149\text{-}881}$)[106]. This biosensor showed improvement in localization over ICUE1 due to removal of a membrane and mitochondria targeting sequence located at the N-terminus. More recently, we developed ICUE3 with an increased

dynamic range by changing the FRET acceptor Citrine to a circularly permuted Venus at lysine 194 (cpV-L194)[107] (Fig. 1.3C). The large dynamic range of ICUE3 (~100% emission ratio change) makes it suitable for subcellular targeting for detecting local cAMP changes (e.g. plasma membrane and nucleus[108], sarcoplasmic reticulum[109], primary cilia[110]) as addition of subcellular localization tags sometimes leads to decreased response amplitudes.

A history of the A-Kinase Activity Reporter

Neuromodulatory signals can be transduced by cAMP and cGMP through their downstream target kinases PKA and PKG, respectively [111]. Although there are no biosensors yet available for PKG activity, the A-kinase activity reporter (AKAR) can report on the kinase activity of PKA [101]. AKAR uses a molecular switch consisting of a phosphoamino acid binding domain linked to a PKA-specific substrate sequence flanked by CFP and YFP. PKA phosphorylation of its substrate induces binding of the phosphorylated substrate to the phosphoamino acid binding domain, leading to an increase in FRET. AKAR1 displayed an irreversible FRET response, which prevented continuous monitoring of PKA dynamics. This was presumably due to the high affinity of the 14-3-3 binding domain for the substrate as tight binding may prevent phosphatases from dephosphorylating the substrate and reversing the FRET response. This was overcome by the generation of AKAR2 that utilized the lower binding affinity forkhead-associated domain 1 (FHA1) and exhibited a reversible FRET response [112]. The kinetics of AKAR2 were improved in AKAR2.2 by replacing the dimeric forms of ECFP and Citrine with versions that resist dimerization. The dynamic range was doubled in AKAR3 by replacing the YFP acceptor in AKAR2 with cpV-E172 [113]. The dynamic range of AKAR was further

enhanced with latest version, AKAR4, by replacing ECFP with Cerulean [114] (Fig. 1.3E). Due to the amplification of the cAMP signal by PKA phosphorylation activity, PKA activity reporters may be able to detect signals not picked up by cAMP binding probes. Recently, a modified AKAR probe named ^{Aq}AKAR^{Cit}, was generated by replacing Cerulean with Aquamarine, a newly engineered CFP variant that has mutations T65S and H148G [115]. These modifications to ECFP increased its photophysical properties and reduced its environmental sensitivity to low pH.

A history of the cGMP Energy Transfer Sensor Derived from PDE5A

Like cAMP, cGMP has had the attention of groups specialized in biosensor development to effectively monitor cGMP in living cells. Some examples include the Cygnet probes[116], cGES-GKIB[117] and the cGi series based on tandem CNBDs from PKG1α. The cGMP probe cGES-DE5 was developed by Nikolaev *et al.* in order to monitor cGMP levels inside living cells.[117] The acronym stands for cGMP energy transfer sensor derived from PDE5A. The sensing unit of cGES-DE5 is the regulatory GAF-A domain from PDE5A and the reporting unit is comprised of EYFP at the N-terminus and ECFP at the C-terminus (Fig. 1.3D). The regulatory GAF-A domain from PDE5A binds cGMP and undergoes a conformational change, bringing the two FPs close together and facilitating FRET (Fig. 1.3D).[118, 119] In conjunction with this probe, the authors developed a similar sensor based on PDE2 and PKGIB, but found cGES-DE5 to be the best with high selectivity for cGMP/cAMP and a large FRET response. This single-chain cGMP probe generates a 40% increase in emission ratio, representing a two-fold improvement over the older Cygnet construct[116], making it an attractive alternative to previous cGMP biosensors.

Utilizing cyclic nucleotide biosensors to study neuronal differentiation

As mentioned previously, cAMP and cGMP are involved in many biological processes. As an example of utilizing cGES-DE5A to solve a biological problem, a study by Shelly *et al*. used ICUE3 and cGESDE5 to study neuronal development.[70] cAMP is a well-known determinant of axonal polarization, whereas cGMP has been implicated in dendrite differentiation.[120, 121] The authors conducted several experiments using primary rat cortical and hippocampal neurons transfected with ICUE3 or cGES-DE5. Exposing a neurite tip to cAMP agonists using glass beads caused a cAMP increase in the exposed neurite and a decrease in the other neurites. The same stimulation caused a decrease in cGMP in the stimulated neurite, and an increase in the distal neurites. This phenomenon was dubbed long range inhibition of cAMP. The authors argue for a mechanism of axon/dendrite polarization that involves localized increases of cAMP and cGMP and activation of their downstream effectors. Thus, ICUE3 and cGES-DE5A were used together to study the impact of reciprocal regulation of cyclic nucleotides in the developing nervous system. The ability of these genetically encoded biosensors to report free cyclic nucleotide dynamics in living cells with high spatial and temporal resolution makes them a very powerful tool for understanding the molecular mechanisms underlying critical biological processes.

Advantages and limitations of FRET-based biosensors

Enzyme-linked immunosorbent assay and radioimmunoassays are sensitive,

specific, and provide a snapshot of the biochemical state of a population of cells. However, these assays require many cells, lack spatial information and measure total levels of cyclic nucleotides. Early studies on cyclic nucleotide compartmentation comes from the use of cyclic nucleotide gated ion channels, but these were limited by single compartment localization and lack of generalizability[122].

FP based biosensors have many advantages over traditional biochemical techniques including their ability to: 1) measure free cyclic nucleotides in live cells, 2) provide information on temporal dynamics, 3) provide information on spatially compartmentalized nucleotides, 4) report on the cyclic nucleotide status of single cells, and 5) provide a quantitative ratiometric readout. Because these biosensors are genetically encodable, they are produced by the cell and can be continuously monitored in live cells to track cyclic nucleotide dynamics. By attaching subcellular targeting sequences to the N- or C- termini of the biosensor, it can report on dynamics within specific compartments or microdomains. Furthermore, genetically encoded biosensors help uncover the complexities of subcellular signaling events at the level of individual cells. This information generates insights into single cell behaviors and reveals variations between cells.

The ability to provide a quantitative measurement of intracellular cyclic nucleotides is an attractive feature of ratiometric biosensors like ICUE3 and cGES-DE5A. By using the ratio of acceptor emission over donor emission upon donor excitation, some experimental variations such as light source and cell thickness are minimized making it possible to use calibration curves to help determine nucleotide concentration. This can be accomplished by obtaining lysate from a cell expressing a biosensor and adding known concentrations of cAMP or cGMP while monitoring the FRET ratio using a fluorimeter.

The FRET ratio can then be correlated to the concentration of free cyclic nucleotide in live cells[123] In addition, single chain FRET biosensors do not have the problem of unequal donor-acceptor expression. Taken together, the many advantages offered by genetically encoded biosensors for cyclic nucleotides make them a great option for researchers wishing to study real-time cyclic nucleotide signaling.

Every technology has limitations that need to be kept in mind when using the technology to answer biological questions. In the case of genetically encoded cyclic nucleotide biosensors, endogenous signaling pathways may be impacted by the introduction of a cyclic nucleotide biosensor. Due to the high affinity of CNBDs for their cyclic nucleotides, overexpressing them may buffer cAMP or cGMP, leaving the cell without enough cyclic nucleotide to complete the signaling process. Therefore, one needs to assess any perturbations to cell by comparing cyclic nucleotide dependent signal transduction responses between cells transfected with a biosensor versus a control GFP. Because every FRET reporter has a set dynamic range and cyclic nucleotide sensitivity, the level of cyclic nucleotide may not be faithfully reported. For example, the FRET change might plateau while the concentration of cyclic nucleotide is still increasing. This limitation can be addressed by designing sensors with varying sensitivities to cAMP and cGMP. If a particular signaling phenomenon induces small changes in cAMP for example, a biosensor with a high sensitivity should be able to detect it. This same biosensor may not be suitable however, for larger increases that saturate it early on during generation of cAMP. Therefore, a biosensor with a less sensitive FRET response would be more appropriate. To this extent, Russwurm *et al.* have developed a series of FRET sensors for cGMP based on the tandem GAF domains of PKG called cGi-500, cGi-3000 and cGi-6000, where the

numbers refer to the EC_{50} values for cGMP.[124] Lastly, cyclic nucleotide specificity must be high in order to accurately report on cyclic nucleotide levels. Some domains bind to other cyclic nucleotides in addition to the target, making it difficult to study signaling in complex interacting systems.

Significance

The second messengers cAMP and cGMP transduce many neuromodulatory signals from hormones and neurotransmitters into specific functional outputs. Their production, degradation and signaling are spatiotemporally regulated to achieve high specificity in signal transduction. The development of genetically encodable fluorescent biosensors has provided researchers with useful tools to study these versatile second messengers and their downstream effectors with unparalleled spatial and temporal resolution in cultured cells, tissues, and living animals.

Although there has been significant progress made in understanding how the specific signaling of cyclic nucleotide second messengers is achieved, the mechanistic details in complex cell types like neurons are only just beginning to surface. Current and future fluorescent protein reporters will be essential to elucidate the role of cyclic nucleotide signaling dynamics in the functions of individual neurons and their networks.

Chapter 2

AKAP-mediated feedback control of cAMP gradients in developing hippocampal neurons

This chapter has been adapted from a manuscript recently submitted to Nature Chemical Biology.

Introduction

Neuronal development is an intricate, multi-stage process[92] in which the transition from progenitor cell to fully developed neuron depends on spatiotemporally regulated signaling events. Polarized growth is a particularly crucial aspect of this process, with individual neurons relying on coordinated pathways to ensure the proper development of a spatially distinct axon and dendrites[125]. Among these, 3'5' cyclic adenosine monophosphate (cAMP) signaling, a pathway that is essential for many neuronal functions[33], is known to be a critical axon determinant[98].

cAMP is generated by adenylyl cyclases (ACs) and degraded by phosphodiesterases (PDEs); the free cAMP concentration in the cell is therefore dictated by the balance of these enzymatic activities. cAMP then binds and activates effector proteins such as protein kinase A (PKA) and exchange protein activated by cAMP (Epac), which play crucial roles in developing axons. For example, BDNF has been shown to elevate cAMP/PKA activity in the axon, leading to additional BDNF release and increased plasma membrane insertion of the BDNF receptor, TrkB, resulting in continued cAMP/PKA signaling and effectively generating a nested positive feedback loop in the nascent axon[95]. Similarly, Epac activation was shown to result in increased growth cone turning and neurite outgrowth, as well as axon regeneration in DRG neurons[48]. In hippocampal neurons, Epac regulates axon elongation via the activation of Rap1B and the subsequent activation of PI3K[47]. PKA and Epac have also been shown to play opposing roles. For example, in embryonic DRG neurons, growth cone attraction to morphogens was shown to be mediated by Epac, while repulsion was mediated by PKA[45].

cAMP signaling specificity is often achieved by confining cAMP elevations to discrete subcellular compartments[114, 126]. For example, asymmetric cAMP signaling can directly influence the formation of a single axon and multiple dendrites. Specifically, axonal cAMP elevations were found to have long-range inhibitory effects on dendritic cAMP levels in hippocampal neurons (HNs), with the local elevation of cAMP at a nascent neurite leading to decreased cAMP levels in the remaining neurites[70]. Compartmentalization of the cAMP signaling machinery itself[61, 127] can further refine the spatial control of cAMP dynamics to modulate cell physiology. Adenylyl cyclase 5 (AC5), for example, was previously shown to be enriched in the distal axon and growth cone[128]. Nevertheless, cAMP dynamics have not been systematically examined in subcompartments of developing neurons.

At the PKA level, spatial compartmentalization is directly controlled by A-kinase anchoring proteins (AKAPs)[60, 129, 130], with many different AKAPs acting as scaffolds for the PKA holoenzyme, adenylyl cyclases, phosphodiesterases, phosphatases, and ion channels[131]. The AKAP microdomain localizes the regulators and effectors of PKA signaling and serves to spatially control PKA function by binding the RII subunit of PKA[132], the major regulatory subunit in neurons[133]. Thus, any PKA signaling that contributes to the initiation of morphological compartmentation exists within a scaffold of PKA regulators and effectors[134]. However, despite efforts to understand the role of AKAPs in neuronal excitability and synaptic responses[33, 131], there has not been significant inquiry into the role AKAPs play in neuronal development.

Here, we utilized genetically encoded fluorescence resonance energy transfer (FRET)-based biosensors to investigate cAMP/PKA signaling dynamics in stage-three to

stage-four primary rat HNs[135]. Neurons at these stages have nascent and spatially distinct dendrites and axons in the process of elongation. Using these probes, we uncovered a developmentally timed, axon-directed cAMP gradient that is maintained by AKAP-anchored PKA activity and that is critical for ensuring proper axonal development. Our results suggest that, although cAMP and PKA are widely regarded as playing a positive role in promoting and establishing neuronal polarity, axon elongation, and guidance[31, 45, 128, 136, 137], these signaling molecules in fact play a more nuanced role in shaping neuronal development than previously appreciated.

Results

Comparing spatial cAMP signaling in hippocampal neurons at different developmental stages

As first demonstrated by the pioneering work of Dotti *et al.*[92, 138], the stages of neuronal development can be defined *in vitro* by plating HNs onto polylysine-coated glass coverslips. Between the time of plating and 7 days in culture, neurons proceed through five main stages of growth. At stage one (0 h), the neuron is uniform in shape, with small, lamellar protrusions extending from the cell body. At stage two (12 h), the neuron forms immature neurites. At stage three (36 h), the cell begins to specify the fate of one of these neurites to grow rapidly and form the axon. At stage four (4 days), the dendrites begin to grow. At stage five and beyond (>7 days), the neuron begins to mature. We therefore used rat (*Rattus norvegicus*) HNs grown for five days *in vitro* (DIV5) to investigate the molecular activities involved in neurite outgrowth.

We first used the genetically encoded FRET-based cAMP biosensor ICUE3 (Fig. 2.1a)[107] to analyze the activity and regulation of cAMP in living neurons. ICUE3 contains a truncated version of Epac1 (aa 149-881) sandwiched between ECFP (donor) and cpVenus-L194 (acceptor), wherein the binding of cAMP results in a conformational change in this truncated Epac1 and an increase in the donor-to-acceptor (C/Y) emission ratio. Using this probe, we observed a range of emission ratio changes in different regions of DIV5 HNs upon bath stimulation with 50 μM forskolin (Fsk), a general activator of transmembrane ACs; on average, the ratio increases were significantly lower in the soma, dendrites, and proximal axon (21.8±3.7%, 24.5±3.7%, and 30.6±5.0%, respectively) than in the middle and distal axon (41.8±5.3% and 47.8±5.7%; mean±SEM, n=12) (Fig. 2.1b-d), indicating the presence of a gradient of cAMP signaling towards the axon in these cells. These data are consistent with previously suggested axonal-dendritic differences in cAMP[128] and further define axonal subcompartments that show distinct cAMP characteristics.

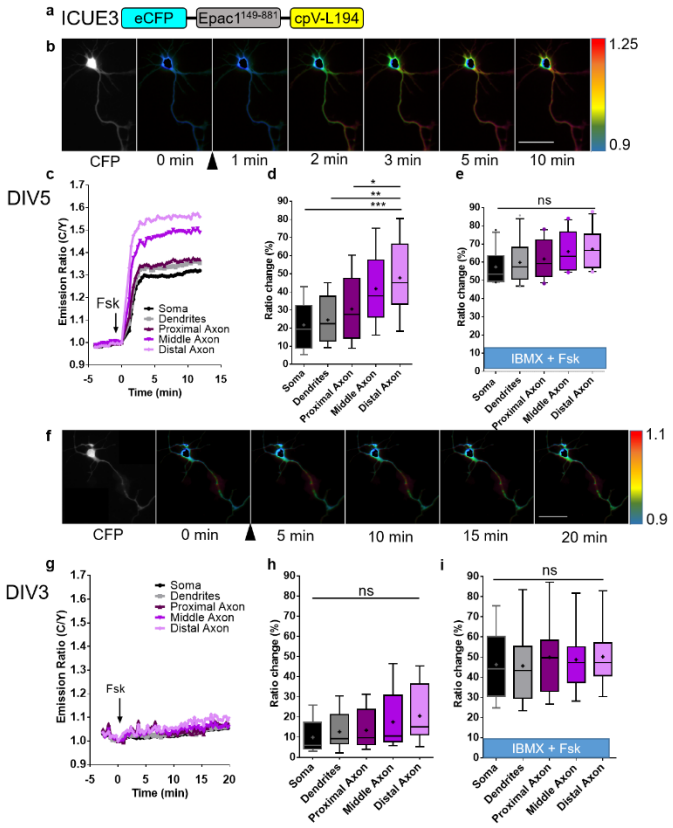

Figure 2.1. Spatial regulation of cAMP production in early polarized hippocampal neurons.

(a) Schematic illustrating the domain structure of the cAMP biosensor ICUE3, which uses Epac1$^{149\text{-}881}$ as the sensing domain and eCFP/cpV-L194 as the FRET pair. (b) Pseudocolored images showing the responses of ICUE3 to 50 µM Fsk in a DIV5 HN. Arrowhead indicates time of drug addition. Warmer colors correspond to higher cyan/yellow (C/Y) emission ratios. Scale bar, 50 µm. (c) Representative time-course of the emission ratio changes in the soma, dendrites, proximal axon, middle axon, and distal axon from the cell in a. (d) Average ICUE3 responses induced by Fsk stimulation in each region of DIV5 HNs (n=12 from five preparations; *p=0.032, **p=0.0023, and ***p=0.0009 according to two-tailed Student's t-test). (e) Average ICUE3 responses induced by IBMX followed by 50 µM Fsk in each region of DIV5 HNs (n=10, from three preparations). No significant differences were observed among the regions in response to Fsk following IBMX treatment. (f) Pseudocolored images showing the responses of ICUE3 to 50 µM Fsk in the DIV3 HN. Arrowhead indicates time of drug addition. Warmer colors correspond to higher C/Y emission ratios. Scale bar, 50 µm. (g) Representative time-course of the emission ratio changes in the different regions in response to 50 µM Fsk in the DIV3 HN from panel f. (h) Average cAMP increase induced by Fsk stimulation in each region of DIV3 HNs (n=8 from three preparations). (i) Average cAMP increase induced by IBMX followed by 50 µM Fsk in each region of DIV3 HNs (n=8 from three preparations). Data in d, e, h, and i are shown as box-and-whisker plots, with the box showing the median, 25% quartile, and 75% quartile, and the whiskers designating the 5th and 95th percentiles; a "+" indicates the mean. ns, not significant.

Although axonal-dendritic differences in cAMP have previously been suggested to assist in neuronal development[70, 95], cAMP gradients have yet to be investigated at different stages of development. We therefore compared the cAMP dynamics of DIV5 HNs with those of less-developed DIV3 HNs. Overall, we observed a weaker and more uniform ICUE3 response to Fsk stimulation in DIV3 cells compared with that in DIV5 cells, with a gradual increase of ~15% over 20 min and no significant differences in the different cellular regions (Fig. 2.1f-h). Thus, neurons at different developmental stages have different capacities for generating cAMP gradients.

Because such capacities originate from balanced actions of ACs and PDEs[139], we next tested the role of PDEs in generating the cAMP gradient observed in DIV5 cells. Interestingly, treatment with the general PDE inhibitor 3-isobutyl 1-methylxanthine (IBMX) revealed a weak axon-directed cAMP response in these cells (Fig 2.2a), with subsequent Fsk stimulation producing a large, uniform ratio increase of ~50-60% (Fig. 2.1e). DIV3 HNs treated with IBMX similarly exhibited a small, axon-directed increase in cAMP (Fig 2.2b), followed by a larger, uniform increase in emission ratio upon Fsk stimulation (Fig. 2.1i). Treatment with the isoform-specific inhibitors rolipram (PDE4 specific) and milrinone (PDE3 specific) followed by Fsk revealed that PDE4 is the dominant isoform at DIV3, as well as at DIV5, as rolipram pretreatment mimicked the effect of IBMX on potentiating the Fsk-induced response, in contrast to milrinone pretreatment (Fig 2.3a,b). Collectively, these data reveal differences in cAMP signaling within neuronal compartments and between HNs at different developmental stages. Specifically, both DIV3 and DIV5 HNs displayed higher AC activity towards the axon, yet DIV3 HNs appeared to possess stronger PDE activity compared with DIV5 HNs. Our

results suggest that this imbalance in favor of PDE activity contributes to the lower stimulated cAMP production observed in newly polarized, DIV3 cells. On the other hand, the lower axonal PDE activity in DIV5 HNs may allow polarized AC activity to induce the formation of a steep cAMP gradient, with higher cAMP levels in more distal regions of the axon compared to other regions of the cell.

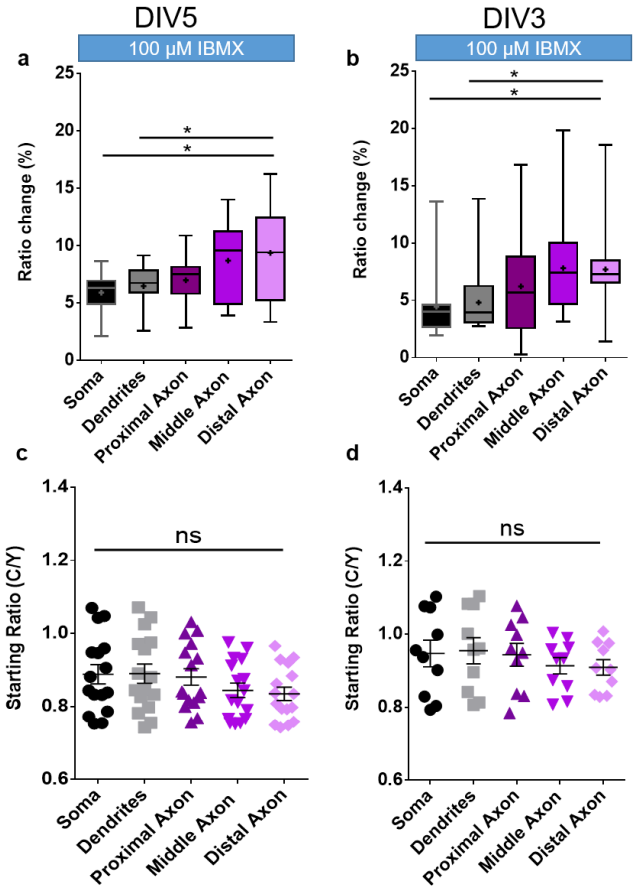

Figure 2.2. PDE activity affects cAMP dynamics in developing neurons.
(a) Average ICUE3 responses induced by 100 µM IBMX in DIV5 HNs (n=12 from three preparations; Distal vs Soma *p=0.018, Distal vs Dendrites *p=0.043, according two-tailed Student's t-test). (b) Average ICUE3 responses induced by 100 µM IBMX in DIV3 HNs (n=18 from three preparations, Distal vs Soma *p= 0.013, Distal vs Dendrites *p=0.029 according to two-tailed Student's t-test). (c) Average ICUE3 starting ratios in DIV5 HNs. (d) Average ICUE3 starting ratios in DIV3 HNs; ns, not significant. Data in a and b are shown as box-and-whisker plots, with the box showing the median, 25% quartile, and 75% quartile, and the whiskers designating the 5th and 95th percentiles; a "+" indicates the mean.

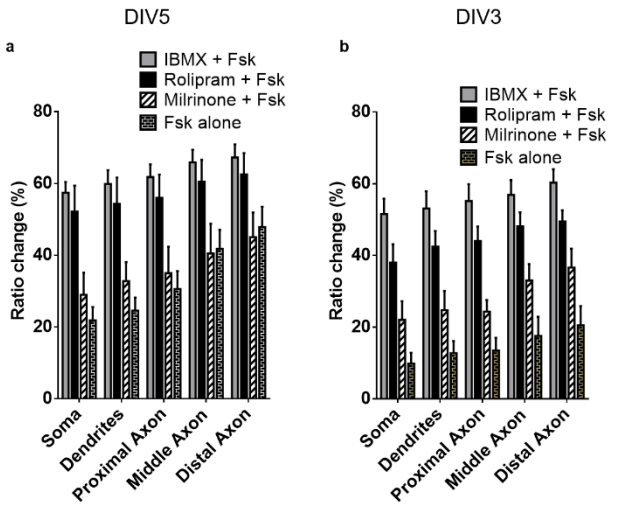

Figure 2.3. PDE4 is the dominant cAMP phosphodiesterase in hippocampal neurons. (a) Average ICUE3 responses to 100 μM IBMX+50 μM Fsk (n=10 from three preparations), 10 μM rolipram+50 μM Fsk (n=8 from three preparations), 10 μM milrinone+50 μM Fsk (n=7 from three preparations), or 50 μM Fsk alone (n=12 from three preparations, data shown previously) in DIV5 HNs. (b) Average ICUE3 responses to 100 μM IBMX+50 μM Fsk (n=9 from three preparations), 10 μM rolipram+50 μM Fsk (n=11 from three preparations), 10 μM milrinone+50 μM Fsk (n=7 from three preparations), or 50 μM Fsk alone (n=8 from three preparations, data shown previously) in DIV3 HNs. Fsk-alone data are reproduced from Figure 2.1. Bars represent mean±S.E.M.

Compartmental PKA activity in hippocampal neurons at different developmental stages

Because PKA is directly downstream of cAMP, we wanted to know if PKA activity follows the axon-directed cAMP gradient observed above. We therefore transfected DIV5 and DIV3 HNs with the PKA activity biosensor AKAR4[114] that contains a PKA substrate sequence and phosphoamino acid-binding domain (FHA1) sandwiched between Cerulean (donor) and cpVenus-E172 (acceptor) and reports on PKA activity via increases in the acceptor-to-donor (Y/C) emission ratio (Fig. 2.4). However, AKAR4-expressing DIV5 and DIV3 HNs both responded to 50 μM Fsk stimulation with uniform FRET ratio increases (~40%) among all the regions (Fig. 2.4). Cells expressing a negative-control reporter (AKAR4-TA), in which the target Thr is mutated to Ala, showed no response to 50 μM

Fsk, confirming that these responses are due to PKA activity (Fig. 2.5). Subsequent treatment with 100 µM IBMX failed to elicit any additional increase in both DIV5 and DIV3 cells (Fig. 2.4), indicating that the AKAR4 response was fully saturated.

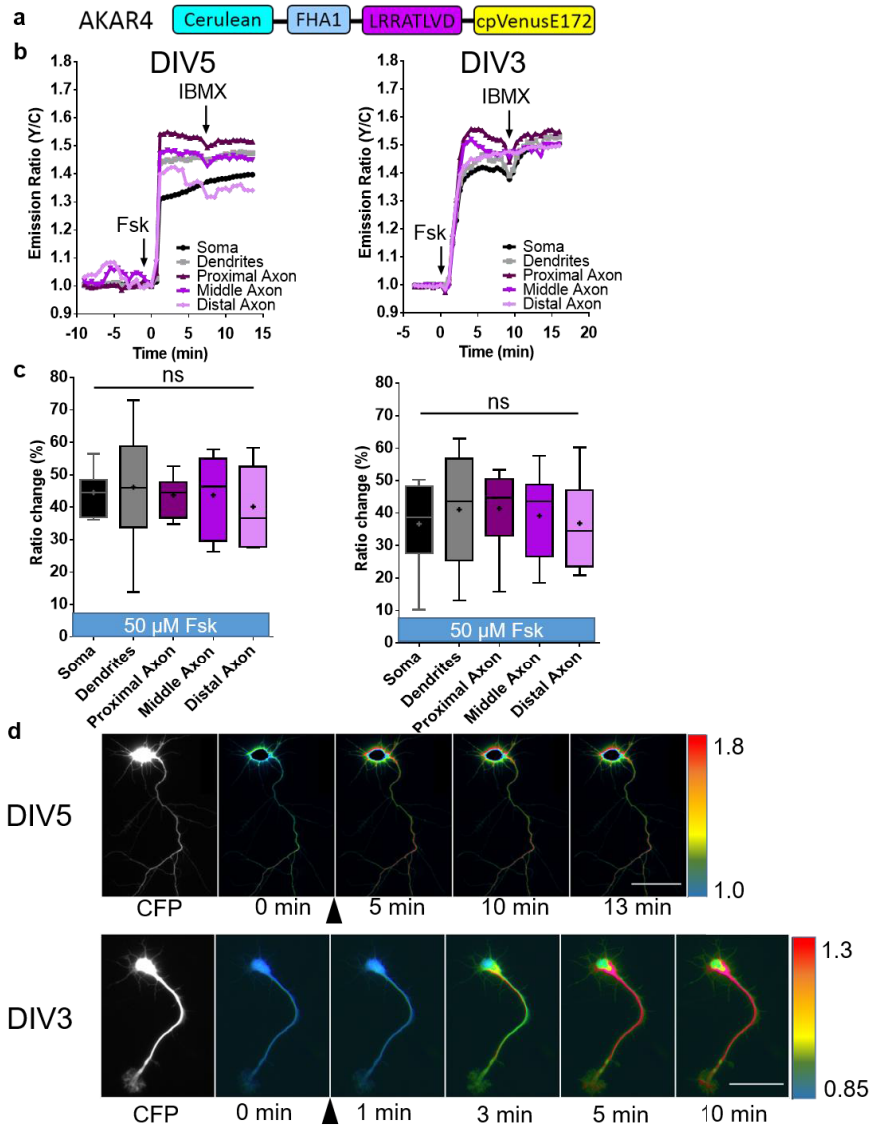

Figure 2.4. The AKAR4 response is saturated by treatment with 50 µM Fsk.
(a) Schematic illustrating the domain structure of AKAR4. AKAR4 contains an FHA1 domain fused to a PKA substrate (LRRATLVD) as the sensing domain and Cerulean/cpVenus-E172 as the donor/acceptor FRET pair. (b) Representative time-course of AKAR4 emission ratio changes in a DIV5 (left) and DIV3 HN (right) in response to 50 µM Fsk. (c) Average AKAR4 responses induced by 50 µM Fsk in DIV5 (left, n=7 from four preparations) and DIV3 HNs (right, n=10 from three preparations). Both DIV5 and DIV3 HNs exhibit a maximal response that is not further affected by PDE inhibition with

100 µM IBMX. (d) Pseudocolored images showing the responses of AKAR4 to 50 µM Fsk in the DIV5 (top) and DIV3 HN (bottom) from panel b. Arrowheads indicate the time of drug addition. Warmer colors correspond to higher Y/C emission ratios. Scale bar, 50 µm. Data in c are shown as box-and-whisker plots, with the box showing the median, 25% quartile, and 75% quartile, and the whiskers designating the 5th and 95th percentiles; a "+" indicates the mean; ns, not significant, *p<0.05, according to two-tailed Student's t-test.

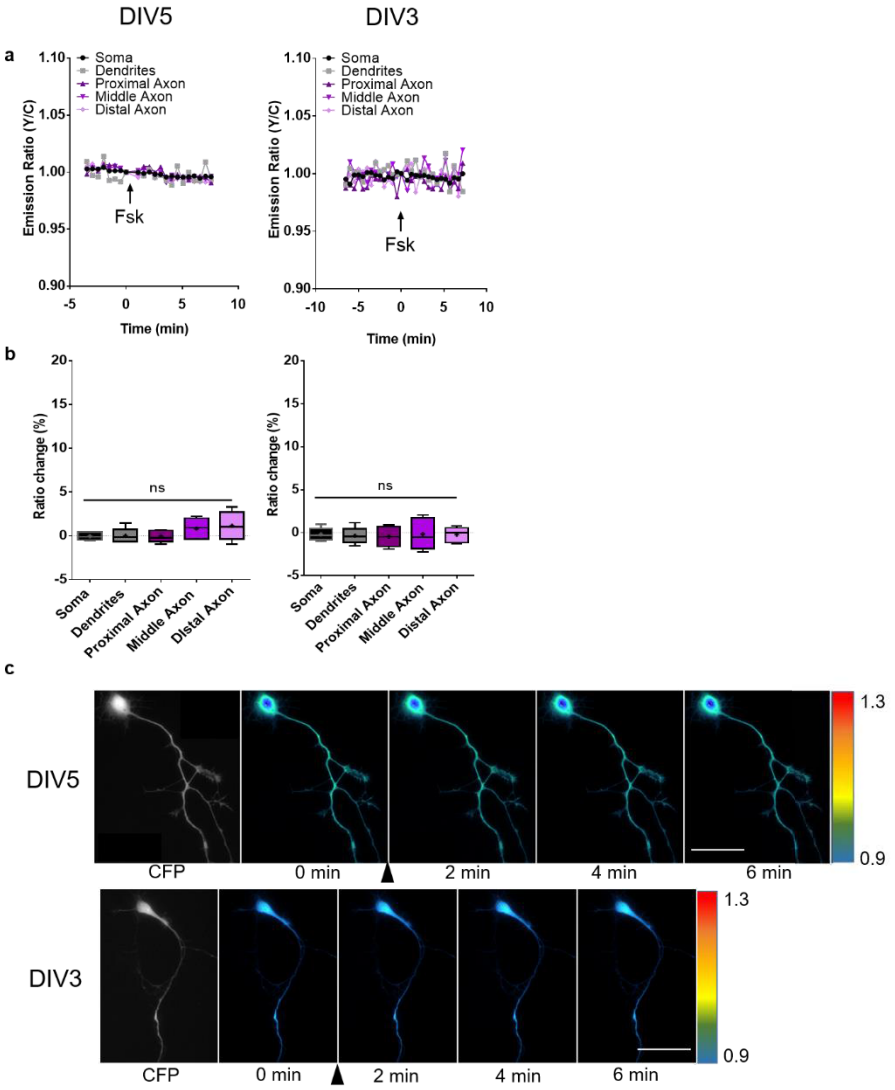

Figure 2.5. The AKAR4-TA control reporter does not exhibit a response to 50 µM Fsk. (a) Representative time-course of AKAR4-TA in a DIV5 (left) and DIV3 HN (right) treated with 50 µM Fsk. (b) Average AKAR4-TA response in DIV5 (left, n=5 from one preparation) and DIV3 HNs (right, n=5 from preparation) to 50 µM Fsk. (c) Pseudocolored images showing the response of AKAR4-TA to 50 µM Fsk in the DIV5 (top) and DIV3 HN (bottom) from panel a. Arrowheads indicate the time of drug addition. Warmer colors correspond to higher Y/C emission ratios. Scale bar, 50 µm. Data in b are shown box-and-

whisker plots, with the box showing the median, 25% quartile, and 75% quartile, and the whiskers designating the 5th and 95th percentiles; a "+" indicates the mean.

Because cAMP binds to PKA with an ~1000 fold higher affinity compared with Epac[140], we suspected that the saturating effect of 50 μM Fsk stimulation was masking the underlying spatial differences in PKA activity. We therefore tested whether submaximal stimulation would reveal a PKA gradient. Indeed, treating DIV5 cells with tenfold less (500 nM) Fsk generated an axon-directed PKA activity gradient that paralleled the cAMP response (Fig. 2.6a,b; left). On the other hand, DIV3 cells showed only small (~5%) responses to the low dose of Fsk, with no significant differences between the regions (Fig. 2.6a,b; right). Pretreating DIV3 HNs with IBMX resulted in an ~40% ratio increase in response to 500 nM Fsk, whereas IBMX treatment alone produced an ~50% ratio increase in DIV5 HNs, confirming that the reporter was functioning normally (Fig. 2.6c).

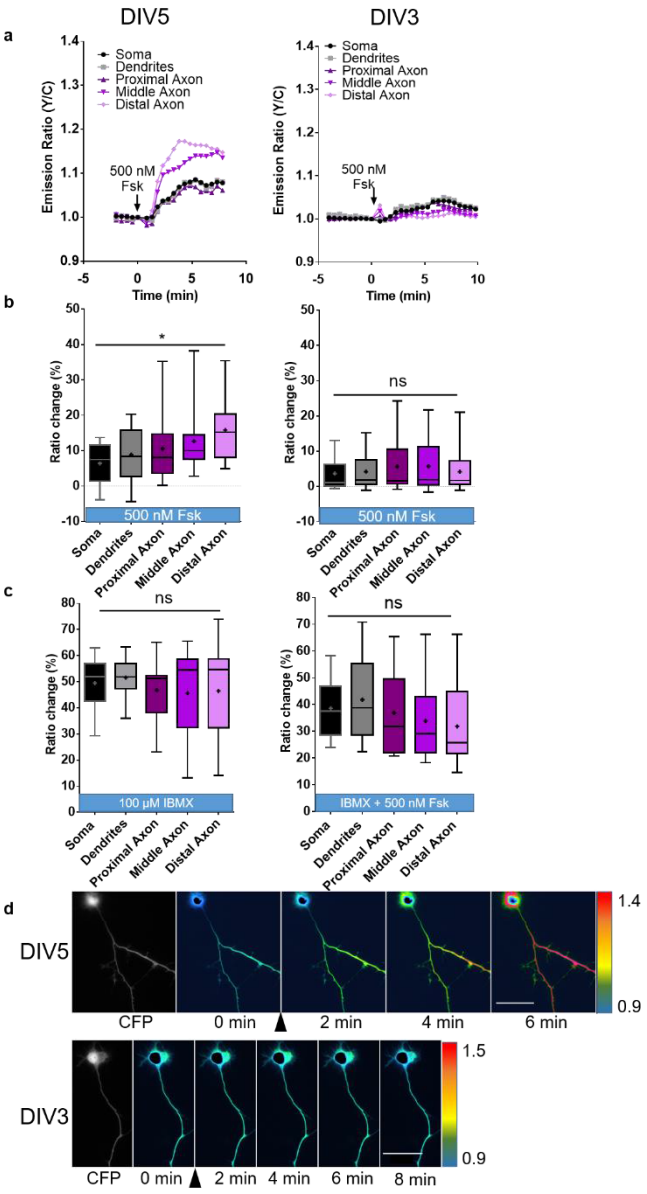

Figure 2.6. Spatial regulation of PKA activity in early polarized hippocampal neurons.

(a) Representative time-course of the AKAR4 emission ratio changes in the different compartments of a DIV5 (left) and DIV3 HN (right) in response to 500 nM Fsk. (b) Average AKAR4 responses induced by 500 nM Fsk in DIV5 (left, n=10 from four preparations; *p=0.012 according to two-tailed Student's t-test) and DIV3 HNs (right, n=14 from three preparations). (c) Average AKAR4 response induced by 100 µM IBMX in DIV5 HNs (left, n=9, from three preparations) and 100 µM IBMX followed by 500 nM Fsk in DIV3 HNs (right, n=15 from three preparations). (d) Pseudocolored images showing the responses of AKAR4 to 500 nM Fsk in the DIV5 (top) and DIV3 (bottom) HN from panel a. Arrowheads indicate the time of drug addition. Warmer colors correspond to higher yellow/cyan (Y/C) emission ratios. Scale bar, 50 µm. Data in b and c are shown as box-and-whisker plots, with the box showing the median, 25% quartile, and 75% quartile,

and the whiskers designating the 5th and 95th percentiles; a "+" indicates the mean. ns, not significant.

We also observed a clear, axon directed gradient in the AKAR4 starting ratio in DIV5 HNs (Fig. 2.7). Although control cells expressing AKAR4-TA also exhibited higher starting ratios in the distal axon, possibly due to slightly higher levels of the probe in this region, the starting ratio differences were steeper with AKAR4 than with AKAR4-TA in DIV5 HNs (Fig 2.7), whereas both AKAR4 and AKAR4-TA exhibited similar starting ratio differences in DIV3 HNs (Fig. 2.7), suggesting the presence of a bona fide gradient of basal PKA activity in resting DIV5 HNs. These data indicate that PKA follows the cAMP response pattern seen in DIV5 HNs, with an axon-directed gradient of PKA activity, whereas more immature HNs lack such a gradient.

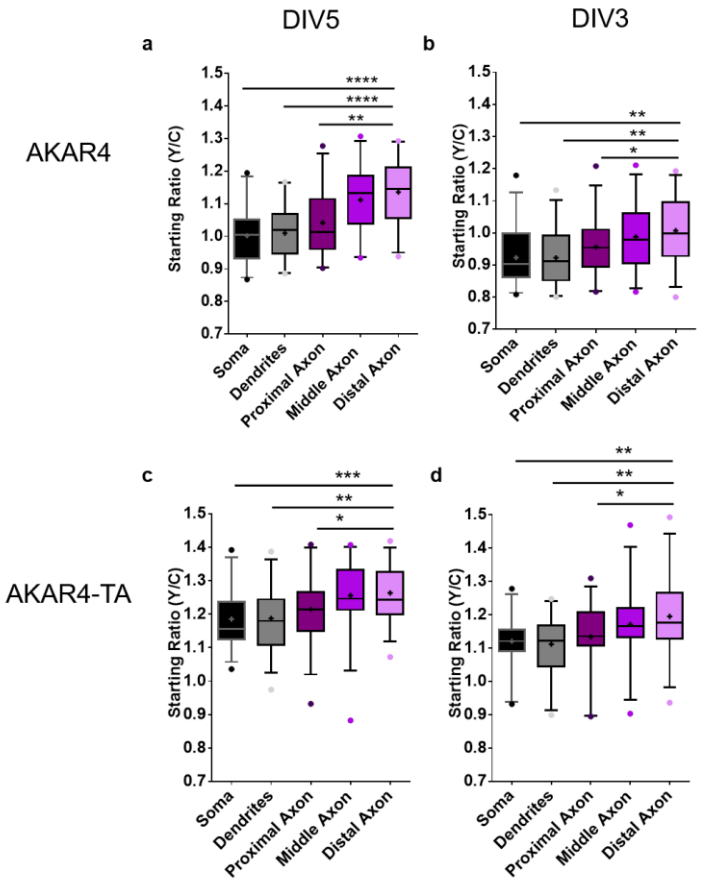

Figure 2.7. Basal PKA activity in developing neurons.
(a) Average starting Y/C emission ratio in DIV5 HNs expressing AKAR4 (n=20 from five preparations). (b) Average starting Y/C emission ratio in DIV3 HNs expressing AKAR4 (n=31 from four preparations). (c) Average starting Y/C emission ratio in DIV5 HNs expressing AKAR4-TA (n=30 from three preparations). (d) Average starting Y/C emission ratio inDIV3 HNs expressing AKAR4-TA (n=28 from three preparations). Data are shown as box-and-whisker plots, with the box showing the median, 25% quartile, and 75% quartile, and the whiskers designating the 5th and 95th percentiles; a "+" indicates the mean; *p<0.05, **p<0.01, ***p<0.001, ****p<0.0001 according to two-tailed Student's t-test.

AKAP anchoring is required for basal PKA activity in the axon in hippocampal neurons

Because AKAP anchoring plays a role in spatially restricting PKA in cells, we next investigated whether the PKA gradient in DIV5 HNs depends on AKAP anchoring. To this end, we treated cells with a cell-permeable form of Ht31 (st-Ht31), a peptide derived from

AKAP-Lbc[132, 141] that is known to disrupt PKA RII binding to AKAPs. In DIV5 HNs, st-Ht31 treatment led to a minimal change in the PKA activity within the somatodendritic compartment and a larger decrease in the axonal regions (Fig. 2.8a,b; left). On the other hand, DIV3 HNs exhibited no significant change in PKA activity among the different regions (Fig. 2.8a,b; right) following st-Ht31 treatment. DIV5 HNs transfected with the negative-control reporter exhibited no change upon st-Ht31 treatment (Fig. 2.9). These results further support our conclusion that the starting ratio differences in DIV5 HNs correspond to differential PKA activity and reveal that the axonal PKA gradient is promoted by AKAP anchoring.

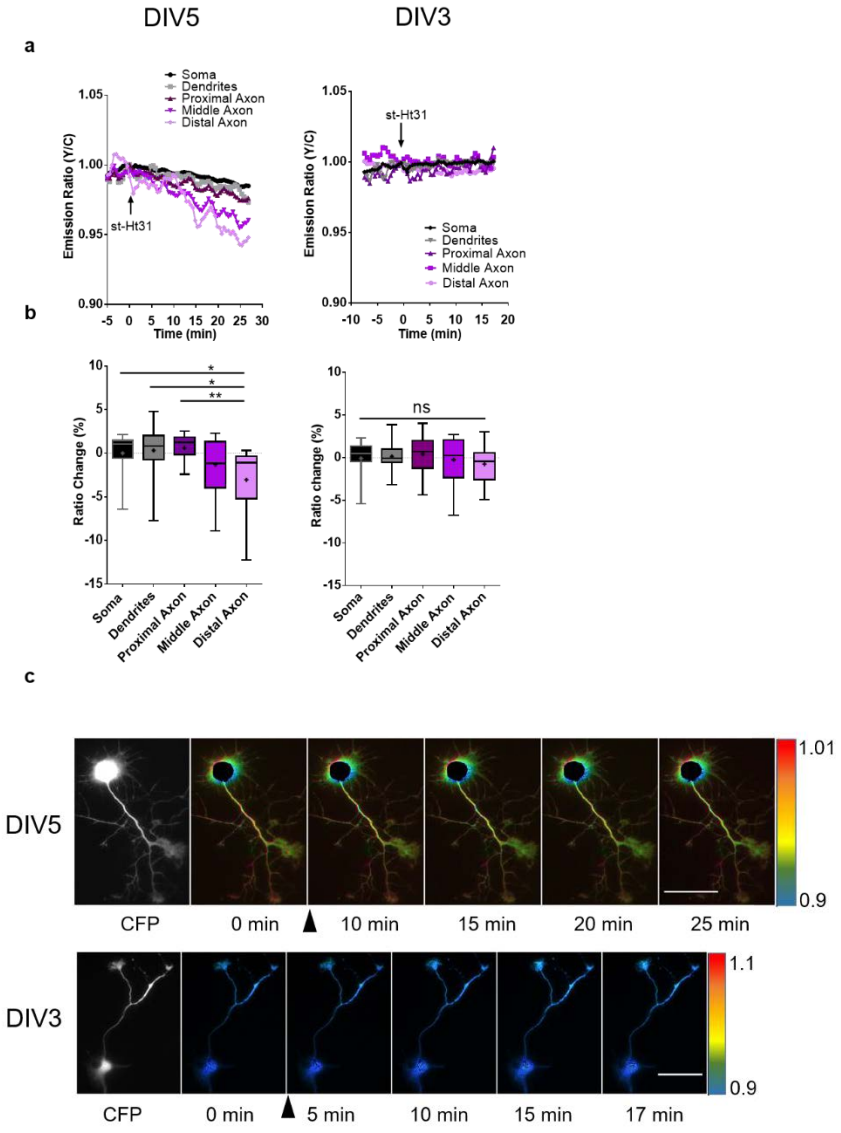

Figure 2.8. Acute disruption of AKAP anchoring decreases PKA activity in the axon. (a) Representative time-course of the AKAR4 emission ratio changes of a DIV5 (left) and DIV3 HN (right) in response to 10 µM st-Ht31. (b) Average AKAR4 response induced by 10 µM st-Ht31 in DIV5 (left, n=15 from three preparations; Distal vs Soma *p=0.012, Distal vs Dendrites *p=0.011, and Distal vs Proximal **p=0.0017 according to two-tailed Student's t-test) and DIV3 HNs (right, n=16 from three preparations). (c) Pseudocolored images showing the responses of AKAR4 to 10 µM st-Ht31 in the DIV5 (top) or DIV3 (bottom) HN from panel a. Arrowheads indicate the time of drug addition. Warmer colors correspond to higher Y/C emission ratios. Scale bar, 50 µm. Data in b are shown as box-and-whisker plots, with the box showing the median, 25% quartile, and 75% quartile, and the whiskers designating the 5th and 95th percentiles; a "+" indicates the mean. ns, not significant.

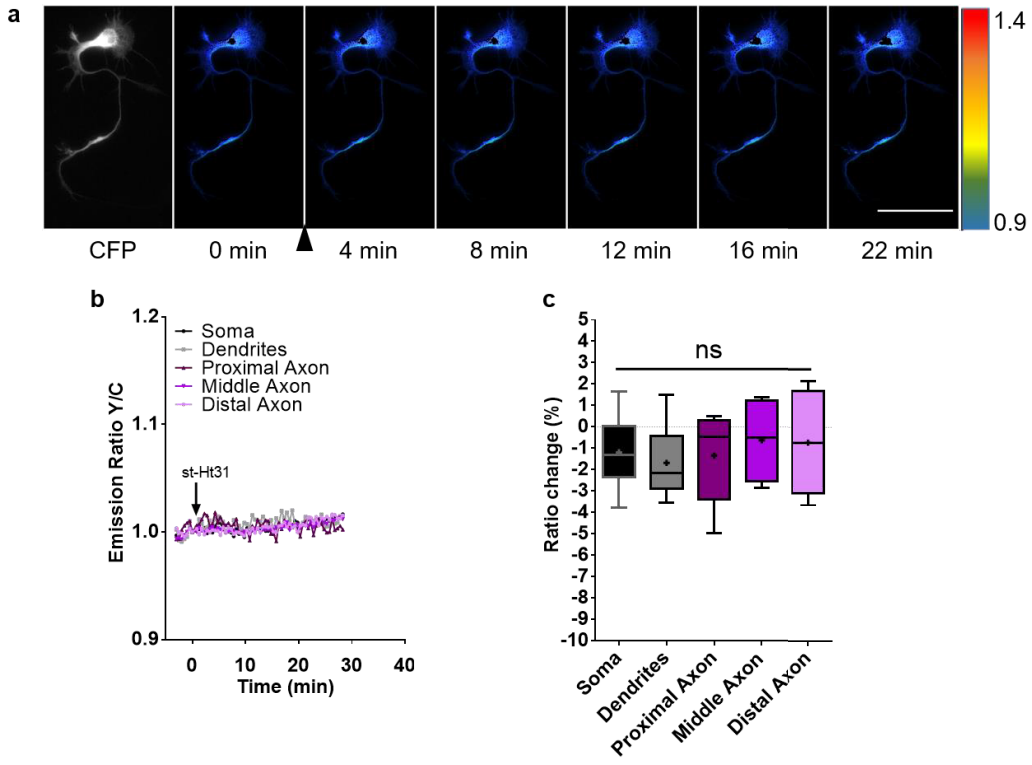

Figure 2.9. DIV5 HNs expressing AKAR4-TA do not respond to 10 µM st-Ht31. (a) Pseudocolored images showing the response of AKAR4-TA in a DIV5 HN treated with 10 µM st-Ht31. Arrowhead indicates the time of drug addition. Warmer colors correspond to higher Y/C emission ratios. Scale bar, 50 µm. (b) Representative time-course of the AKAR4-TA response from the cell in a. (c) Average response of DIV5 HNs expressing AKAR4-TA treated with 10 µM st-Ht31 (n=6 from two preparations). Data in c are shown as a box-and-whisker plot, with the box showing the median, 25% quartile, and 75% quartile, and the whiskers designating the 5th and 95th percentiles; a "+" indicates the mean; ns, not significant according to Student's t-test.

Delocalizing PKA enhances axon elongation in hippocampal neurons

We next investigated the functional role of AKAP-mediated PKA compartmentalization in axon development. PKA plays a well-known role in promoting axonogenesis[28, 31, 94] and AKAP anchoring promotes the specificity of PKA signaling in part by localizing PKA near its downstream substrates Thus, we hypothesized that the AKAP anchoring of PKA would have a pro-axonogenic effect in developing HNs. To test this hypothesis, we treated newly plated HNs (16-20 h *in vitro*) with st-Ht31 to disrupt

AKAP-PKA anchoring and then performed immunostaining to detect Tau1, an axon-specific marker, as well as MAP2, a dendrite specific marker, after 72 h *in vitro* (DIV3) (Fig. 2.10). Axon growth was assessed by measuring the length of the longest Tau1-positive neurite extending from the soma of each cell. Based on the reported positive role of PKA in axon development, we expected the disruption of PKA anchoring to have a detrimental effect on axon outgrowth. Surprisingly, however, we observed significantly longer neurites in DIV3 HNs treated with st-Ht31 compared with control HNs treated with DMSO, and treatment with a scrambled peptide (st-Ht31p) had no effect on neurite length (Fig. 2.10b-d,i). Furthermore, PKA inhibition by either H89, KT5720, or Rp-8-Br-cAMPShad no effect on axon elongation (Fig. 2.10e-g,i). The enhancement of neurite outgrowth with st-Ht31 was also dose dependent, with increasing doses of st-Ht31 progressively increasing neurite length (Fig. 2.11).

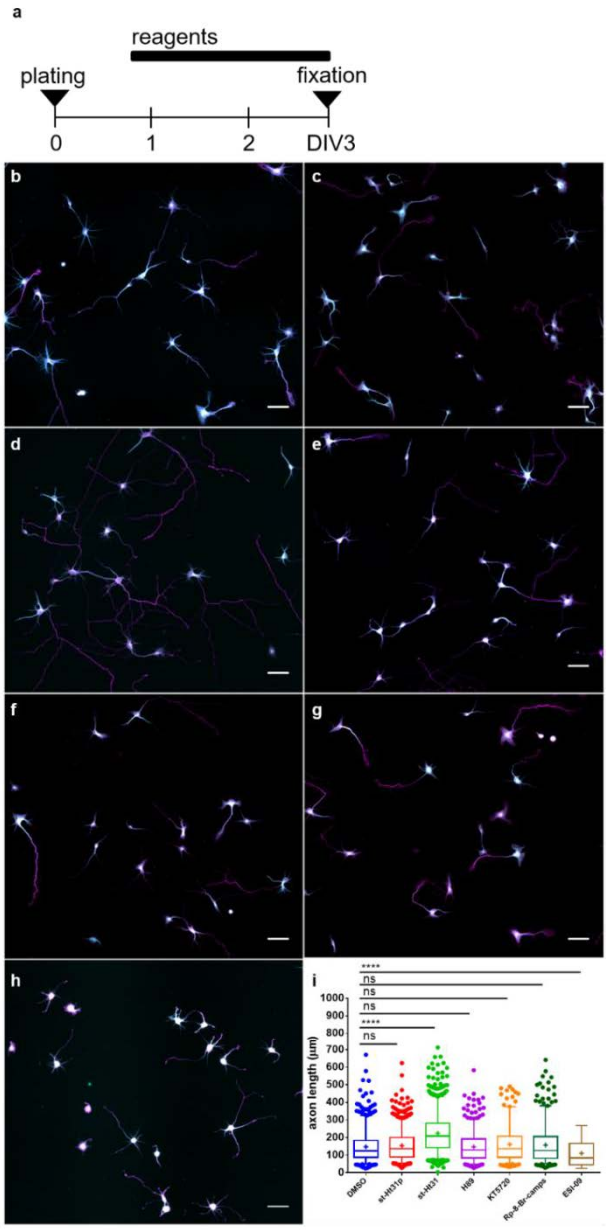

Figure 2.10. Disruption of AKAP anchoring increases axon outgrowth in undifferentiated HNs.

(a) Schematic of experimental design: newly plated cells (DIV0) were treated with various compounds after ~16 h in vitro. HNs were then fixed at DIV3 for immunostaining. (b-h) Representative images of DIV3 HNs immunolabeled with Tau1 (magenta) and MAP2 (cyan) and treated for ~48 h with (b) DMSO, (c) 20 µM st-Ht31p, (d) 20 µM st-Ht31, (e) 10 µM H89, (f) 400 nM KT5720, (g) 200 µM Rp-8-Br-camps, and (h) 15 µM ESI-09. Scale bar, 50 µm. ****p<0.0001 according to two-tailed Student's t-test. (i) Box-and-whisker plots summarizing the axon length following the indicated treatments. The box shows the median, 25% quartile, and 75% quartile, and the whiskers designate the 5th and 95th percentiles; a "+" indicates the mean. Each bar contains pooled data from at least 170 cells and three preparations.

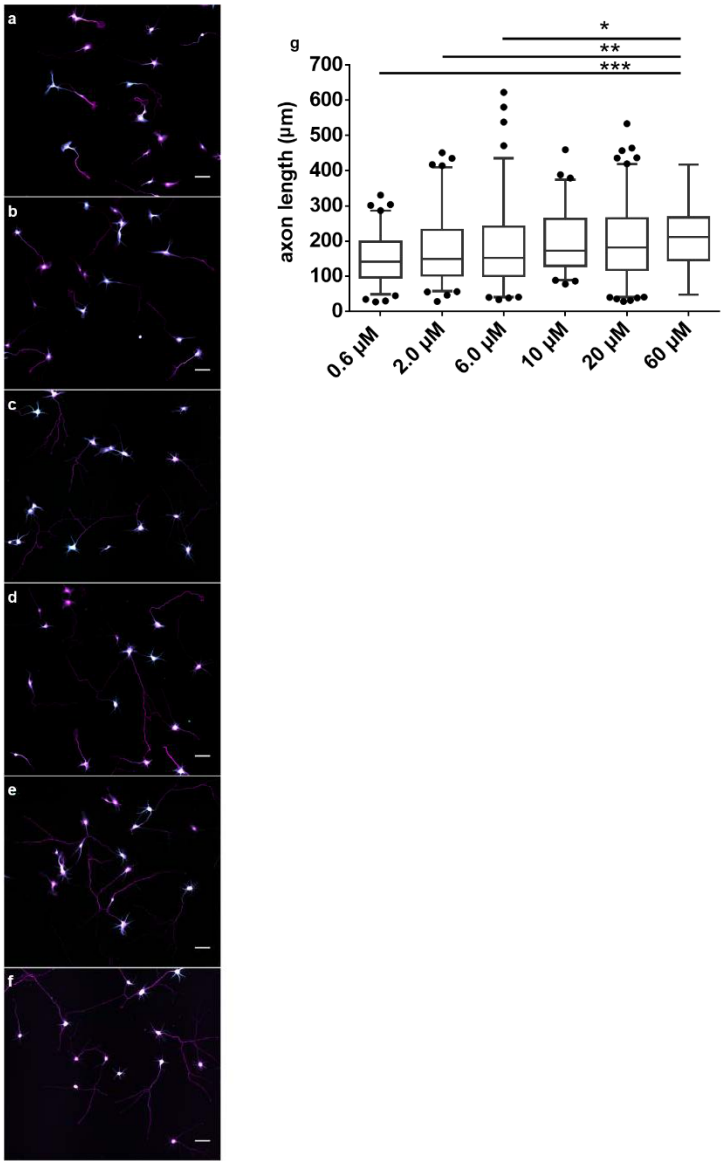

Figure 2.11. Disruption of AKAP anchoring increases axon outgrowth in undifferentiated HNs.

(a-e) Representative montage of DIV3 HNs immunostained with Tau1 (magenta) and MAP2 (cyan) and treated with increasing doses of st-Ht31 for 48 h: (a) 0.6 µM, (b) 2.0 µM, (c) 6.0 µM, (d) 10.0 µM, (e) 20 µM, or (f) 60 µM. Scale bar, 50 µm. (g) Average neurite length for cells treated with increasing doses of st-Ht31 for 48 h Data in f shown as box-and-whisker plots from >60 cells from one culture. The box shows the median, 25% quartile, and 75% quartile, and the whiskers designating the 5th and 95th percentiles; *p<0.05, **p<0.01, ***p<0.001, ****p<0.0001 according to two-tailed Student's t-test.

Disrupting AKAP-PKA anchoring enhances the cAMP gradient in DIV3 hippocampal neurons

Combined with our previous observation that axonal PKA activity is supported by AKAP anchoring, the fact that disrupting the PKA-AKAP microdomain enhances axon elongation suggests that AKAP-anchored PKA acts to limit axon elongation during early developmental timepoints. These results are surprising because cAMP and PKA are thought to promote axon polarization and elongation and because AKAP anchoring helps support PKA function. We therefore investigated whether the st-Ht31 effect on axon length was related to the observed spatial differences in cAMP signaling. To this end, we treated ICUE3-expressing DIV3 HNs with st-Ht31 followed by Fsk. The addition of st-Ht31 yielded small increases in cAMP levels, with a slightly larger increase in the axon, and subsequent stimulation with Fsk produced a steep, axon-directed cAMP gradient (Fig. 2.12a-c). Comparing the Fsk-induced ICUE3 response in DIV3 HNs with and without st-Ht31 pretreatment revealed a significant difference in cAMP levels in the distal axon (Fig. 2.12d). In fact, this gradient was very similar to that observed in DIV5 HNs treated with Fsk alone (Fig. 2.1 and Fig. 2.12e). These data imply that delocalizing PKA from the AKAP microdomain actually enhances cAMP accumulation in DIV3 HNs, especially in distal regions of the axon. Hence, younger neurons with delocalized PKA exhibited cAMP gradients typically seen only in older neurons.

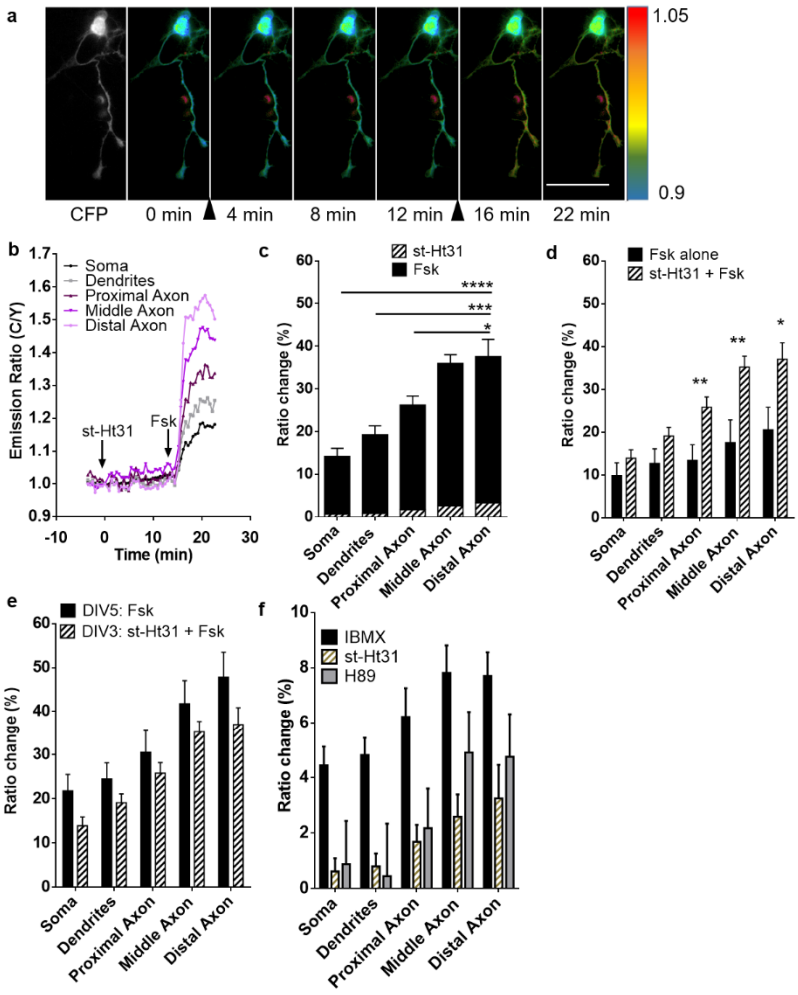

Figure 2.12. Acute disruption of AKAP anchoring increases cAMP and reveals an axon-directed cAMP gradient in developing HNs.
(a) Pseudocolored images showing the response of ICUE3 to 10 µM st-Ht31 followed by 50 µM Fsk in a DIV3 HN. Arrowheads indicate the time of drug addition. Warmer colors correspond to higher C/Y emission ratios. Scale bar, 50 µm (b) Representative time-course of the ICUE3 emission ratio changes in the different regions of the DIV3 HN shown in a. (c) Stacked comparison of ICUE3 responses induced by st-Ht31 (striped bars) and Fsk addition (black bars) (n=11 from three preparations; *p=0.0231, ***p=0.0006, ****p<0.0001 according to two-tailed Student's t-test). (d) Comparison of ICUE3 responses in each region of DIV3 HNs treated with Fsk in the presence (black bars, n=8 from three preparations) and absence (striped bars, n=11 from three preparations) of st-Ht31 pretreatment, Distal Axon *p=0.020, Middle Axon **p=0.0044, Proximal Axon **p=0.0084 according to two-tailed Student's t-test (e) Comparison of Fsk-induced ICUE3 response in each region in DIV5 HNs (n=12, data reproduced from Fig. 2.1d) with that of DIV3 HNs pretreated with 10 µM st-Ht31 (n=11). (f) Comparison of IBMX- (n=18, from three preparations), st-Ht31- (n=11 from three preparations), and H89-induced (n=9, from three preparations) ICUE3 responses in DIV3 HNs. Bars in c-f represent mean±S.E.M.

Model of developmentally regulated cAMP signaling in hippocampal neurons

Our results suggest that PKA acts as a local negative-feedback regulator of cAMP signaling within an AKAP microdomain in developing neurons. Indeed, we found that directly inhibiting PKA also produced a trend of an axon-directed cAMP gradient in DIV3 HNs (Fig. 2.13), confirming that PKA activity has a negative effect on cAMP levels in these cells.

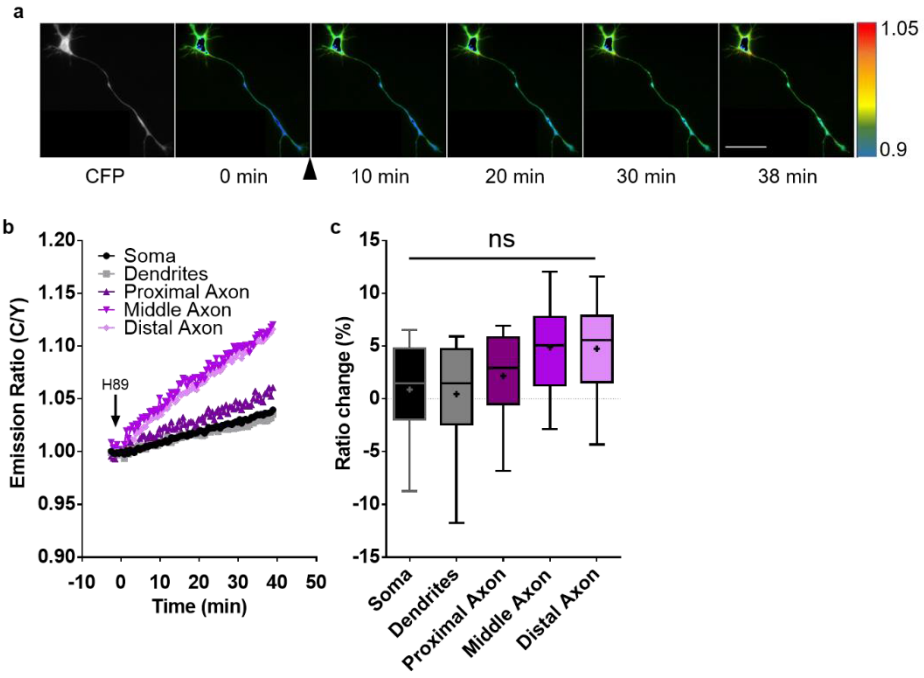

Figure 2.13. H89 increases cAMP in the distal axon of DIV3 HNs.
(a) Pseudocolored image showing the responses of ICUE3 in a DIV3 HN to 10 µM H89. Arrowhead indicates the time of drug addition. Warmer colors correspond to higher C/Y emission ratios. Scale bar, 50 µm. (b) Representative time-course of the ICUE3 response in the cell from a. (c) Average response of DIV3 HNs expressing ICUE3 treated with 10 µM H89 (n=9 from three preparations). Data in c shown as box-and-whisker plots, with the box showing the median, 25% quartile, and 75% quartile, and the whiskers designating the 5th and 95th percentiles; a "+" indicates the mean; ns, not significant according to two-tailed Student's t-test.

Two possible mechanisms could explain this effect: the PKA-mediated inhibition of ACs such as AC V and VI[142, 143] or the PKA-mediated activation of PDEs such as PDE4[144].

However, the fact that PDE inhibition revealed elevated axonal cAMP levels in DIV3 HNs (Fig. 2.2) is inconsistent with a model of local AC inhibition, which would instead predict either the absence of a gradient or lower axonal cAMP levels following PDE inhibition. Furthermore, comparing the responses of ICUE3-expressing DIV3 HNs to IBMX, H89, and st-Ht31 indicated that the cAMP response to PDE inhibition was qualitatively similar to the axon-directed cAMP gradient produced by either inhibiting or delocalizing PKA (Fig. 2.12f). The cAMP gradient was steeper following both AKAP disruption and PKA inhibition compared with PDE inhibition (Figure 2.14), which is consistent with the targeted disruption of local PKA-PDE feedback versus more general inhibition.

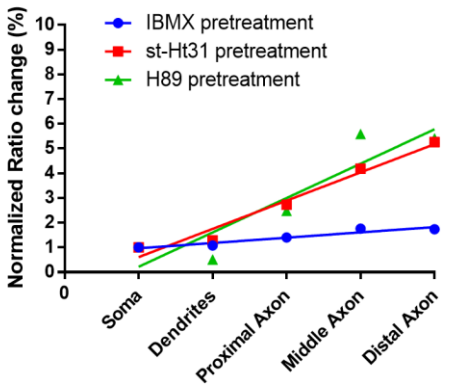

Figure 2.14. Comparison of cAMP gradients generated by IBMX, st-Ht31, and H89 treatment in DIV3 HNs.
Average ICUE3 responses of DIV3 HNs to 100 µM IBMX, 10 µM st-Ht31, or 10 µM H89 in each region from Fig. 2.12f. Lines indicate the results from a linear regression analysis. For each treatment, the average responses in each region were normalized to the average response in the soma.

Thus, our data support a model (Fig. 2.15) in which PKA and PDE form an AKAP-anchored signaling microdomain in the developing axon of immature (e.g., DIV3) HNs. Basally active PKA phosphorylates and activates co-anchored PDE that locally degrades cAMP, thereby forming a negative feedback loop that dampens axonal cAMP signaling

and limits axon elongation. Disrupting this AKAP-anchored feedback circuit leads younger cells to mimic more mature (e.g., DIV5) HNs, in which the feedback circuit is absent, by prematurely forming an axon-directed cAMP gradient that drives axon elongation.

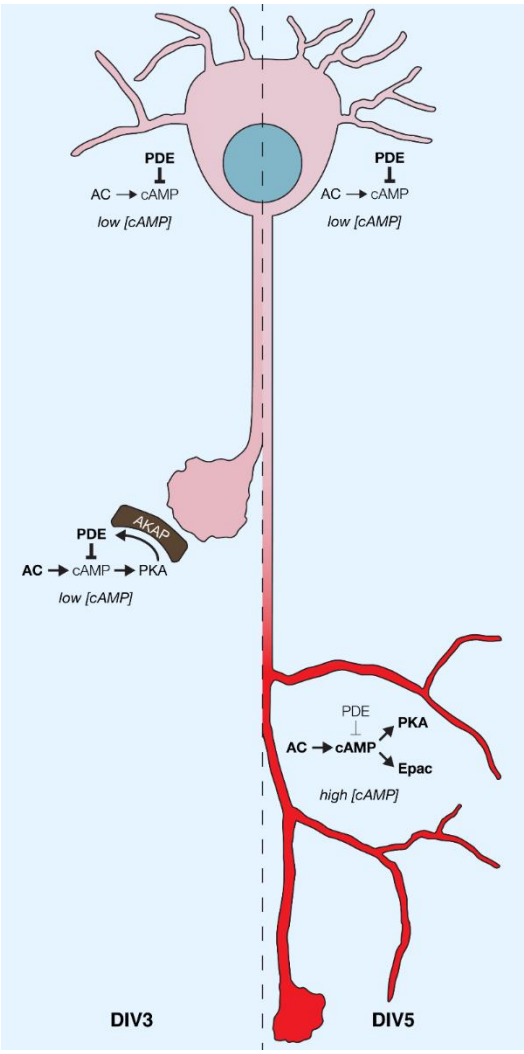

Figure 2.15. Model of compartmentalized cAMP signaling in developing HNs.
At early stages of growth (DIV3, left), PDEs have high activity, and the neuron exhibits a shallow gradient of cAMP from the distal axon to the somatodendritic region. The PDE activity in the soma of a DIV3 cell keeps [cAMP] low, while AKAP-mediated PKA-to-PDE feedback dampens [cAMP] in the distal axon, thereby restraining axon outgrowth. At later stages of growth (DIV5, right), high PDE activity keeps [cAMP] low in the soma, while the absence of PKA-mediated negative feedback in the axon enables the formation of a steep [cAMP] gradient, with the highest [cAMP] in the distal axon, leading to the activation of downstream effectors such as Epac and PKA, which regulate axon growth. Red coloring indicates cAMP levels.

Discussion

cAMP/PKA signaling is essential to neuronal development and growth. Some of the earliest studies on the role of cAMP in axon biology focused on axon guidance, indicating that local sources of cAMP can act as attractants for growth cones[136, 145]. Recent work on axon formation also showed that neurons prefer to grow axons on cAMP-laden stripes and are repelled by stripes containing inhibitory cAMP analogs or PKA inhibitors[70], while individual neurites exposed to a local source of cAMP tended to turn into axons rather than dendrites. Our investigation revealed growth stage-specific cAMP gradients and suggests that a steeper cAMP gradient is correlated with enhanced axon elongation. These findings are in keeping with past observations of spatially regulated cAMP signaling during axon development, such as local elevations in cAMP within the growth cones of *Xenopus* spinal neurons[146]. Although local signaling events can often be driven by the spatial distribution of signaling factors such as ACs[128], our analyses did not reveal any clear spatial differences in the distribution of AC or PDEs in either DIV3 or DIV5 HNs that could give rise to the signaling patterns observed in the present study (Fig. 2.16a-c).

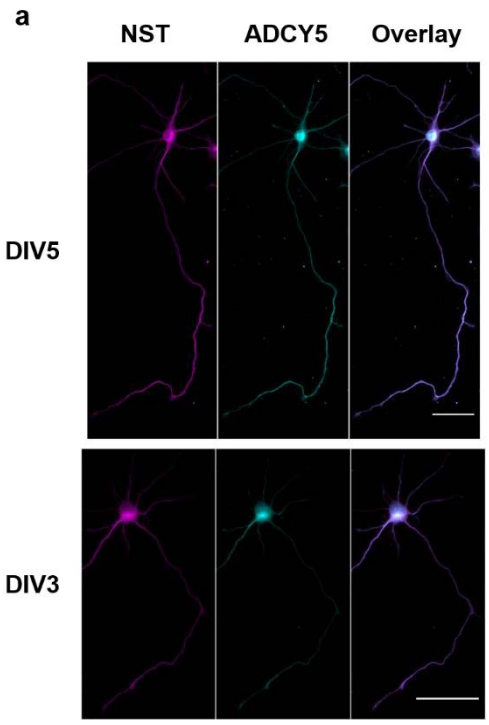

Figure 2.16. Expression of cAMP signaling enzymes in hippocampal neurons.
(a) Immunostaining for ADCY5 and NST in DIV5 (top) and DIV3 (bottom) HNs. Left, NST (general morphology marker, magenta); middle, ADCY5 (cyan); right, overlay. Scale bar, 50 μm.

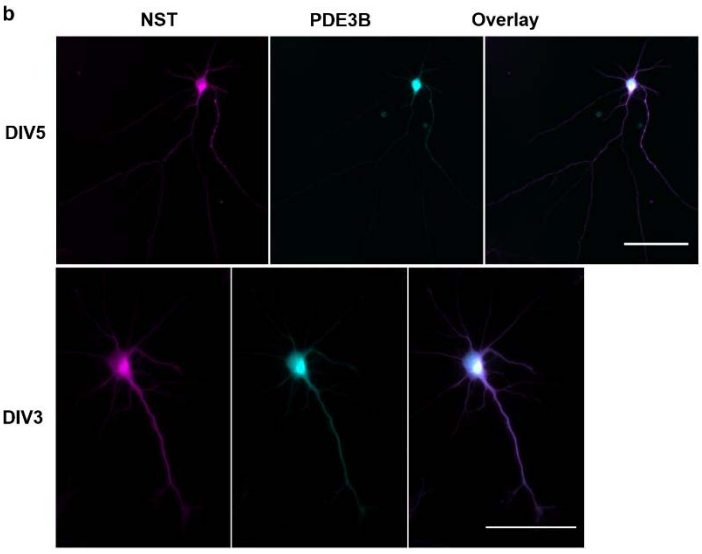

Figure 2.16. Expression of cAMP signaling enzymes in hippocampal neurons.
(b) Immunostaining for PDE3B and NST in DIV5 (top) and DIV3 (bottom) HNs. Left, NST (general morphology marker, magenta); middle, PDE3B (cyan); right, overlay. Scale bar, 50 μm.

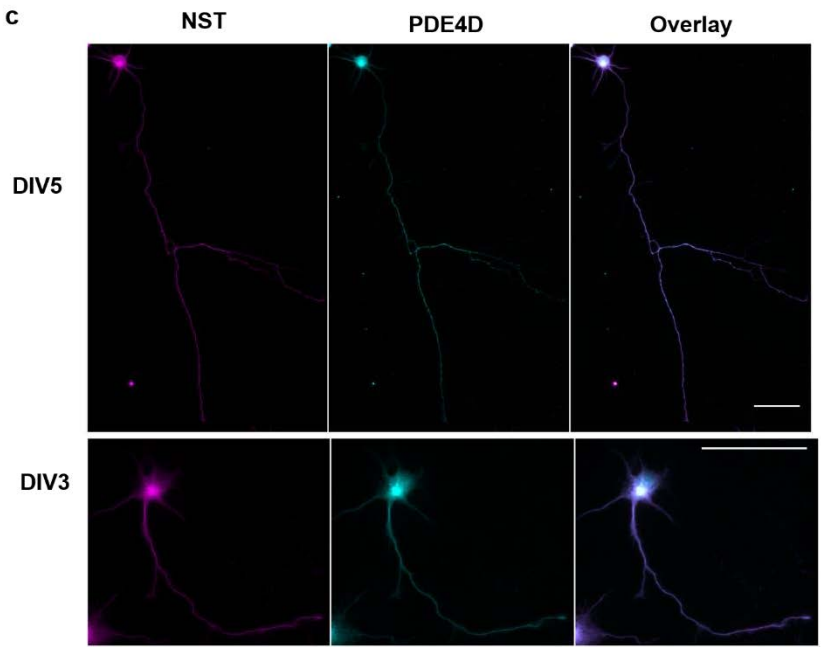

Figure 2.16. Expression of cAMP signaling enzymes in hippocampal neurons.
(c) Immunostaining for PDE4D and NST in DIV5 (top) and DIV3 (bottom) HNs. Left, NST (general morphology marker, magenta); middle, PDE4D (cyan); right, overlay. Scale bar, 50 μm.

The geometry of neuronal subcompartments has also been shown to play a role in determining local cAMP concentrations, which can help explain the generation of gradients in thin processes. Modeling work in recent years has revealed that molecules such as cAMP can become concentrated in compartments with high surface-to-volume ratios, i.e., thinner processes, as the rate of production generally exceeds that of diffusion in these thin compartments[147]. Furthermore, concentration is also positively correlated with increasing distance from the soma[147]. In fact, dendritic geometry has been shown to counteract the effects of increasing distance from the soma to enhance cAMP-dependent nuclear signaling[148]. In our study, we found no obvious correlation between distance from the soma and axonal diameter in ICUE3-expressing DIV5 neurons (Fig 2.17), suggesting that the

gradient of cAMP accumulation that we observed in these cells is not significantly influenced by axonal geometry.

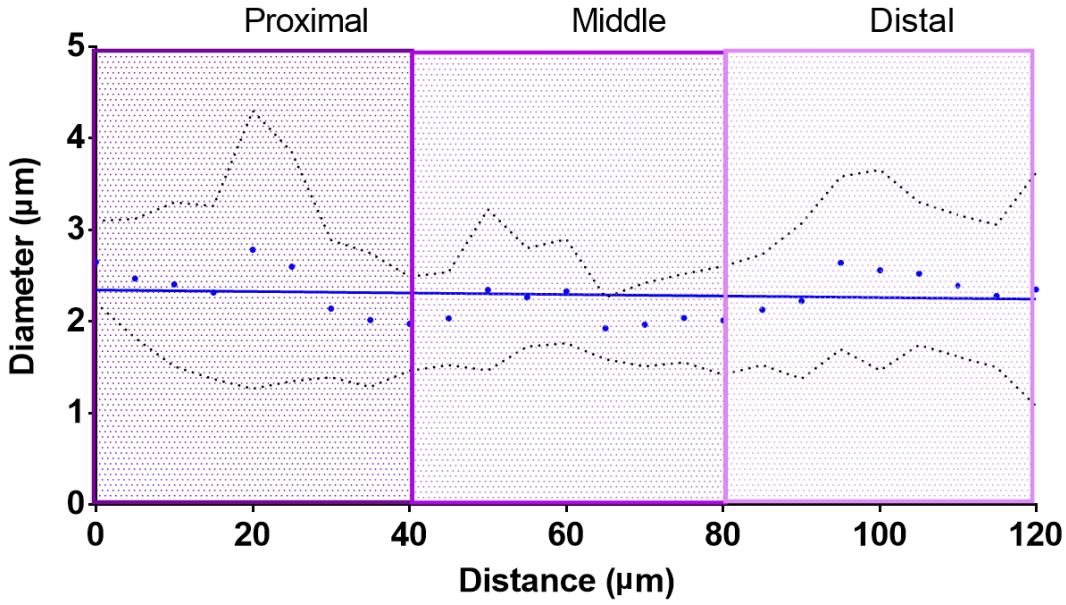

Figure 2.17. Comparison of the diameter to distance measurements of DIV5 HNs expressing ICUE3.
The proximal, middle, and distal regions of the cells show no significant differences in diameter according to two-way ANOVA. Linear regression analysis also shows that the slope does not significantly differ from zero.

Our findings also complicate the role of PKA in axonogenesis. Previously, PKA-dependent phosphorylation of LKB1 was shown to promote axon formation both *in vitro* and *in vivo* through the activation of SAD kinases[31, 93, 94], which show elevated activity in the distal axon[149]. In the present study, we observed that disrupting PKA compartmentalization in DIV3 HNs not only led to higher axonal cAMP but also increased axon elongation. On the other hand, AKAP disruption had no effect on axon length in DIV5 HNs, despite causing an apparent increase in somatodendritic cAMP accumulation (Fig. 2.18 and 2.19).

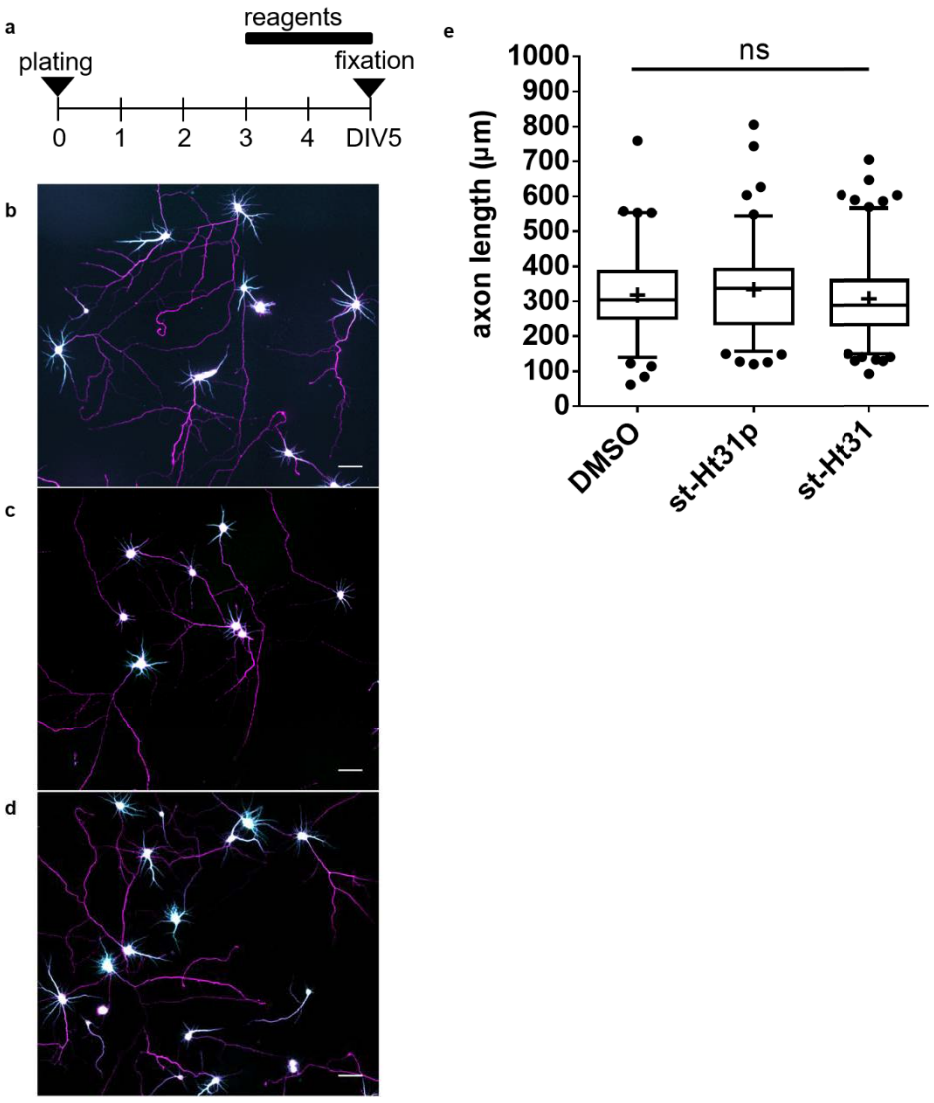

Figure 2.18. Disruption of AKAP anchoring does not increase neurite outgrowth in differentiated HNs. (a) Schematic of experimental design for i: DIV0 and treated after ~72 hours *in vitro*. HNs were fixed at DIV5 for immunostaining. Montage of representative images from the three treatments: (b) DMSO, (c) st-Ht31p, and (d) st-Ht31. Scale bar, 50 µm. (e) Axon lengths for each treatment are shown as box-and-whisker plots, with the box showing the median, 25% quartile, and 75% quartile, and the whiskers designating the 5th and 95th percentiles; a "+" indicates the mean. Data are pooled from at least three preparations; ns, not significant according to one-way ANOVA.

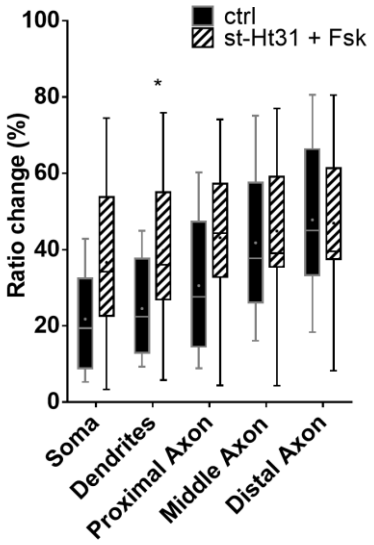

Figure 2.19. st-Ht31 increases somatodendritic cAMP in DIV5 HNs.
Average response of DIV5 HNs expressing ICUE3 treated with 50 µM Fsk alone (black bars, n=12 from three preparations) or 10 µM st-Ht31+50 µM Fsk (striped bars, n=9 from three preparations). Data are shown as box-and-whisker plots, with the box showing the median, 25% quartile, and 75% quartile, and the whiskers designating the 5th and 95th percentiles; a "+" indicates the mean; *$p<0.05$, according to two-tailed Student's t-test.

These results suggest a specific role for axonal PKA activity in blocking axon elongation in immature HNs, which is a departure from the established, exclusively positive role of PKA in axon development. It is possible that axonal PKA in fact plays a dual role as both a positive and negative regulator of axon elongation through LKB1 and cAMP, respectively. This complexity may account for the lack of observed effects on axon growth when PKA activity was inhibited directly (Fig. 2.10), as both the negative and positive PKA pathways would be blocked. Furthermore, recent work has shown that Epac is also necessary for axon extension[150,47], and the increased cAMP levels caused by delocalizing PKA in developing HNs likely also enhance axon outgrowth through the activation of Epac (Fig. 2.15). Indeed, PKA and Epac1 were both clearly expressed in these cells (Fig. 2.20a-d), and experiments performed using ESI-09, an Epac1-specific inhibitor,

confirm the critical role of Epac signaling in axon outgrowth in developing hippocampal neurons (Fig. 2.10h, i).

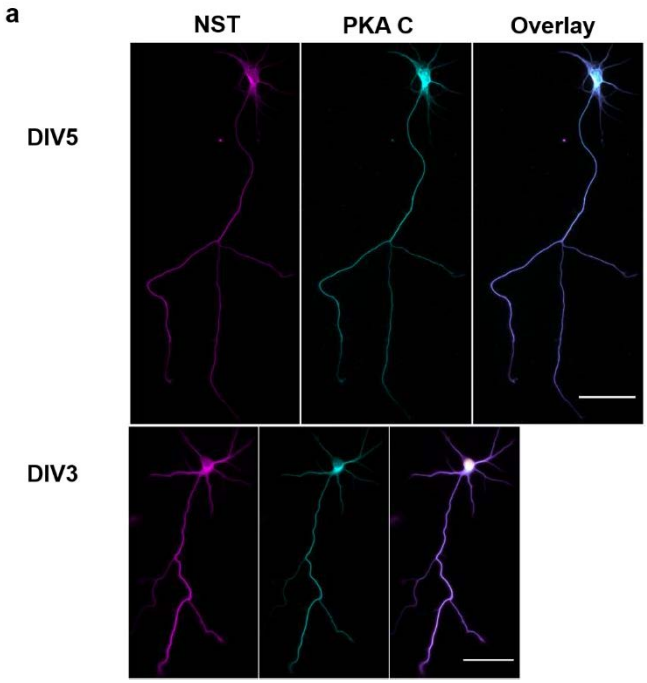

Figure 2.20. Expression of cAMP effectors in hippocampal neurons.
(a) Immunostaining for PKA C and NST in DIV5 (top) and DIV3 (bottom) HNs. Left, NST (general morphology marker, magenta); middle, PKA C (cyan); right, overlay. Scale bar, 50 µm.

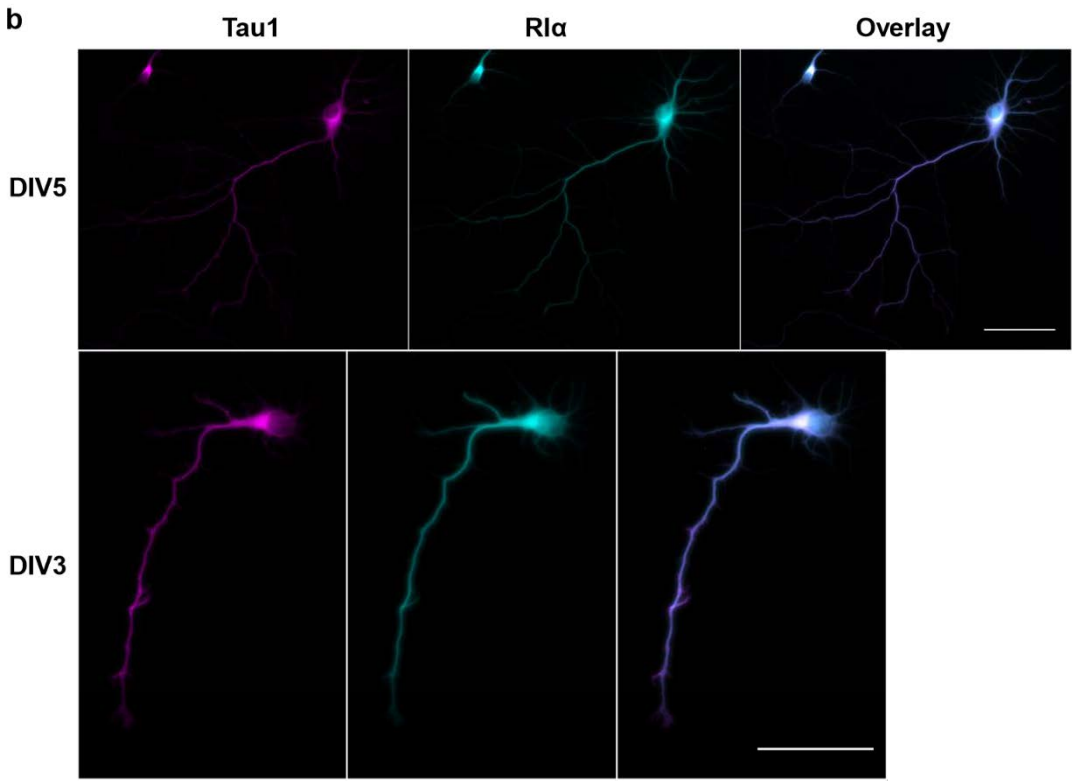

Figure 2.20. Expression of cAMP effectors in hippocampal neurons.
(b) Immunostaining for RIα and Tau1 in DIV5 (top) and DIV3 (bottom) HNs. Left, Tau1 (axon marker, magenta); middle, RIα (cyan); right, overlay. Scale bar, 50 μm.

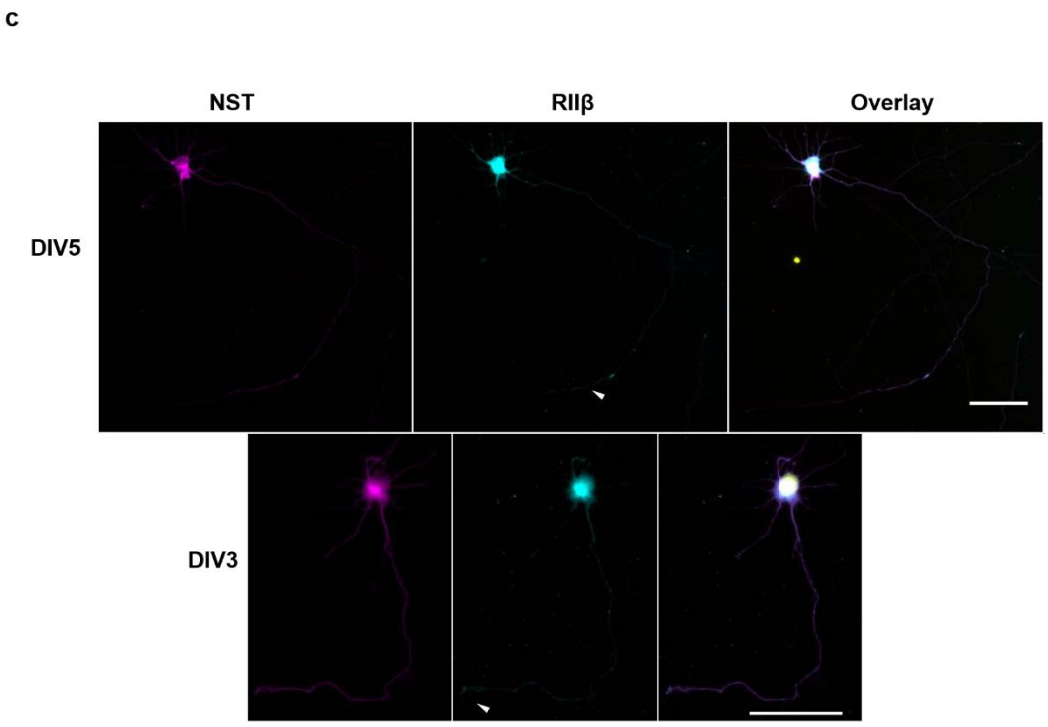

Figure 2.20. Expression of cAMP effectors in hippocampal neurons.
(c) Immunostaining for RIIβ and NST in DIV5 (top) and DIV3 (bottom) HNs. Left, NST (general morphology marker, magenta); middle, RIIβ (cyan); right, overlay. Scale bar, 50 μm.

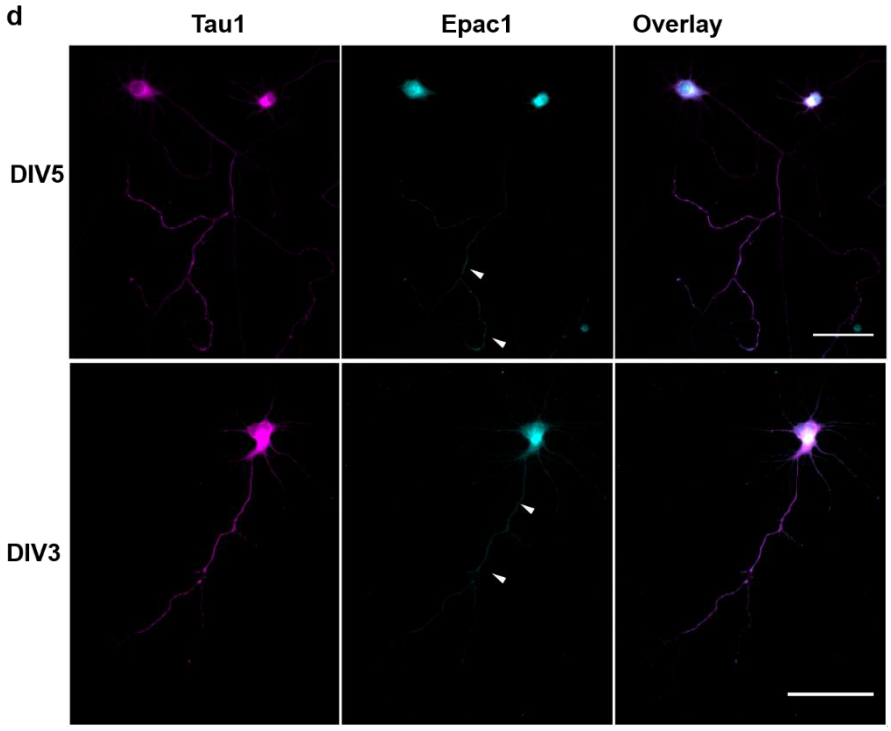

Figure 2.20. Expression of cAMP effectors in hippocampal neurons.
(d) Immunostaining for Epac1 and Tau1 in DIV5 (top) and DIV3 (bottom) HNs. Left, Tau1 (axon marker, magenta); middle, Epac1 (cyan); right, overlay. Scale bar, 50 μm.

The effects of delocalizing PKA using st-Ht31 specifically highlight the importance of AKAP-compartmentalized PKA activity in developing HNs, and are consistent with previous findings of PKA compartmentalization within specific neuronal structures[151]. AKAPs often act to facilitate PKA signaling by colocalizing PKA with downstream targets[129 32] and by coupling PKA activity to specific upstream signals[152]. However, AKAP anchoring can also play a major role in shaping the dynamics of both PKA and cAMP signaling by localizing PKA with regulatory proteins such as PDEs[153,154], and our results indicate that this type of "regulatory" AKAP microdomain is central to directing the course of axon elongation in developing HNs. For instance, AKAP12/Gravin, which binds both PKA and PDE4D, can be found throughout mouse HNs[155] and in punctate structures in NT2-N human model neurons[156]. Another PKA/PDE4D3 scaffold, AKAP9 can assemble signaling platforms on centrosomes, and its splice variant Yotiao has also been shown to bind NMDA subunits[157], although Yotiao has not been shown to bind to PDEs. Interestingly, WAVE-1 knockout mice exhibit clear changes in brain structure and behavioral deficits[158], and knocking down WAVE-1 in HNs reduces axon length[159]; however, WAVE-1 has also not been demonstrated to bind PDEs. Lastly, mAKAP, which binds Epac1, PKA, PDE4D3 and ACs, has been found to promote axon elongation and survival in injured retinal ganglion cells, but not during normal growth[160]. Nevertheless, the mAKAP signalosome may also play a role in coordinating cAMP signaling in different neuronal cell types, including HNs. However, while we were able to detect the expression of these and other AKAPs in DIV5 and DIV3 HNs, our initial analyses did not uncover

any obvious differences in expression or localization that might explain the signaling differences between these developmental stages (Fig. 2.21a-e). It therefore remains to be seen which specific AKAP is responsible for the localized effects observed in our study.

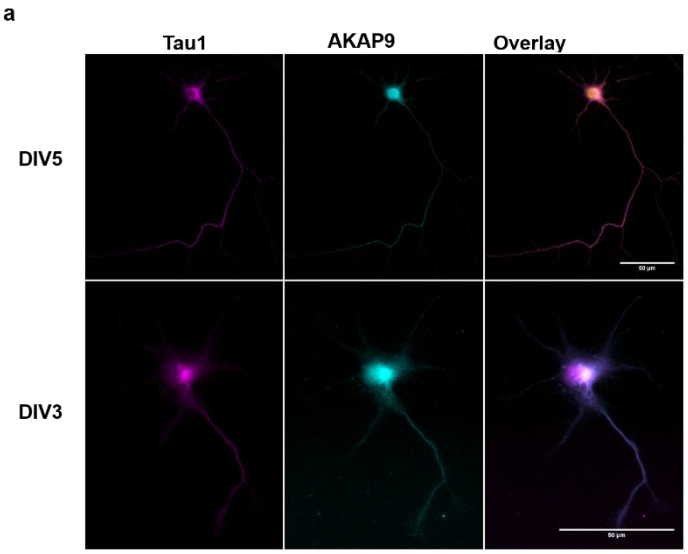

Figure 2.21. AKAP expression in hippocampal neurons.
(a) Immunostaining for AKAP9 and Tau1 in DIV5 (top) and DIV3 (bottom) HNs. Left, Tau1 (axon marker, magenta); middle, AKAP9 (cyan); right, overlay. Scale bar, 50 μm.

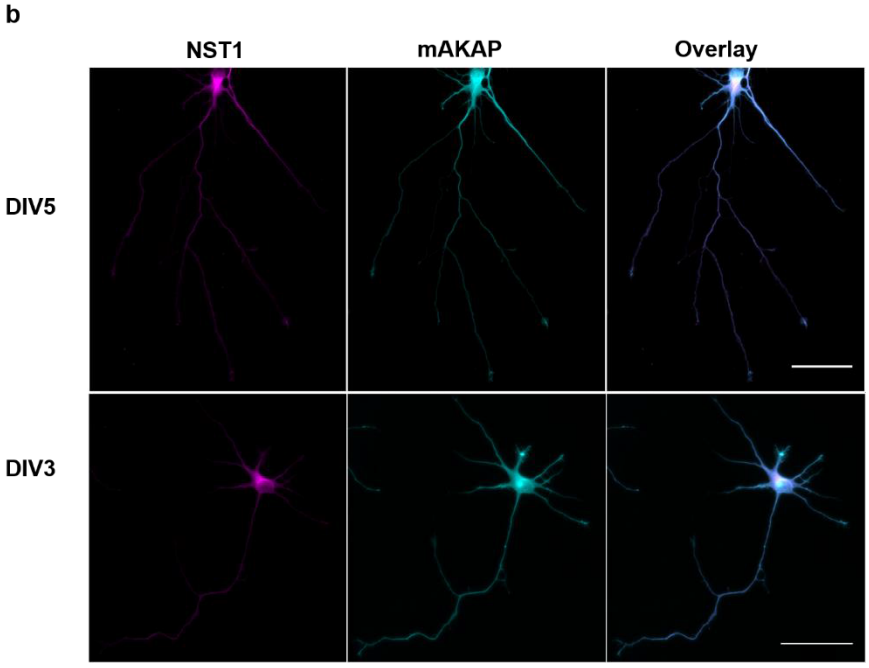

Figure 2.21. AKAP expression in hippocampal neurons.
(b) Immunostaining for mAKAP and NST in DIV5 (top) and DIV3 (bottom) HNs. Left, NST (general morphology marker, magenta); middle, mAKAP (cyan); right, overlay. Scale bar, 50 µm.

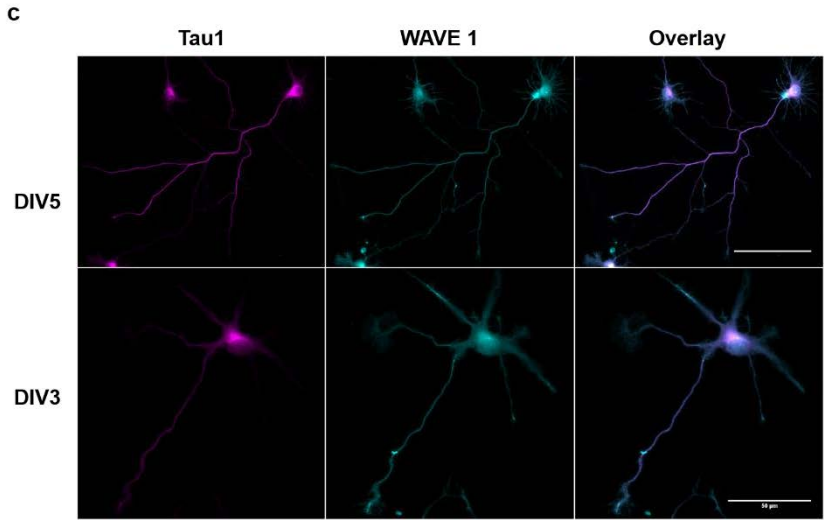

Figure 2.21. AKAP expression in hippocampal neurons.
(c) Immunostaining for WAVE-1 and Tau1 in DIV5 (top) and DIV3 (bottom) HNs. Left, Tau1 (general morphology marker, magenta); middle, WAVE-1 (cyan); right, overlay. Scale bar, 50 µm.

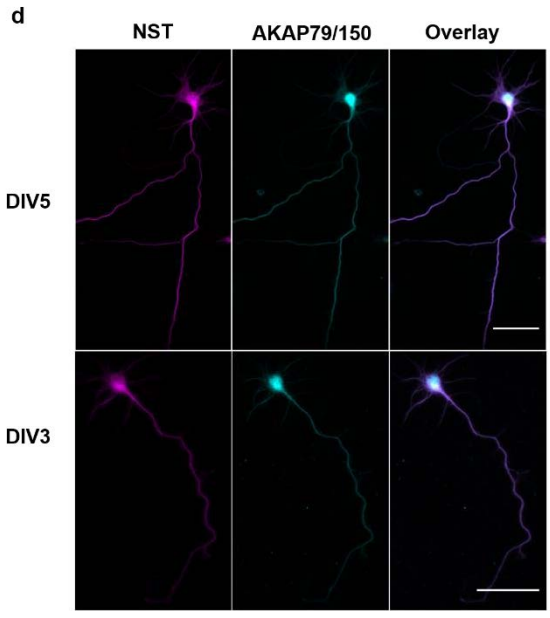

Figure 2.21. AKAP expression in hippocampal neurons.

(d) Immunostaining for AKAP79/150 and NST in DIV5 (top) and DIV3 (bottom) HNs. Left, NST (general morphology marker, magenta); middle, AKAP79/150 (cyan); right, overlay. Scale bar, 50 μm.

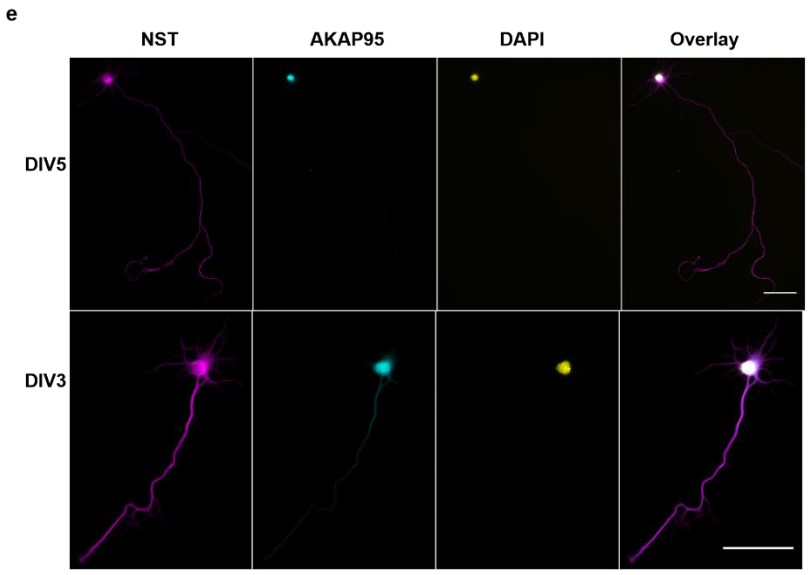

Figure 2.21. AKAP expression in hippocampal neurons.
(e) Immunostaining for AKAP95 and NST in DIV5 (top) and DIV3 (bottom) HNs. First panel, NST (general morphology marker, magenta); second panel, AKAP9 (cyan); third panel, DAPI (nucleus, yellow); last panel, overlay. Scale bar, 50 μm.

Our work using cultured rat HNs as a model system has established the functional relevance of AKAP-mediated cAMP/PKA compartmentalization in neuronal differentiation and development. Future studies of the various AKAPs will help drive our understanding of cAMP signaling regulation in neuronal development.

Significance

PKA has long been suggested to play a positive role in axon development. Here, we add a complex element of negative feedback inhibition to axonal PKA activity that dampens axon growth by suppressing local cAMP levels in immature hippocampal neurons. Our study thus establishes a completely new role for PKA as a negative regulator

of axonal development and demonstrates that PKA plays a much more complex role in neuronal development than was previously known. Precise spatial control can therefore allow a signaling molecule to play seemingly opposite functional roles in the same cell.

Materials and Methods

Reagents

Papain Dissociation System was purchased from Worthington (Lakewood, NJ). Neurobasal was purchased from Invitrogen (21103-049). B27 was purchased from Gibco (17504044). Pen-Strep was purchased from Thermo-Fisher (15140122). GlutaMax was purchased from Gibco (35050061). Poly-D-Lysine (PDL) was purchased from Sigma (P6407). Lipofectamine LTX was purchased from Invitrogen (15338030). Forskolin (Fsk, 344270) and 3-isobutyl-1-methylxanthine (IBMX, 410957) were purchased from Calbiochem and used at a final concentration of 500 nM or 50 μM (Fsk) and 100 μM (IBMX)[161 162, 163]. H89 was purchased from Sigma (B1427) and used at a concentration of 10 μM[81, 164]. KT5720 (K7361), Rp-8-Br-cAMPS(B1381), and ESI-09 (SML0814) were purchased from Sigma. St-Ht31 (V8211) and st-Ht31p (V8221) were purchased from Promega. Paraformaldehyde solution (16%) was purchased from Electron Microscopy Sciences (15700, 4% final dilution). Rabbit anti-Tau1 (ab64193, 1:100 dilution) and mouse anti-NST (ab14545, 1:1000 dilution) were purchased from Abcam. Mouse-anti MAP2 (1:500, MAB3418) was purchased from Millipore. Rabbit anti-AKAP79 (1:100, sc10764), rabbit anti-AKAP95 (1:100, sc10766), rabbit anti-PDE3B (1:100, sc-20793), rabbit anti-PDE4D (1:100, sc-25814) and mouse anti-Epac (1:100, sc-28366) were purchased from Santa Cruz Biotechnology. Mouse anti-AKAP9 (1:100, NB100-74351)

was purchased from Novus Biological. Mouse anti-WAVE 1 (1:100, ab106516) and rabbit anti-ADCY5/6 (1:100, ab196748) were purchased from Abcam. Rabbit anti-PKA (Cα) (1:100, ab4782) was purchased from Cell Signaling Technologies. Mouse anti-PKA RIIβ (1:100, 610625) and mouse anti-PKA RIα (1:100, 610165) were purchased from BD Biosciences. Goat anti-mouse Alexa-Fluor 488 (A-11001, 1:1000 dilution) and goat anti-rabbit Alex-Fluor 568 (A-11036, 1:1000 dilution) were purchased from ThermoFisher Scientific. Prolong Gold antifade mounting reagent was purchased from Life Technologies (P36930).

Cell Culture

Primary rat hippocampal neurons - Hippocampi were dissected from E18 Sprague Dawley rat (*Rattus norvegicus*) pups (Harlan, Indianapolis, IN) in ice-cold Hank's Balanced Salt Solution (HBSS) supplemented with 20 mM HEPES, pH 7.4, 5 mM D-glucose, 0.23 mM sodium pyruvate, and 0.5% pen-strep and were dissociated using the Papain Dissociation System according the manufacturer's instructions. Dissociated HNs were re-suspended in Neurobasal medium supplemented with 2.0% B27 supplement, 0.5% pen-strep and 2.0 mM Glutamax. Each separate preparation contained pooled tissues from a single litter (~10-12 pups), with one preparation performed per week. Approximately $1.0x10^5$ cells were plated onto 35-mm nitric acid-treated glass-bottom imaging dishes coated with 150 μg/mL PDL. Cells were given a 50% media change every three days to restore glucose levels to 3.0 mM as previously described[165]. Cells were cultured at 37°C in a humidified incubator at 5% CO_2. At DIV2 or DIV4, cells were transfected with Lipofectamine LTX according to manufacturer's instructions and imaged after 24 h.

Live-cell Imaging

Cells were washed twice with HBSS prior to imaging and maintained in the dark at 37°C. DMSO, Fsk, IBMX, H89 and st-Ht31 were added as indicated. Dual emission ratio imaging was performed on a Zeiss AxioObserver Z1 microscope (Carl Zeiss, Thornwood, NY) equipped with a 40x/1.3 NA objective and a Photometrics Evolve 512 EMCCD (Photometrics, Tucson, AZ) controlled by METAFLUOR 7.7 software (Molecular Devices, Sunnyvale, CA). Images were acquired using a 420DF20 excitation filter, a 450DRLP dichroic mirror, and two emission filters (475DF40 for CFP and 535DF25 for YFP) alternated by a Lambda 10-2 filter-changer (Sutter Instruments, Novato, CA). Exposure times ranged between 50 and 500 ms, and images were acquired every 30 s. Images were analyzed in METAFLUOR 7.7 by defining a single region of interest (ROI) for the dendrites and for the soma, with the axon separated into three equal-length ROIs of ~40-50 µm (Fig. 2.22). The proximal axon region is defined as the length of axon extending directly from the soma, and the middle and distal axon regions correspond the next two equal-length segments after the proximal segment. The same axon segments were analyzed for both DIV3 and DIV5 HNs.

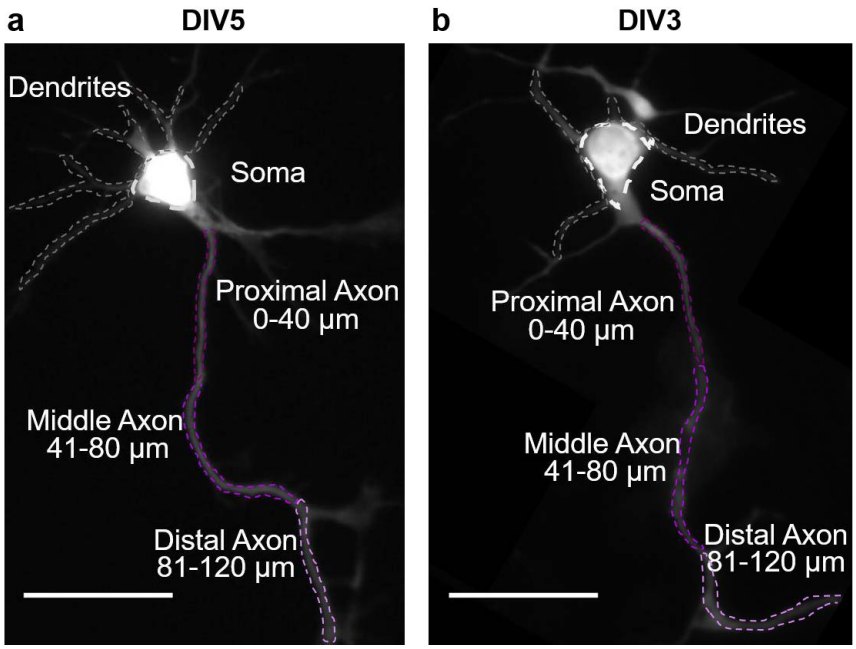

Figure 2.22. Regions of interest for analysis of FRET data in HNs.
Examples of a (a) DIV5 and (b) DIV3 HN illustrating the regions of interest examined in this study: Soma (white), Dendrites (gray), Proximal Axon (dark purple), Middle Axon (purple), Distal Axon (pink). Scale bar, 40 µm.

Only one cell could be imaged per dish, and data were averaged across multiple independent dishes and across multiple cell preparations. Fluorescence images in each channel were background-corrected by subtracting the fluorescence intensity of an ROI corresponding to a background region with no cells from the emission intensities of cells expressing fluorescent biosensors. The biosensors used in this study contain cyan fluorescent protein (CFP) as the donor and yellow fluorescent protein (YFP) as the acceptor. Three channels were captured per image acquisition: CFP (direct donor excitation and emission), YFP-FRET (donor-sensitized acceptor emission), and YFP (direct acceptor excitation and emission). Emission ratios (CFP/YFP-FRET) for ICUE3 and (YFP-FRET/CFP) for AKAR4 were then calculated for the different ROIs at each timepoint. Emission ratios were normalized by dividing the ratio at each timepoint by the value

immediately before drug addition. Pseudocolor ratiometric images were scaled to the indicated upper and lower bounds for emission ratios. In some cases, the cell body of the neuron is brighter than the rest of the cell and therefore appears black or pink. The color of the soma is not an indication of intensity saturation. The pseudocolor images were not used for data analysis.

Immunocytochemistry

Approximately $2.0x10^4$ HNs were cultured on nitric acid-washed, PDL-coated 15-mm glass coverslips for ~16-20 h, treated with the indicated drugs, and cultured for an additional 48 h. At DIV3, cells were fixed with 4% PFA for 20 min at room temperature. Free PFA was quenched with 100 mM glycine in HBSS. Cells were then permeabilized and preincubated in blocking buffer (5% goat serum, 0.2% BSA, 0.1% Triton-X 100, and 0.01% NaN_3 in HBSS) for 30 min. The cells were incubated overnight at 4°C with the following primary antibodies in blocking buffer: rabbit Tau1 and mouse NST. On the following day, the cells were washed 3 times in HBSS and incubated with goat anti-rabbit Alexa-Fluor-568 or goat anti-mouse Alexa-Flour-488 secondary antibody for 2 h at room temperature in the dark. Cells were then washed once with HBSS, counterstained with 1 mg/mL Hoechst stain to visualize the nuclei, and washed another 3 times with HBSS. Prolong Gold anti-fade mounting reagent was used to mount coverslips for imaging on a Zeiss LSM700 inverted confocal microscope (Zeiss, Oberkochen, Germany). All image were processed using ImageJ software (NIH, Bethesda, MD) and the Simple Neurite Tracer plugin[166].

Statistical Analysis

Graphs were plotted using GraphPad Prism 6 (GraphPad, La Jolla, CA), and all statistical analyses were performed using the same software. Sample size was not predetermined prior to performing the experiments, Cells were excluded from data acquisition when axons and dendrites were not obviously developed. Pairwise comparisons were performed using two-sided Student's t-test, and statistical significance was set at $p<0.05$. Global comparisons of sensor responses were performed using one- or two-way ordinary ANOVA analysis, and statistical significance was set at $p<0.05$. Bar graphs depict the mean±S.E.M. For box-and-whisker plots, the box shows the median, 25% quartile, and 75% quartile, and the whiskers designating the 5th and 95th percentiles; the mean value is indicated with a "+". Investigators were not blinded to the group allocation during analysis.

Chapter 3

Dynamics of cGMP in subcellular compartments

Introduction

Compartmentalization of cellular signaling allows cells to control a signal's specificity, duration, and magnitude[167]. One method a cell uses to compartmentalize signals is by organizing signaling components into discrete signaling microdomains[168]. Examples of discrete subcellular locations are the surfaces of organelles like the plasma membrane (PM) rafts, and non-raft PM regions, nucleus, mitochondria, and endoplasmic reticulum (ER). Each of these locations and organelles have unique profiles of different signaling pathways, which endow them with specialized function. For example, the membrane rafts are small, rigid platforms made up of cholesterol and glycosphingolipids, which serve as organizing centers for membrane components such as receptors, ion channels, and other enzymes to regulate signaling pathways[169].

The cyclic guanosine monophosphate (cGMP) signaling pathway is found in all organisms from bacteria to humans. Some of its many functions includes regulating gene expression[170], cell proliferation[171, 172], and cell metabolism[173]. Specialized cells like cardiomyocytes utilize cGMP for proper ventricular function in the heart. Smooth muscle cells use cGMP to relax blood vessels, and neurons use cGMP signaling in differentiation and development. cGMP is produced by enzymes that catalyze the conversion of GTP in a cyclization reaction to generate cGMP. In rod photoreceptors, a high cGMP concentration activates cGMP-gated sodium channels, which keeps cells depolarized in the dark[174, 175]. In cortical neurons, dendrite outgrowth stimulated by Semaphorin3A was mediated by increases in cGMP[99]. Sema3a simultaneously suppresses axon outgrowth via the mutual inhibition of cAMP leading to reduced PKA activity, which inhibits LKB1, activates GSK3β, and prevents axon polarization. This study highlights the important interplay between cAMP and cGMP, whose actions are mutually antagonistic in certain situations[56].

Soluble guanylyl cyclases are found throughout the cell and are stimulated by nitric oxide (NO) while particulate guanylyl cyclases are transmembrane receptors for natriuretic peptides like ANP[176]. cGMP is regulated by the enzymatic activity of phosphodiesterases (PDEs) that catalyze its hydrolysis and prevent saturation of the cell with the second messenger. Understanding how cGMP signals are distributed within living cells in space and time helps researchers connect signaling responses to specific biological outcomes.

Traditional methods of studying biochemical activity are insufficient to provide a high resolution map of spatiotemporal signaling dynamics in living cells. Fluorescence resonance energy transfer (FRET) biosensors are well suited to provide such information with using a ratiometric fluorescence intensity readout[135]. These powerful probes can be used to visualize molecular activity with high spatial and temporal resolution in real time in living cells. Nikolaev *et al.* have constructed FRET-based cGMP biosensors using the cyclic nucleotide binding domain (CNBD) GAF-A from PDE5A as the sensing unit sandwiched between the reporting unit fluorescent protein donor ECFP and acceptor EYFP[117]. When cGMP binds to the sensing unit, it induces a conformational change and increases FRET in the reporting unit. To better understand compartmentalized cGMP signaling, we targeted the cGMP energy transfer sensor derived from PDE5A (cGES-DE5) to multiple locations within the cell using localization sequences to deliver the reporter to the proper subcellular compartment. We found that cGMP dynamics are differentially regulated in signaling microdomains and depend on the type of stimulation used to elevate cGMP.

Results

Generation and expression of organelle specific cGMP reporters

We first constructed the genetically encoded FRET-based cGMP biosensor cGES-DE5 (Fig. 3.1a) by cloning the GAF-A domain from PDE5A and inserting it between ECFP and EYFP in cGES-DE2, another cGMP reporter generated by Nikolaev *et al*.[117]. In this sensor, the binding of cGMP results in a conformational change in the PDE5A GAF-A domain and an increase in the acceptor-to-donor (Y/C) emission ratio. Using this probe, we observed emission ratio increases (Fig 3.1b) in Cos-7 cells treated with 80 μM sodium nitroprusside (SNP), a nitric oxide donor and general activator of soluble ACs, which confirmed SNP can elevate cGMP levels inside Cos-7 cells[177]. The normal, unmodified reporter has a diffuse localization when expressed in Cos-7 cells. We appended signal sequences to cGES-DE5 in order to localize the sensor to different subcellular compartments including the general PM, membrane rafts, the nucleus, mitochondria, and the ER (Fig. 3.1c-h). The PM localized reporters were constructed using lipid modification domains. The non-membrane raft PM targeted reporter cGES-DE5 K-Ras utilizes a CaaX (C = cysteine, a = aliphatic amino acid, and X = any amino acid) sequence combined with a stretch of lysine residues to anchor the reporter to the PM. The N-terminus of Lyn kinase tethers the Lyn cGES-DE5 reporter to the membrane rafts via myristoylation and palmitoylation[114, 178]. Nuclear targeting was achieved with a nuclear localization signal[105]. An N-terminal motif from DAKAP1a, a mitochondrial outer membrane protein, was used to generate mito cGES-DE5[105], and an N-terminal targeting motif from cytochrome P450 was used for ER cGES-DE5[179].

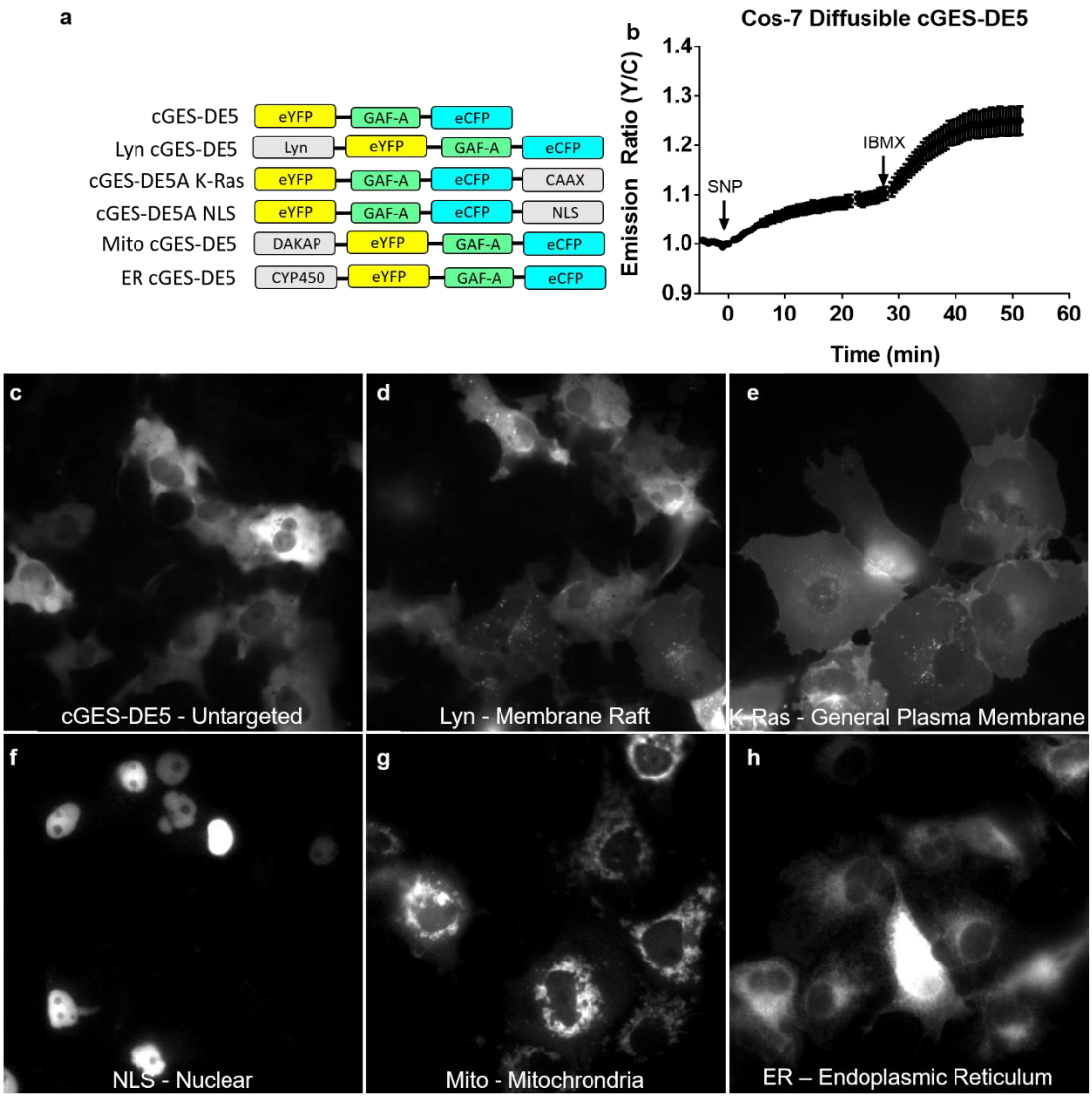

Figure 3.1 Design and localization of original and targeted cGES-DE5 constructs in Cos-7 cells.

(a) Illustration of cGES-DE5 constructs with targeting signal sequences at the N- and C-termini. (b) Average emission ratio YFP-FRET/CFP response curve of diffusible cGES-DE5 expressing Cos-7 cells (n=10) to 80 µM SNP and 100 µM IBMX. CFP images of Cos-7 cells expressing organelle specific cGES-DE5 constructs: (c) untargeted, (d) membrane rafts, (e) general PM, (f) nucleus, (g) mitochondria, and (h) ER.

Characterizing the sGC generated cGMP dynamics using os-cGES-DE5 reporters in Cos-7 cells

The average SNP stimulated emission ratio change was significantly different between the whole cell, membrane rafts, general PM, and the nucleus (7.95±0.98%, 4.96±0.65%, and 2.94±1.08% and 9.31±1.95% respectively, n=14≥ cells) (Fig. 3.2a), indicating that cGMP generated by the activation of sGCs is not uniform in all locations. Addition of IBMX to Cos-7 cells after treatment with SNP increased the emission ratio of each sensor to 22.14±2.08%, 18.07±1.36%, 11.64±2.53%, and 28.65±3.37% (mean±S.E.M.; n≥14) in the whole cell, membrane rafts, PM, and nucleus, respectively. These data are consistent with the known effects of PDE activity on cyclic nucleotide second messengers and further demonstrate the presence of this regulation in multiple cellular locations. To help characterize the sensors further, we calculated the SNP response as a percentage of the cumulative SNP + IBMX response. The data indicates that the compartment specific SNP response is not equal and further supports the idea that cGMP dynamics differ between subcellular compartments.

So far, we have shown that compartmentalized cGMP signaling stimulated by SNP is under the regulation of PDE activity. Inhibiting PDEs at the basal state can reveal the basal activity of sGC in the absence of any stimulation. Addition of IBMX to Cos-7 cells basally produced a minimal amount of cGMP indicating that sGC activity is generally low (Fig. 3.2c). As expected, subsequent addition of SNP produced a larger cGMP response than with SNP treatment alone. Interestingly, cGES-DE5 localized to the general PM (cGES-DE5 K-Ras) had the lowest response of all the versions despite the treatment order.

However, the cGES-DE5 K-Ras SNP response was similar to the other locations when calculated as a percentage of the max response.

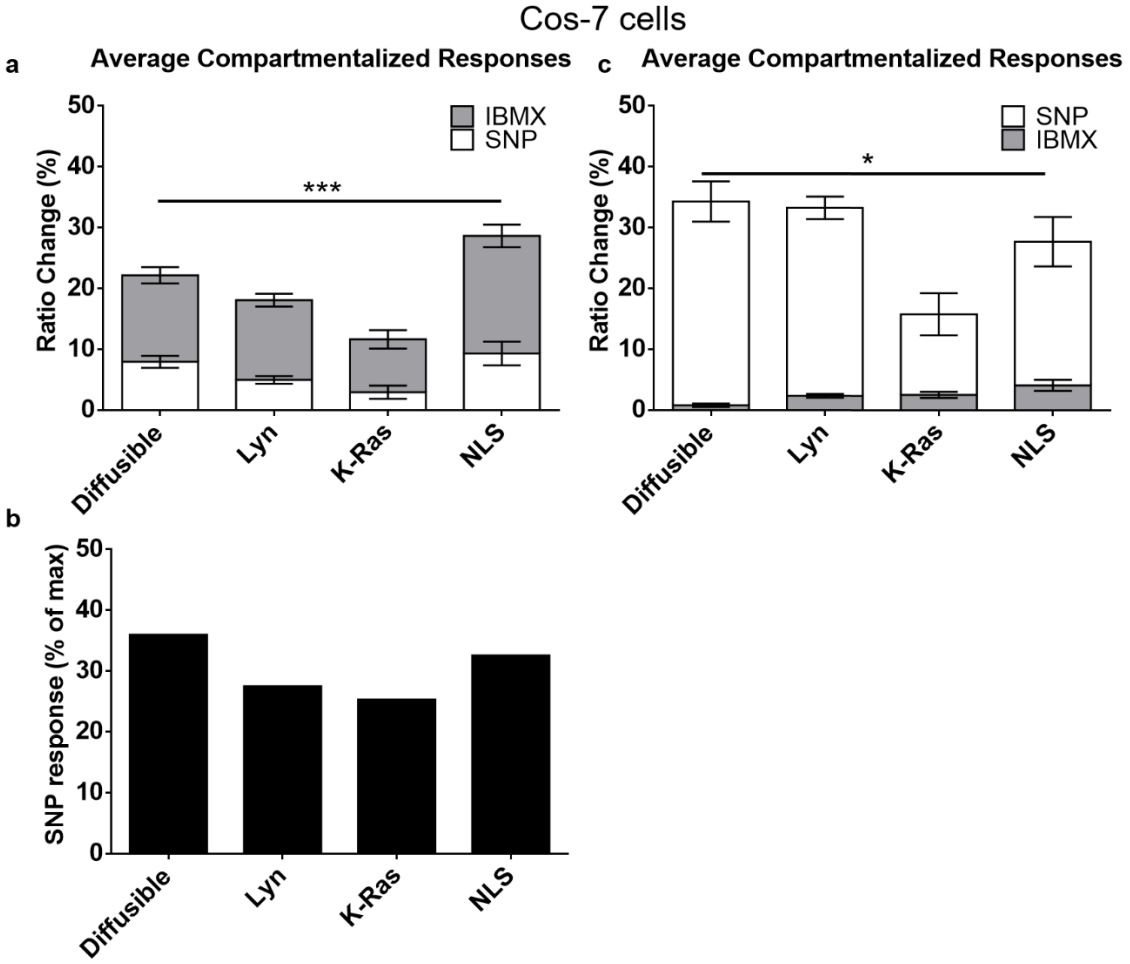

Figure 3.2 Differential cGMP responses in subcellular locations of Cos-7 cells.
(a) Average responses represented as stacked bars to 80 µM SNP (white) followed by 100 µM IBMX (gray) in Cos-7 cells expressing cGES-DE5 localized to the general cell, membrane rafts, PM, and nucleus localized versions. Data shown as mean±S.E.M. *** indicates $p<0.001$ according to one-way ANOVA. (b) Average SNP response as a percent of the cumulative SNP + IBMX response. (c) Average responses to 100 µM IBMX (gray) followed by 80 µM SNP (white) in Cos-7 cells expressing cGES-DE5 localized to the general cell, membrane rafts, PM, and nucleus localized versions. Data shown as mean±S.E.M. * indicates $p<0.05$ according to one-way ANOVA.

Characterizing the pGC generated cGMP dynamics using os-cGES-DE5 reporters in HeLa cells

In cells, sGC and pGC are the cGMP generating enzymes stimulated by NO and natriuretic peptides like ANP, respectively. Because we are interested in the compartmentalization of cGMP signaling, and cGMP enzymes are differentially localized in the cell, we tested the stimulation of NPR1, the receptor for ANP, in Cos-7 cells and the associated cGMP responses. Surprisingly, we were not able to see a significant cGMP response with any of our os-cGES-DE5 reporters (data not shown). We therefore used the HeLa cell line that has been reported to produce cGMP in response to ANP stimulation. HeLa cells expressing the os-cGES-DE5 reporters treated with 10 μM ANP responded with emission ratio increases of 10.0±3.55% (diffusible, n=10), 5.02±1.69% (membrane raft, n=15), 6.21±2.21% (PM, n=26), and 6.14±1.99% (nucleus, n=18) (Fig. 3.3a). Subsequent stimulation with 100 μM IBMX increased the response by ~10% in each region. The cumulative ANP + IBMX response was not significantly different between the regions. These data indicate that the os-cGES-DE5 sensors can detect ANP stimulated cGMP responses and that PDE activity controls the magnitude of cGMP increase in HeLa cells. By calculating the ANP response as a percentage of the cumulative ANP + IBMX response, we show that the diffusible reporter generated the largest ANP response while the membrane raft targeted reporter generated the smallest ANP response. The data indicates that similar to the SNP response in Cos-7 cells, the ANP stimulated pGC activity is compartmentalized. Interestingly, although pGCs are known to localize to the PM, we detected a large increase in the nucleus, which may support fast cGMP diffusion into the nucleus from the membrane.

As we did for Cos-7 cells and the SNP response, we inverted the treatment order of ANP and IBMX to understand the basal pGC activity contribution to compartmentalized cGMP. Addition of IBMX to HeLa cells actually decreased the emission ratio in each cellular compartment, indicating that basal PDE activity positively influences cGMP levels in HeLa cells. Nonetheless, subsequent addition of ANP generated a larger response than ANP alone, similar to the IBMX + SNP response in Cos-7 cells. These data support the idea that PDE activity controls cGMP levels when pGCs are stimulated with ANP.

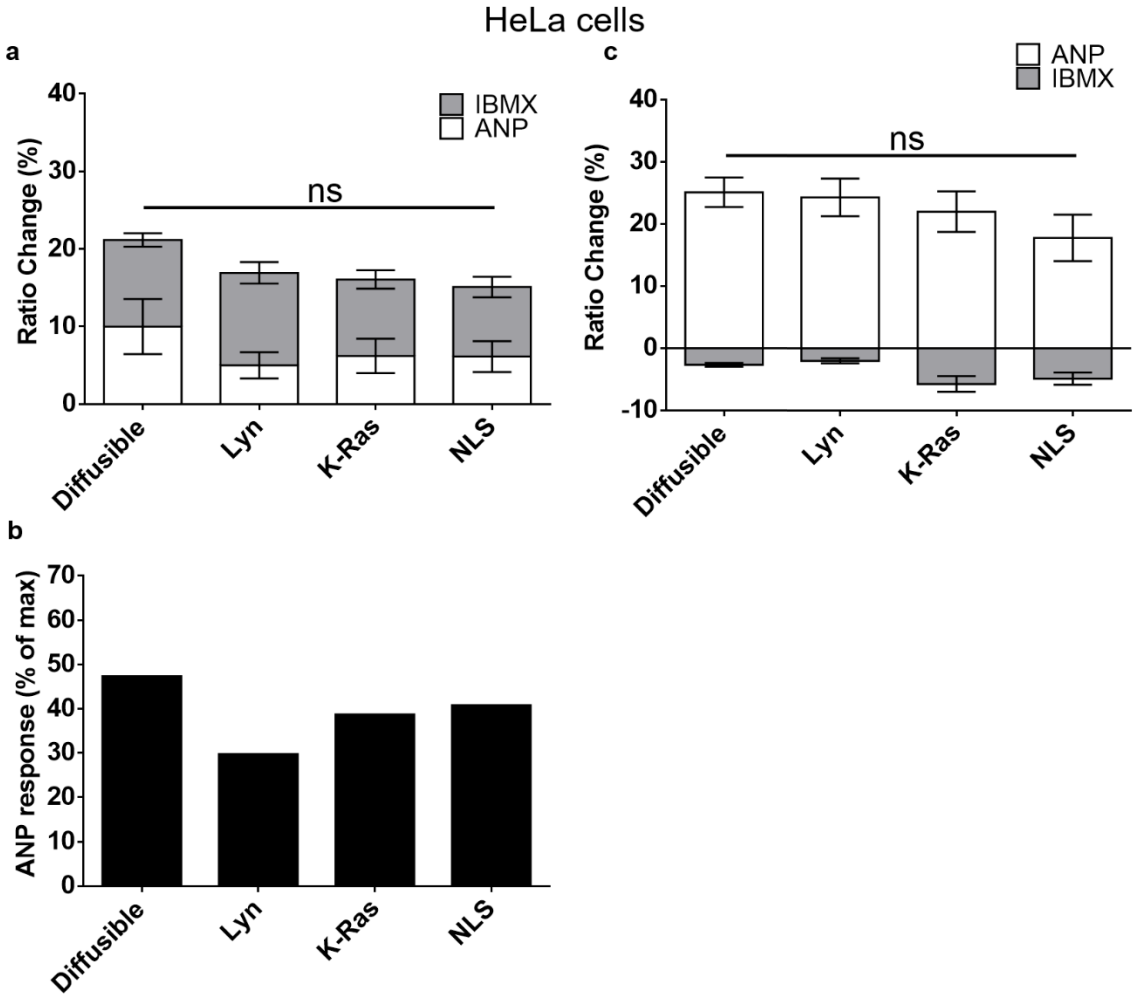

Figure 3.3 Differential cGMP responses in subcellular locations of HeLa cells.

(a) Average responses represented as stacked bars to 10 μM ANP (white) and 100 μM IBMX (gray) in HeLa cells expressing cGES-DE5 localized to the general cell, membrane rafts, PM, and nucleus localized versions. Data shown as mean ±S.E.M. ns, not significant according to one-way ANOVA. (b) Average ANP responses as a percent of the cumulative SNP + IBMX response. (c) Average responses to 100 μM IBMX (gray) followed by 10 μM ANP (white) in Cos-7 cells expressing cGES-DE5 localized to the general cell, membrane rafts, PM, and nucleus localized versions. Data shown as mean ±S.E.M. ns, not significant according to one-way ANOVA.

Membrane raft disruption affects the cGMP levels produced by SNP stimulated sGCs in Cos-7 cells

cGMP signal regulation is achieved by compartmentalization of signaling components including receptors, regulators and effectors into discrete subcellular compartments to enhance signal specificity. The PM microdomains called membrane rafts are rigid structures enriched in cholesterol and glycosphingolipids, which are known to compartmentalize cellular signaling components like the β2-adrenergic receptor for cAMP signaling. Cholesterol depletion by methyl-beta-cyclodextrin (MβCD) is a well-known method to disrupt membrane rafts regions of the PM and has been shown to modulate PM signaling dynamics[114]. We tested the SNP stimulated sGC responses in membrane raft and non-membrane raft microdomains in the presence of MβCD using Cos-7 cells expressing Lyn cGES-DE5 and cGES-DE5 K-Ras, respectively. Cells were pretreated with MβCD for one hour prior to stimulation with the cGMP agonists. We found that disruption of membrane rafts via cholesterol depletion significantly enhanced the SNP stimulated sGC response by ~10% in the membrane raft microdomain (Fig. 3.4a,b). MβCD significantly enhanced the non-membrane raft cGMP response to SNP by ~5% (Fig. 3.4c,d). Together, these results indicate that PM cGMP responses stimulated by sGC activation are

potentiated upon membrane raft disruption, suggesting membrane rafts play a negative role in sGC stimulation of cGMP signaling.

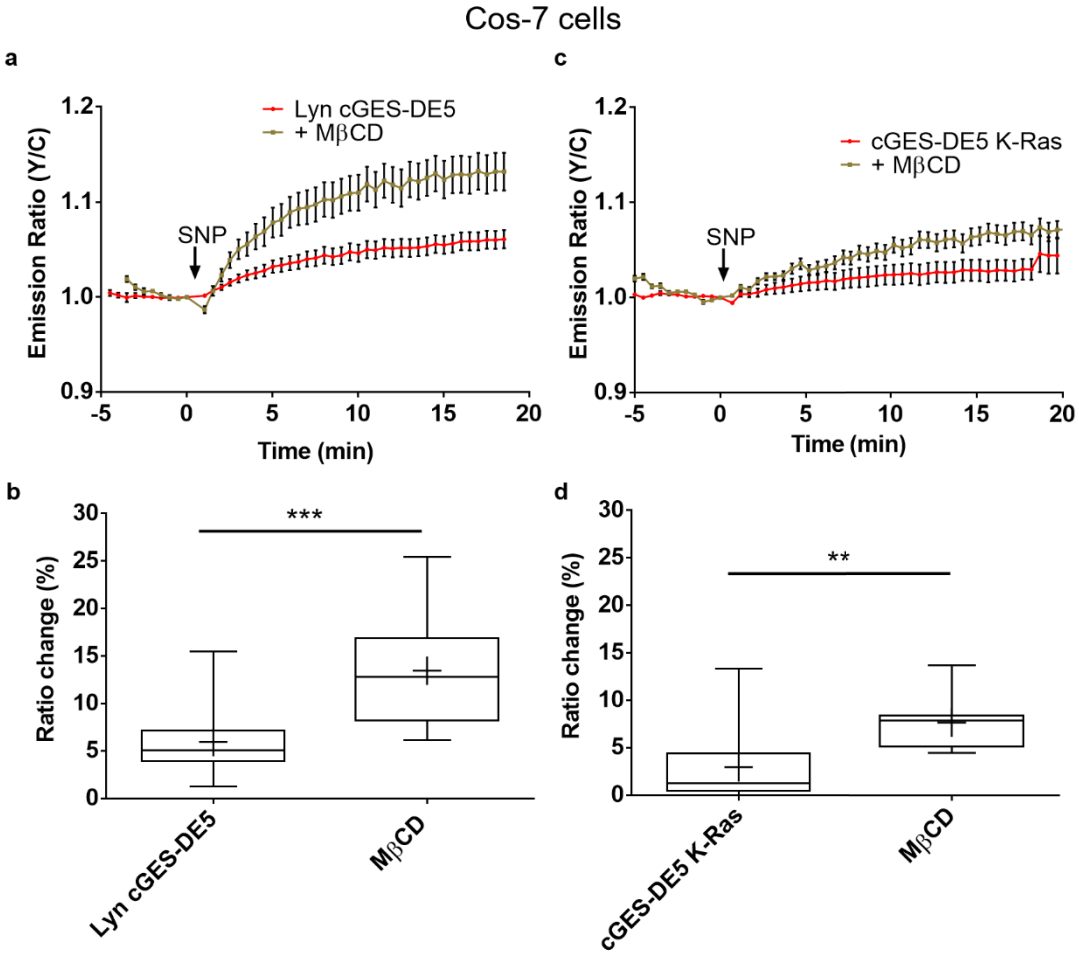

Figure 3.4 Membrane raft disruption affects membrane cGMP responses in Cos-7 cells
(a) Average emission ratio curves (YFP-FRET/CFP) of membrane raft-targeted cGES-DE5 to 80 µM SNP without (red) and with 4 mM MβCD (gold) in Cos-7 cells. (b) Average SNP responses from a. (c) Average emission ratio curves (YFP-FRET/CFP) of PM-targeted cGES-DE5 to 80 µM SNP without (red) and with MβCD (gold) in Cos-7 cells. (d) Average SNP responses from b. Data in b and d are shown as box-and-whisker plots, with the box showing the median, 25% quartile, and 75% quartile, and the whiskers designating the 5th and 95th percentiles; a "+" indicates the mean. *** indicates $p<0.001$, ** indicates $p<0.01$ according to Student's t-test.

We then conducted the same experiment with HeLa cells to determine if the cGMP generated by ANP stimulated pGCs was affected by membrane raft disruption.

Surprisingly, this treatment did not significantly affect ANP stimulated pGC responses within membrane rafts themselves or in non-membrane raft regions (Fig. 3.5). Future experiments will examine whether membrane rafts were disrupted effectively by this treatment. A tentative conclusion is that the pGC signaling is not affected by membrane raft disruption despite being transmembrane proteins.

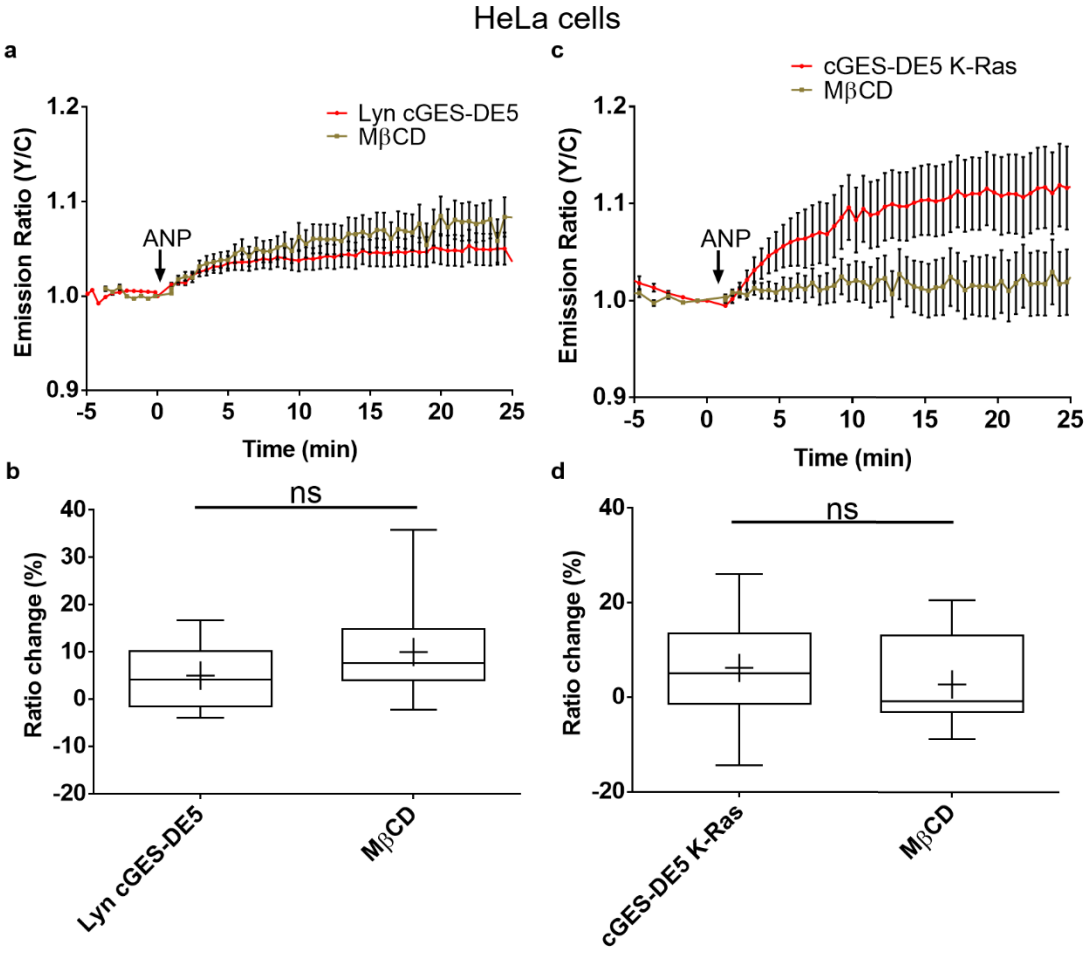

Figure 3.5 Membrane raft disruption affects membrane cGMP responses in HeLa cells

(a) Average emission ratio curves (YFP-FRET/CFP) of membrane raft-targeted cGES-DE5 to 10 µM ANP without (red) and with MβCD (gold) in HeLa cells. (b) Average ANP responses from a. (c) Average emission ratio curves (YFP-FRET/CFP) of PM-targeted cGES-DE5 to 80 µM ANP without (red) and with MβCD (gold) in HeLa cells. (d) Average ANP responses from b. Data in b and d are shown as box-and-whisker plots, with the box showing the median, 25% quartile, and 75% quartile, and the whiskers designating the 5th

and 95th percentiles; a "+" indicates the mean. * indicates $p<0.05$, ns, not significant according to one-way ANOVA.

Discussion

Our study of compartmentalized cGMP signaling suggests that there are differences between subcellular compartments and sources of cGMP production and regulation. First, we observed significant location specific differences in cGMP signaling with SNP stimulation. As the sGC maintains a diffuse localization throughout the cell, the detection of different levels of cGMP activity support the hypothesis that cGMP signaling is differentially regulated within discrete compartments. In fact, the combined nuclear SNP and IBMX generated the largest dynamic range as compared to the other regions. Importantly, the presence of nuclear cGMP as reported by the cGES-DE5 NLS biosensor suggests either sGC is localized to the nucleus or cGMP is able to diffuse quickly from the cytoplasm to the nucleus. Secondly, PDE inhibition prior to SNP revealed low levels of basal sGC activity, whereas SNP stimulation in the presence of PDE inhibition generated a heightened SNP response, suggesting the elevation of cGMP is coupled to and regulated by PDE activity. The responses of the diffusible, raft, and non-raft reporters are also increased when PDEs are inhibited before the addition of SNP, suggesting that there is a temporal component to cGMP activity and that the sequence of activation plays a role in the magnitude of the cGMP response. During the SNP treatment, PDEs are activated and degrade the newly generated cGMP, effectively limiting the maximum concentration of cGMP to be produced. With PDE inhibition, the negative regulation is removed and the cell has a higher potential to generate cGMP. Future studies will examine the contribution of different PDE isoforms to spatiotemporal compartmentalization of cGMP signaling.

In our attempt to understand cGMP signal regulation by different mechanisms, we found that the cGMP response is cell type-dependent. Here, we were not able to activate sGCs in HeLa cells, nor were we able to activate pGCs in Cos-7 cells. Therefore, we could not make direct comparisons between sGC and pGC regulation of cGMP levels in the same cell type. Nonetheless, we analyzed ANP stimulated cGMP responses in HeLa cells and found less variability in the compartmental responses. Still, HeLa cells exhibited a sizeable nuclear cGMP response to ANP. Under the assumption that pGCs are localized to the PM, the data suggests that cGMP is able to diffuse readily into the nucleus to activate any potential effectors that may reside there. The negative regulation of cGMP by PDEs is a general rule and is exemplified by the heightened ANP response when PDEs are inhibited prior to stimulation with ANP.

Our results suggest that membrane rafts play a more important role in shaping the cGMP responses from sGCs than from pGCs. We observed an enhanced cGMP response to SNP in Cos-7 cells upon membrane raft disruption. Surprisingly, the response was increased in both the raft and non-raft compartment. The specific mechanism for the enhancement is unknown, but may be related to a redistribution of signaling components like PDEs or other cGMP binding partners. Alternatively, sGCs present within the raft regions may be under negative regulation and raft disruption releases the inhibition, effectively elevating the potential for sGCs to generate cGMP upon sensing NO.

This study emphasizes the importance of understanding how cellular microdomains regulate cGMP signaling dynamics. Further development of high-resolution, quantitative live-cell imaging techniques will play a critical role in assessing how compartmentalized signaling shapes biologically relevant cellular responses. To this end, we have contributed

to the field a suite of cGMP biosensors that can specifically detect free cGMP at specific organelles. This suite of sensors can be expanded to other locations like the lysosome and golgi, or more specifically, tethered to proteins to detect nanodomain pools of cGMP. os-cGES-DE5 biosensors have allowed us to track subcellular cGMP signaling dynamics in discrete subcellular compartments revealing how cGMP is regulated in different signaling microdomains.

Significance

The cyclic nucleotide cGMP is a critical second messenger molecule responsible for initiating signaling cascades that regulate critical biological functions. It is well appreciated that spatiotemporal compartmentalization of cGMP allows for specific signal transduction through the generation of subcellular pools or microdomains of cGMP signaling. Given that there are two ways to generate cGMP inside of a cell, by activating pGCs or sGCs, it important to understand the spatiotemporal dynamics of cGMP in different subcellular compartments. Although several cGMP biosensors have been developed for detecting free cGMP in the entire cell, there are no biological tools available to study compartmentalized cGMP signaling within living cells in real time. To this end, we have generated a suite of cGMP sensors targeted to specific subcellular compartments using signal sequence targeting motifs. Here, we have characterized the sensors within membrane rafts in the PM, non-membrane rafts regions of the PM, and the nucleus. First, we tested the subcellular cGMP responses with sGC stimulation and pGC stimulation. Interestingly, we observed a lack of pGC stimulation in Cos-7 cells, and a lack of sGC stimulation in HeLa cells. In either cell type, we did not detect a significant difference in cGMP responses between the regions. Next, we found that disruption of PM rafts by

cholesterol depletion changes the sGC stimulated cGMP response indicating the integrity of membrane rafts shapes cGMP dynamics. This study demonstrates that 1) subcellular cGMP dynamics can be detected using FRET-based biosensors, 2) different cell types have different modes of cGMP signaling, and 3) cGMP signaling at the membrane is dependent on the integrity of membrane rafts.

Signal transduction is the process that cells use to respond to their environment and adapt appropriately. Many of signaling pathways rely on second messengers like the cyclic nucleotides to convert the signal from outside to inside of the cell. Once a signal is converted, intracellular signaling mechanisms control the duration and intensity of the response. cGMP is one of the two cyclic nucleotides used for many critical cellular functions. Compartmentalization provides a cell with the ability to control the specificity and response of cellular signals. This work sought to understand how cGMP is regulated in discrete subcellular compartments by utilizing genetically encodable FRET-based biosensors for cGMP targeted to these signaling microdomains. Traditional techniques like western blot and immunoassays do not allow for visualization of signaling dynamics in living cells. The organelle-specific cGES-DE5 sensors overcome these limitations providing a real time ratiometric readout of cGMP signaling in specific locations within the cell. Here, we constructed targeted versions of the sensor using localization signals appended to the N- and C-termini of the reporter. We were able to show that subcellular cGMP activity is indeed different in different cells and confirmed the regulation of cGMP by phosphodiesterases. Altogether, our work introduces a method by which cGMP signals can be tracked in real-time within subcellular compartments of living cells. These sensors can be applied to studies dissecting the mechanisms of action of therapeutics affecting the

cGMP signaling pathway. Furthermore, understanding cGMP compartmentalization using these sensors would greatly benefit preclinical studies involving cardiac myocytes and neurons, which are heavily dependent on cGMP for their functions.

Materials and Methods

Generating os-cGES-DE5 constructs

cGES-DE2 was a gift from the Nikolaev lab and was used as a template for cGES-DE5 created in our lab. The GAF-A domain was cloned from PDE5A using primer amplification and inserted into cGES-DE2 between ECFP and EYFP. cGES-DE5 was targeted to membrane rafts by a 5' myristoylation and palmitoylation lipid modification sequence (GCIKSKRKDK) derived from Lyn kinase and to non-rafts by a 3' farnesylation lipid modification sequence (KKKKKKSKTKCVIM) derived from K-Ras kinase. cGES-DE5 was targeted to the nucleus using a 3' nuclear localization signal (PKKKRKVEDA). cGES-DE5 was targeted to the mitochondria using a 5' targeting motif from DAKAP1a (**M**AIQLRSLFPLALPGMLALLGWWWFFSRKK). cGES-DE5 was targeted to the ER outer membrane using a 5' targeting motif from CYP450 (**M**DPVVVLGLCLSCLLLLSLWKQSYGGG).

Reagents

Sodium Nitroprusside was purchased from Sigma. ANP was purchased from Sigma. 3-isobutyl-1-methylxanthine (IBMX, 410957) were purchased from Calbiochem and used at a final concentration of 100 μM (IBMX)[161 162, 163]. Methyl-β-cyclodextrin (MβCD) was purchased from Sigma.

Cell Culture

Cos-7 and HeLa cells were cultured in DMEM supplemented with 10% FBS and 1% Pen-Strep and maintained at 37 °C with 5% CO_2. For imaging, cells were plated onto sterilized glass cover slips in 35 mm dishes, transfected with Lipofectamine 2000 at 50-60% confluency, and then grown for approximately 24 hours before imaging.

Imaging

Cells were washed twice with Hanks' Balanced Salt Solution (HBSS) and imaged in the dark at room temperature. Cholesterol depletion experiments were carried out by treating cells with 4 mM methyl-β-cyclodextrin (MβCD; Sigma) for 30 minutes at 37 °C before imaging. Cells were treated with SNP, ANP, and IBMX as indicated in the graphs. Images were acquired on an Axiovert 200M microscope (Carl Zeiss, Thornwood, NY) with a cooled charge-coupled device camera (Roper Scientific, Trenton, NJ) controlled by Metafluor 6.2 software (Molecular Devices, Downingtown, PA). Dual emission ratio imaging used a 420DF20 excitation filter, a 450DRLP dichroic mirror, and two emission filters (475DF40 for CFP and 535DF25 for YFP). Exposure time was 50–500 ms and images were acquired every 30 s. Background correction of the fluorescence images was performed by subtracting autofluorescence intensities of untransfected cells or regions of the imaging dish with no cells. Graph curves were normalized by setting the emission ratio before drug addition equal to one.

Chapter 4

Concluding Remarks

Information from the external environment comes to cells in many forms and must be appropriately transduced by cells. From hormones and ions, to small molecules and neurotransmitters, proper conversion of extracellular signals to activate intracellular signal transduction pathways is essential for the proper functioning of cells. Different cell types utilize signal transduction pathways in different ways, but common to all cells is the requirement for appropriate regulation of signaling modules in both space and time. The spatiotemporal regulation of signaling networks is a complex process involving many players and signal transduction events. For cyclic nucleotides, the spatiotemporal compartmentalization is achieved by several methods including physical segregation of enzymes like GPCRs, cyclases, and phosphodiesterases and the activity of these enzymes and cyclic nucleotide effectors helps generate specific cellular responses. Understanding these spatiotemporal dynamics helps us understand where and when a signal is acting, allowing researchers to connect the cellular signals to cellular functions. Studies on signal transduction networks from living cells provide the most relevant information, as the native biological context of the cellular milieu in live cells permits researchers to study the signal transduction pathways as they occur in nature, rather than reconstituting the pathway components *in vitro.* Here, we have shown how FRET-based biosensors expressed in primary neuronal cells and heterologous cell lines can be used as biological tools to study the spatiotemporal dynamics of cyclic nucleotide signaling.

In primary hippocampal neurons, we have used cAMP and PKA biosensors to reveal the gradients of molecular activity in the developing axon which have long been alluded to in the literature as playing an important role in the function of cAMP/PKA signaling. The fact that these axon-directed gradients were growth stage dependent

highlights their role in axon development. We further dissected how PDEs regulate these gradients and by using PDE isoform specific inhibitors showed that PDE4, not PDE3, is a major regulator of cAMP in developing neurons. While our investigation into the regulation of cAMP gradients by PKA, AKAPs, and PDEs revealed a new and unexpected mechanism for controlling axon outgrowth in developing hippocampal neurons, it raises the question of how enhanced cAMP gradients in the axon can drive elongation. It is now well-appreciated that the cAMP effectors Epac1 and PKA both play important roles in axon development. It would therefore be interesting to understand the activity dynamics of Epac itself within the axon and how PKA and Epac interact within AKAP signaling microdomains to engage in axon elongation. Our work also brings AKAPs into the fold of neuronal differentiation and development. While AKAPs have been studied in the context of neuronal excitation and action potentials, researchers have not yet included AKAPs into the discussion of nervous system development. Our work lays the foundation for studying AKAPs in this new context and identifying which AKAPs are most important in the developing axon.

The second study presented here introduces FRET-based biosensors for the study of compartmentalized cGMP signaling which up until this point have not been available. We have designed subcellularly targeted biosensors to sensitively monitor cGMP dynamics with high spatiotemporal resolution. With these tools researchers are now able to study how localized cGMP signaling varies with disease and therapeutic treatment.

The importance of proper signal regulation in cells has been heavily emphasized throughout this work. To achieve specific cellular responses, signals must be tightly regulated and compartmentalized. The critical functions of the cAMP/PKA and

cGMP signaling pathways mean that dysregulation may lead to improper signal transduction; a consequence that may lead to diseased states. The implications of the basic science research presented herein are two-fold: it provides a foundation for future research projects in understanding how cAMP/PKA signaling contributes to the development of the nervous system and delivers tools to further characterize compartmentalized cGMP signaling in different cell systems.

References

1. Nikulina, E. & Filbin, M.T. in Cyclic-Nucleotide Phosphodiesterases In The Central Nervous System 353-374 (John Wiley & Sons, Inc., 2014).
2. Taly, A. Novel approaches to drug design for the treatment of schizophrenia. *Expert Opinion on Drug Discovery* **8**, 1285-1296 (2013).
3. Lim, W.K. GPCR drug discovery: novel ligands for CNS receptors. *Recent Pat CNS Drug Discov* **2**, 107-112 (2007).
4. Antoni, F.A. Molecular Diversity of Cyclic AMP Signalling. *Frontiers in Neuroendocrinology* **21**, 103-132 (2000).
5. Conti, M. & Richter, W. in Cyclic-Nucleotide Phosphodiesterases In The Central Nervous System. (eds. N.J. Brandon & A.R. West) 1-46 (John Wiley & Sons, Inc., 2014).
6. Rich, T.C., Webb, K.J. & Leavesley, S.J. Can we decipher the information content contained within cyclic nucleotide signals? *The Journal of General Physiology* **143**, 17-27 (2014).
7. Sutherland, E.W. & Rall, T.W. Fractionation and characterization of a cyclic adenine ribonucleotide formed by tissue particles. *The Journal of biological chemistry* **232**, 1077-1091 (1958).
8. Stanley McKnight, G. Cyclic AMP second messenger systems. *Current opinion in cell biology* **3**, 213-217 (1991).
9. McCudden, C.R., Hains, M.D., Kimple, R.J., Siderovski, D.P. & Willard, F.S. G-protein signaling: back to the future. *Cellular and molecular life sciences : CMLS* **62**, 551-577 (2005).

10. Hurley, J.H. Structure, Mechanism, and Regulation of Mammalian Adenylyl Cyclase. *Journal of Biological Chemistry* **274**, 7599-7602 (1999).

11. Kamenetsky, M. et al. Molecular details of cAMP generation in mammalian cells: a tale of two systems. *Journal of molecular biology* **362**, 623-639 (2006).

12. Zippin, J.H. et al. Bicarbonate-responsive "soluble" adenylyl cyclase defines a nuclear cAMP microdomain. *The Journal of cell biology* **164**, 527-534 (2004).

13. Fimia, G.M. & Sassone-Corsi, P. Cyclic AMP signalling. *Journal of cell science* **114**, 1971-1972 (2001).

14. Chin, K.V. et al. Reinventing the wheel of cyclic AMP: novel mechanisms of cAMP signaling. *Annals of the New York Academy of Sciences* **968**, 49-64 (2002).

15. Taylor, S.S. et al. PKA: a portrait of protein kinase dynamics. *Biochimica et biophysica acta* **1697**, 259-269 (2004).

16. Skalhegg, B.S. & Tasken, K. Specificity in the cAMP/PKA signaling pathway. Differential expression,regulation, and subcellular localization of subunits of PKA. *Frontiers in bioscience : a journal and virtual library* **5**, D678-693 (2000).

17. Tasken, K. & Aandahl, E.M. Localized effects of cAMP mediated by distinct routes of protein kinase A. *Physiological reviews* **84**, 137-167 (2004).

18. Steinberg, R.A., Cauthron, R.D., Symcox, M.M. & Shuntoh, H. Autoactivation of catalytic (C alpha) subunit of cyclic AMP-dependent protein kinase by phosphorylation of threonine 197. *Molecular and cellular biology* **13**, 2332-2341 (1993).

19. Lowe, E.D. et al. The crystal structure of a phosphorylase kinase peptide substrate complex: kinase substrate recognition. *The EMBO Journal* **16**, 6646-6658 (1997).

20. Cheng, X., Ma, Y., Moore, M., Hemmings, B.A. & Taylor, S.S. Phosphorylation and activation of cAMP-dependent protein kinase by phosphoinositide-dependent protein kinase. *Proceedings of the National Academy of Sciences of the United States of America* **95**, 9849-9854 (1998).

21. Shi, Y. Serine/Threonine Phosphatases: Mechanism through Structure. *Cell* **139**, 468-484.

22. Walsh, D.A., Perkins, J.P. & Krebs, E.G. An adenosine 3',5'-monophosphate-dependant protein kinase from rabbit skeletal muscle. *The Journal of biological chemistry* **243**, 3763-3765 (1968).

23. Brushia, R.J. & Walsh, D.A. Phosphorylase kinase: the complexity of its regulation is reflected in the complexity of its structure. *Frontiers in bioscience : a journal and virtual library* **4**, D618-641 (1999).

24. Lee, J.H. et al. Protein Kinase A subunit balance regulates lipid metabolism in Caenorhabditis elegans and mammalian adipocytes. *Journal of Biological Chemistry* (2016).

25. Hansson, V., Skålhegg, B.S. & Taskén, K. Cyclic-AMP-dependent protein kinase (PKA) in testicular cells. Cell specific expression, differential regulation and targeting of subunits of PKA. *The Journal of Steroid Biochemistry and Molecular Biology* **73**, 81-92 (2000).

26. Yao, H., York, R.D., Misra-Press, A., Carr, D.W. & Stork, P.J.S. The Cyclic Adenosine Monophosphate-dependent Protein Kinase (PKA) Is Required for the Sustained Activation of Mitogen-activated Kinases and Gene Expression by Nerve Growth Factor. *Journal of Biological Chemistry* **273**, 8240-8247 (1998).

27. Shaywitz, A.J. & Greenberg, M.E. CREB: A Stimulus-Induced Transcription Factor Activated by A Diverse Array of Extracellular Signals. *Annual Review of Biochemistry* **68**, 821-861 (1999).

28. Bouchard, J.-F. et al. Protein Kinase A Activation Promotes Plasma Membrane Insertion of DCC from an Intracellular Pool: A Novel Mechanism Regulating Commissural Axon Extension. *The Journal of Neuroscience* **24**, 3040-3050 (2004).

29. Goto, A., Kamioka, Y. & Matsuda, M. PKA modulation of Rac in neuronal cells. *Frontiers in Cellular Neuroscience* **8**, 321 (2014).

30. Cassano, S., Di Lieto, A., Cerillo, R., Avvedimento, E.V. & ¶ Membrane-bound cAMP-dependent Protein Kinase Controls cAMP-induced Differentiation in PC12 Cells. *Journal of Biological Chemistry* **274**, 32574-32579 (1999).

31. Shelly, M., Cancedda, L., Heilshorn, S., Sumbre, G. & Poo, M.-m. LKB1/STRAD Promotes Axon Initiation During Neuronal Polarization. *Cell* **129**, 565-577 (2007).

32. Diering, G.H., Gustina, A.S. & Huganir, R.L. PKA-GluA1 coupling via AKAP5 controls AMPA receptor phosphorylation and cell-surface targeting during bidirectional homeostatic plasticity. *Neuron* **84**, 790-805 (2014).

33. Park, A.J. et al. A presynaptic role for PKA in synaptic tagging and memory. *Neurobiology of Learning and Memory* **114**, 101-112 (2014).

34. Oliveira, R.F., Kim, M. & Blackwell, K.T. Subcellular location of PKA controls striatal plasticity: stochastic simulations in spiny dendrites. *PLoS Comput Biol* **8**, e1002383 (2012).

35. Lepski, G., Jannes, C.E., Nikkhah, G. & Bischofberger, J. ¬cAMP promotes the differentiation of neural progenitor cells in vitro via modulation of voltage-gated calcium channels. *Frontiers in Cellular Neuroscience* **7** (2013).

36. de Rooij, J. et al. Epac is a Rap1 guanine-nucleotide-exchange factor directly activated by cyclic AMP. *Nature* **396**, 474-477 (1998).

37. Gloerich, M. & Bos, J.L. Epac: defining a new mechanism for cAMP action. *Annual review of pharmacology and toxicology* **50**, 355-375 (2010).

38. Tsalkova, T. et al. Isoform-specific antagonists of exchange proteins directly activated by cAMP. *Proceedings of the National Academy of Sciences* **109**, 18613-18618 (2012).

39. Kawasaki, H. et al. A Family of cAMP-Binding Proteins That Directly Activate Rap1. *Science (New York, N.Y.)* **282**, 2275-2279 (1998).

40. Wang, Z. et al. Rap1-mediated activation of extracellular signal-regulated kinases by cyclic AMP is dependent on the mode of Rap1 activation. *Molecular and cellular biology* **26**, 2130-2145 (2006).

41. Rehmann, H., Das, J., Knipscheer, P., Wittinghofer, A. & Bos, J.L. Structure of the cyclic-AMP-responsive exchange factor Epac2 in its auto-inhibited state. *Nature* **439**, 625-628 (2006).

42. Efetova, M. et al. Separate roles of PKA and EPAC in renal function unraveled by the optogenetic control of cAMP levels in vivo. *Journal of cell science* **126**, 778-788 (2013).

43. Hochbaum, D., Hong, K., Barila, G., Ribeiro-Neto, F. & Altschuler, D.L. Epac, in synergy with cAMP-dependent protein kinase (PKA), is required for cAMP-mediated mitogenesis. *The Journal of biological chemistry* **283**, 4464-4468 (2008).

44. Cheng, X., Ji, Z., Tsalkova, T. & Mei, F. Epac and PKA: a tale of two intracellular cAMP receptors. *Acta biochimica et biophysica Sinica* **40**, 651-662 (2008).

45. Murray, A.J., Tucker, S.J. & Shewan, D.A. cAMP-Dependent Axon Guidance Is Distinctly Regulated by Epac and Protein Kinase A. *The Journal of Neuroscience* **29**, 15434-15444 (2009).

46. Kiermayer, S. et al. Epac activation converts cAMP from a proliferative into a differentiation signal in PC12 cells. *Molecular biology of the cell* **16**, 5639-5648 (2005).

47. Muñoz-Llancao, P. et al. Exchange Protein Directly Activated by cAMP (EPAC) Regulates Neuronal Polarization through Rap1B. *The Journal of Neuroscience* **35**, 11315-11329 (2015).

48. Murray, A.J. & Shewan, D.A. Epac mediates cyclic AMP-dependent axon growth, guidance and regeneration. *Molecular and Cellular Neuroscience* **38**, 578-588 (2008).

49. Smith, M., Drummond, G.I. & Khorana, H.G. Cyclic Phosphates. IV.1 Ribonucleoside-3',5' Cyclic Phosphates. A General Method of Synthesis and Some Properties. *Journal of the American Chemical Society* **83**, 698-706 (1961).

50. Ashman, D.F., Lipton, R., Melicow, M.M. & Price, T.D. Isolation of adenosine 3', 5'-monophosphate and guanosine 3', 5'-monophosphate from rat urine. *Biochemical and biophysical research communications* **11**, 330-334 (1963).

51. Murad, F., Mittal, C.K., Arnold, W.P., Katsuki, S. & Kimura, H. Guanylate cyclase: activation by azide, nitro compounds, nitric oxide, and hydroxyl radical and inhibition by hemoglobin and myoglobin. *Advances in cyclic nucleotide research* **9**, 145-158 (1978).

52. Forstermann, U. et al. Isoforms of nitric oxide synthase. Characterization and purification from different cell types. *Biochemical pharmacology* **42**, 1849-1857 (1991).

53. Arnold, W.P., Mittal, C.K., Katsuki, S. & Murad, F. Nitric oxide activates guanylate cyclase and increases guanosine 3':5'-cyclic monophosphate levels in various tissue preparations. *Proceedings of the National Academy of Sciences of the United States of America* **74**, 3203-3207 (1977).

54. de Bold, A.J., Borenstein, H.B., Veress, A.T. & Sonnenberg, H. A rapid and potent natriuretic response to intravenous injection of atrial myocardial extract in rats. *Life sciences* **28**, 89-94 (1981).

55. McDonald, L.J. & Murad, F. Nitric Oxide and Cyclic GMP Signaling. *Experimental Biology and Medicine* **211**, 1-6 (1996).

56. Zaccolo, M. & Movsesian, M.A. cAMP and cGMP Signaling Cross-Talk: Role of Phosphodiesterases and Implications for Cardiac Pathophysiology. *Circulation research* **100**, 1569-1578 (2007).

57. Zaccolo, M. & Stangherlin, A. in Cyclic-Nucleotide Phosphodiesterases In The Central Nervous System. (eds. N.J. Brandon & A.R. West) 59-76 (John Wiley & Sons, Inc., 2014).

58. Terrin, A. et al. PGE1 stimulation of HEK293 cells generates multiple contiguous domains with different [cAMP]: role of compartmentalized phosphodiesterases. *The Journal of cell biology* **175**, 441-451 (2006).

59. Biswas, K.H., Sopory, S. & Visweswariah, S.S. The GAF domain of the cGMP-binding, cGMP-specific phosphodiesterase (PDE5) is a sensor and a sink for cGMP. *Biochemistry* **47**, 3534-3543 (2008).

60. Esseltine, J.L. & Scott, J.D. AKAP signaling complexes: pointing towards the next generation of therapeutic targets? *Trends in Pharmacological Sciences* **34**, 648-655 (2013).

61. Castro, L.R. et al. Type 4 phosphodiesterase plays different integrating roles in different cellular domains in pyramidal cortical neurons. *The Journal of neuroscience : the official journal of the Society for Neuroscience* **30**, 6143-6151 (2010).

62. Neves, S.R. Modeling of spatially-restricted intracellular signaling. *Wiley Interdiscip Rev Syst Biol Med* **4**, 103-115 (2012).

63. Taussig, R. & Gilman, A.G. Mammalian Membrane-bound Adenylyl Cyclases. *Journal of Biological Chemistry* **270**, 1-4 (1995).

64. Xia, Z., Choi, E.J., Wang, F., Blazynski, C. & Storm, D.R. Type I calmodulin-sensitive adenylyl cyclase is neural specific. *Journal of neurochemistry* **60**, 305-311 (1993).

65. Hu, C.L. et al. Adenylyl cyclase type 5 protein expression during cardiac development and stress. *American journal of physiology. Heart and circulatory physiology* **297**, H1776-1782 (2009).

66. Polleux, F., Morrow, T. & Ghosh, A. Semaphorin 3A is a chemoattractant for cortical apical dendrites. *Nature* **404**, 567-573 (2000).

67. Zaccolo, M. cAMP signal transduction in the heart: understanding spatial control for the development of novel therapeutic strategies. *British journal of pharmacology* **158**, 50-60 (2009).

68. Baillie, G.S. Compartmentalized signalling: spatial regulation of cAMP by the action of compartmentalized phosphodiesterases. *FEBS journal* **276**, 1790-1799 (2009).

69. Kerfant, B.-G. et al. PI3Kγ Is Required for PDE4, not PDE3, Activity in Subcellular Microdomains Containing the Sarcoplasmic Reticular Calcium ATPase in Cardiomyocytes. *Circulation research* **101**, 400-408 (2007).

70. Shelly, M. et al. Local and Long-Range Reciprocal Regulation of cAMP and cGMP in Axon/Dendrite Formation. *Science (New York, N.Y.)* **327**, 547-552 (2010).

71. Bender, A.T. & Beavo, J.A. Cyclic Nucleotide Phosphodiesterases: Molecular Regulation to Clinical Use. *Pharmacological Reviews* **58**, 488-520 (2006).

72. Houslay, M.D. Underpinning compartmentalised cAMP signalling through targeted cAMP breakdown. *Trends in biochemical sciences* **35**, 91-100 (2010).

73. Logue, J.S. & Scott, J.D. Organizing signal transduction through A-kinase anchoring proteins (AKAPs). *FEBS Journal* **277**, 4370-4375 (2010).

74. Colledge, M. & Scott, J.D. AKAPs: from structure to function. *Trends in cell biology* **9**, 216-221 (1999).

75. Skroblin, P., Grossmann, S., Schafer, G., Rosenthal, W. & Klussmann, E. Mechanisms of protein kinase A anchoring. *International review of cell and molecular biology* **283**, 235-330 (2010).

76. Taylor, S.S., Ilouz, R., Zhang, P. & Kornev, A.P. Assembly of allosteric macromolecular switches: lessons from PKA. *Nat Rev Mol Cell Biol* **13**, 646-658 (2012).

77. Bauman, A.L. et al. Dynamic regulation of cAMP synthesis through anchored PKA-adenylyl cyclase V/VI complexes. *Molecular cell* **23**, 925-931 (2006).

78. Stangherlin, A. & Zaccolo, M. Local Termination of 3′-5′-Cyclic Adenosine Monophosphate Signals: The Role of A Kinase Anchoring Protein–Tethered Phosphodiesterases. *Journal of cardiovascular pharmacology* **58**, 345-353 (2011).

79. Redden, J.M. & Dodge-Kafka, K.L. AKAP phosphatase complexes in the heart. *J Cardiovasc Pharmacol* **58**, 354-362 (2011).

80. Hoshi, N., Langeberg, L.K., Gould, C.M., Newton, A.C. & Scott, J.D. Interaction with AKAP79 modifies the cellular pharmacology of PKC. *Molecular cell* **37**, 541-550 (2010).

81. Dodge-Kafka, K.L. et al. The protein kinase A anchoring protein mAKAP coordinates two integrated cAMP effector pathways. *Nature* **437**, 574-578 (2005).

82. Oliveria, S.F., Dell'Acqua, M.L. & Sather, W.A. AKAP79/150 Anchoring of Calcineurin Controls Neuronal L-Type Ca²⁺ Channel Activity and Nuclear Signaling. *Neuron* **55**, 261-275.

83. Diviani, D. & Scott, J.D. AKAP signaling complexes at the cytoskeleton. *Journal of cell science* **114**, 1431-1437 (2001).

84. Wong, W. & Scott, J.D. AKAP signalling complexes: focal points in space and time. *Nat Rev Mol Cell Biol* **5**, 959-970 (2004).

85. Beene, D.L. & Scott, J.D. A-kinase anchoring proteins take shape. *Current opinion in cell biology* **19**, 192-198 (2007).

86. Carr, D.W., Hausken, Z.E., Fraser, I., Stofko-Hahn, R.E. & Scott, J.D. Association of the type II cAMP-dependent protein kinase with a human thyroid RII-anchoring protein. Cloning and characterization of the RII-binding domain. *Journal of Biological Chemistry* **267**, 13376-13382 (1992).

87. Kennedy, E.J. & Scott, J.D. Selective disruption of the AKAP signaling complexes. *cAMP Signaling: Methods and Protocols*, 137-150 (2015).

88. Craig, A.M., Jareb, M. & Banker, G. Neuronal polarity. *Current opinion in neurobiology* **2**, 602-606 (1992).

89. Bartlett, W.P. & Banker, G.A. An electron microscopic study of the development of axons and dendrites by hippocampal neurons in culture. I. Cells which develop without intercellular contacts. *The Journal of neuroscience : the official journal of the Society for Neuroscience* **4**, 1944-1953 (1984).

90. Caceres, A., Banker, G., Steward, O., Binder, L. & Payne, M. MAP2 is localized to the dendrites of hippocampal neurons which develop in culture. *Brain research* **315**, 314-318 (1984).

91. Bartlett, W.P. & Banker, G.A. An electron microscopic study of the development of axons and dendrites by hippocampal neurons in culture. II. Synaptic relationships. *The Journal of neuroscience : the official journal of the Society for Neuroscience* **4**, 1954-1965 (1984).

92. Dotti, C., Sullivan, C. & Banker, G. The establishment of polarity by hippocampal neurons in culture. *The Journal of Neuroscience* **8**, 1454-1468 (1988).

93. Shelly, M. & Poo, M.-M. Role of LKB1-SAD/MARK pathway in neuronal polarization. *Developmental Neurobiology* **71**, 508-527 (2011).

94. Barnes, A.P. et al. LKB1 and SAD Kinases Define a Pathway Required for the Polarization of Cortical Neurons. *Cell* **129**, 549-563 (2007).

95. Cheng, P.L. et al. Self-amplifying autocrine actions of BDNF in axon development. *Proceedings of the National Academy of Sciences of the United States of America* **108**, 18430-18435 (2011).

96. Peace, A.G. & Shewan, D.A. New perspectives in cyclic AMP-mediated axon growth and guidance: The emerging epoch of Epac. *Brain research bulletin* **84**, 280-288 (2011).

97. Zhou, Z. et al. Photoactivated adenylyl cyclase (PAC) reveals novel mechanisms underlying cAMP-dependent axonal morphogenesis. *Scientific reports* **5**, 19679 (2016).

98. Pasterkamp, R.J. Getting neural circuits into shape with semaphorins. *Nat Rev Neurosci* **13**, 605-618 (2012).

99. Shelly, M. et al. Semaphorin3A Regulates Neuronal Polarization by Suppressing Axon Formation and Promoting Dendrite Growth. *Neuron* **71**, 433-446 (2011).

100. Nishiyama, M. et al. Semaphorin 3A induces CaV2.3 channel-dependent conversion of axons to dendrites. *Nat Cell Biol* **13**, 676-685 (2011).

101. Zhang, J., Ma, Y., Taylor, S.S. & Tsien, R.Y. Genetically encoded reporters of protein kinase A activity reveal impact of substrate tethering. *Proceedings of the National Academy of Sciences* **98**, 14997-15002 (2001).

102. Tsien, R.Y. The green fluorescent protein. *Annu Rev Biochem* **67**, 509-544 (1998).

103. Sample, V., Newman, R.H. & Zhang, J. The structure and function of fluorescent proteins. *Chemical Society Reviews* **38**, 2852-2864 (2009).

104. Newman, R.H., Fosbrink, M.D. & Zhang, J. Genetically Encodable Fluorescent Biosensors for Tracking Signaling Dynamics in Living Cells. *Chemical Reviews* **111**, 3614-3666 (2011).

105. DiPilato, L.M., Cheng, X. & Zhang, J. Fluorescent indicators of cAMP and Epac activation reveal differential dynamics of cAMP signaling within discrete subcellular compartments. *Proceedings of the National Academy of Sciences of the United States of America* **101**, 16513-16518 (2004).

106. Violin, J.D. et al. β2-Adrenergic Receptor Signaling and Desensitization Elucidated by Quantitative Modeling of Real Time cAMP Dynamics. *Journal of Biological Chemistry* **283**, 2949-2961 (2008).

107. DiPilato, L.M. & Zhang, J. The role of membrane microdomains in shaping [small beta]2-adrenergic receptor-mediated cAMP dynamics. *Molecular BioSystems* **5**, 832-837 (2009).

108. Sample, V. et al. Regulation of nuclear PKA revealed by spatiotemporal manipulation of cyclic AMP. *Nat Chem Biol* **8**, 375-382 (2012).

109. Liu, S. et al. Phosphodiesterases coordinate cAMP propagation induced by two stimulatory G protein-coupled receptors in hearts. *Proceedings of the National Academy of Sciences* **109**, 6578-6583 (2012).

110. Marley, A., Choy, R.W. & von Zastrow, M. GPR88 reveals a discrete function of primary cilia as selective insulators of GPCR cross-talk. *PLoS One* **8**, e70857 (2013).

111. Giese, K.P. & Mizuno, K. The roles of protein kinases in learning and memory. *Learn Mem* **20**, 540-552 (2013).

112. Zhang, J., Hupfeld, C.J., Taylor, S.S., Olefsky, J.M. & Tsien, R.Y. Insulin disrupts beta-adrenergic signalling to protein kinase A in adipocytes. *Nature* **437**, 569-573 (2005).

113. Allen, M.D. & Zhang, J. Subcellular dynamics of protein kinase A activity visualized by FRET-based reporters. *Biochemical and biophysical research communications* **348**, 716-721 (2006).

114. Depry, C., Allen, M.D. & Zhang, J. Visualization of PKA activity in plasma membrane microdomains. *Molecular BioSystems* **7**, 52-58 (2011).

115. Erard, M. et al. Minimum set of mutations needed to optimize cyan fluorescent proteins for live cell imaging. *Molecular BioSystems* **9**, 258-267 (2013).

116. Honda, A. et al. Spatiotemporal dynamics of guanosine 3',5'-cyclic monophosphate revealed by a genetically encoded, fluorescent indicator. *Proceedings of the National Academy of Sciences of the United States of America* **98**, 2437-2442 (2001).

117. Nikolaev, V.O., Gambaryan, S. & Lohse, M.J. Fluorescent sensors for rapid monitoring of intracellular cGMP. *Nat Meth* **3**, 23-25 (2006).

118. Martinez, S.E., Heikaus, C.C., Klevit, R.E. & Beavo, J.A. The structure of the GAF A domain from phosphodiesterase 6C reveals determinants of cGMP binding, a conserved binding surface, and a large cGMP-dependent conformational change. *The Journal of biological chemistry* **283**, 25913-25919 (2008).

119. Martinez, S.E. et al. The two GAF domains in phosphodiesterase 2A have distinct roles in dimerization and in cGMP binding. *Proceedings of the National Academy of Sciences of the United States of America* **99**, 13260-13265 (2002).

120. Zheng, J.Q., Zheng, Z. & Poo, M. Long-range signaling in growing neurons after local elevation of cyclic AMP-dependent activity. *The Journal of cell biology* **127**, 1693-1701 (1994).

121. Cheng, P.-l. & Poo, M.-m. Early Events in Axon/Dendrite Polarization. *Annual Review of Neuroscience* **35**, 181-201 (2012).

122. Rochais, F. et al. Negative feedback exerted by cAMP-dependent protein kinase and cAMP phosphodiesterase on subsarcolemmal cAMP signals in intact cardiac myocytes: an in vivo study using adenovirus-mediated expression of CNG channels. *The Journal of biological chemistry* **279**, 52095-52105 (2004).

123. Thunemann, M., Fomin, N., Krawutschke, C., Russwurm, M. & Feil, R. Visualization of cGMP with cGi biosensors. *Methods Mol Biol* **1020**, 89-120 (2013).

124. Russwurm, M. et al. Design of fluorescence resonance energy transfer (FRET)-based cGMP indicators: a systematic approach. *Biochem J* **407**, 69-77 (2007).

125. Barnes, A.P. & Polleux, F. Establishment of axon-dendrite polarity in developing neurons. *Annu Rev Neurosci* **32**, 347-381 (2009).

126. Gervasi, N. et al. Dynamics of protein kinase A signaling at the membrane, in the cytosol, and in the nucleus of neurons in mouse brain slices. *The Journal of neuroscience : the official journal of the Society for Neuroscience* **27**, 2744-2750 (2007).

127. Nikolaev, V.O. et al. Beta2-adrenergic receptor redistribution in heart failure changes cAMP compartmentation. *Science (New York, N.Y.)* **327**, 1653-1657 (2010).

128. del Puerto, A. et al. Adenylate cyclase 5 coordinates the action of ADP, P2Y1, P2Y13 and ATP-gated P2X7 receptors on axonal elongation. *Journal of cell science* **125**, 176-188 (2012).

129. Murphy, Jonathan G. et al. AKAP-Anchored PKA Maintains Neuronal L-type Calcium Channel Activity and NFAT Transcriptional Signaling. *Cell reports* **7**, 1577-1588 (2014).

130. Sanderson, J.L. & Dell'Acqua, M.L. AKAP Signaling Complexes in Regulation of Excitatory Synaptic Plasticity. *The Neuroscientist* **17**, 321-336 (2011).

131. Carnegie, G.K. & Scott, J.D. A-kinase anchoring proteins and neuronal signaling mechanisms. *Genes & Development* **17**, 1557-1568 (2003).

132. Carr, D.W., Hausken, Z.E., Fraser, I.D., Stofko-Hahn, R.E. & Scott, J.D. Association of the type II cAMP-dependent protein kinase with a human thyroid RII-anchoring protein. Cloning and characterization of the RII-binding domain. *Journal of Biological Chemistry* **267**, 13376-13382 (1992).

133. Ventra, C. et al. The Differential Response of Protein Kinase A to Cyclic AMP in Discrete Brain Areas Correlates with the Abundance of Regulatory Subunit II. *Journal of Neurochemistry* **66**, 1752-1761 (1996).

134. Taylor, S.S., Zhang, P., Steichen, J.M., Keshwani, M.M. & Kornev, A.P. PKA: Lessons Learned after Twenty Years. *Biochimica et biophysica acta* **1834**, 1271-1278 (2013).

135. Gorshkov, K. & Zhang, J. Visualization of cyclic nucleotide dynamics in neurons. *Frontiers in Cellular Neuroscience* **8** (2014).

136. Lohof, A., Quillan, M., Dan, Y. & Poo, M. Asymmetric modulation of cytosolic cAMP activity induces growth cone turning. *The Journal of Neuroscience* **12**, 1253-1261 (1992).

137. Song, H.-j., Ming, G.-l. & Poo, M.-m. cAMP-induced switching in turning direction of nerve growth cones. *Nature* **388**, 275-279 (1997).

138. Goslin, K. & Banker, G. Experimental observations on the development of polarity by hippocampal neurons in culture. *The Journal of cell biology* **108**, 1507-1516 (1989).

139. Dessauer, C.W. Adenylyl Cyclase–A-kinase Anchoring Protein Complexes: The Next Dimension in cAMP Signaling. *Molecular Pharmacology* **76**, 935-941 (2009).

140. Dao, K.K. et al. Epac1 and cAMP-dependent Protein Kinase Holoenzyme Have Similar cAMP Affinity, but Their cAMP Domains Have Distinct Structural Features and Cyclic Nucleotide Recognition. *Journal of Biological Chemistry* **281**, 21500-21511 (2006).

141. Vijayaraghavan, S., Goueli, S.A., Davey, M.P. & Carr, D.W. Protein Kinase A-anchoring Inhibitor Peptides Arrest Mammalian Sperm Motility. *Journal of Biological Chemistry* **272**, 4747-4752 (1997).

142. Chen, Y. et al. Adenylyl cyclase 6 is selectively regulated by protein kinase A phosphorylation in a region involved in Gα(s) stimulation. *Proceedings of the National Academy of Sciences of the United States of America* **94**, 14100-14104 (1997).

143. Iwami, G. et al. Regulation of adenylyl cyclase by protein kinase A. *The Journal of biological chemistry* **270**, 12481-12484 (1995).

144. Mika, D. & Conti, M. PDE4D phosphorylation: A coincidence detector integrating multiple signaling pathways. *Cellular signalling* (2015).

145. Song, H.J., Ming, G.L. & Poo, M.M. cAMP-induced switching in turning direction of nerve growth cones. *Nature* **388**, 275-279 (1997).

146. Nicol, X., Hong, K.P. & Spitzer, N.C. Spatial and temporal second messenger codes for growth cone turning. *Proceedings of the National Academy of Sciences of the United States of America* **108**, 13776-13781 (2011).

147. Neves, S.R. et al. Cell Shape and Negative Links in Regulatory Motifs Together Control Spatial Information Flow in Signaling Networks. *Cell* **133**, 666-680 (2008).

148. Li, L., Gervasi, N. & Girault, J.-A. Dendritic geometry shapes neuronal cAMP signalling to the nucleus. *Nat Commun* **6** (2015).

149. Ramamurthy, S., Chang, E., Cao, Y., Zhu, J. & Ronnett, G.V. AMPK Activation Regulates Neuronal Structure in Developing Hippocampal Neurons. *Neuroscience*.

150. Zhou, Z. et al. Photoactivated adenylyl cyclase (PAC) reveals novel mechanisms underlying cAMP-dependent axonal morphogenesis. *Scientific reports* **5**, 19679 (2016).

151. Zhong, H. et al. Subcellular dynamics of type II PKA in neurons. *Neuron* **62**, 363-374 (2009).

152. Deming, P.B. et al. Anchoring of Protein Kinase A by ERM (ezrin-radixin-moesin) proteins is required for proper netrin signaling through DCC (deleted in colorectal cancer). *Journal of Biological Chemistry* (2015).

153. Dodge-Kafka, K.L. et al. The protein kinase A anchoring protein mAKAP coordinates two integrated cAMP effector pathways. *Nature* **437**, 574-578 (2005).

154. Terrin, A. et al. PKA and PDE4D3 anchoring to AKAP9 provides distinct regulation of cAMP signals at the centrosome. *The Journal of cell biology* **198**, 607-621 (2012).

155. Gelman, I.H., Tombler, E. & Vargas, J. A Role for SSeCKS, a Major Protein Kinase C Substrate with Tumour Suppressor Activity, in Cytoskeletal Architecture, Formation of Migratory Processes, and Cell Migration During Embryogenesis. *The Histochemical Journal* **32**, 13-26.

156. Piontek, J. & Brandt, R. Differential and regulated binding of cAMP-dependent protein kinase and protein kinase C isoenzymes to gravin in human model neurons: Evidence that gravin provides a dynamic platform for the localization for kinases during neuronal development. *The Journal of biological chemistry* **278**, 38970-38979 (2003).

157. Vardjan, N., Kreft, M. & Zorec, R. Dynamics of β-adrenergic/cAMP signaling and morphological changes in cultured astrocytes. *Glia* **62**, 566-579 (2014).

158. Soderling, S.H. et al. Loss of WAVE-1 causes sensorimotor retardation and reduced learning and memory in mice. *Proceedings of the National Academy of Sciences of the United States of America* **100**, 1723-1728 (2003).

159. Kawano, Y. et al. CRMP-2 is involved in kinesin-1-dependent transport of the Sra-1/WAVE1 complex and axon formation. *Molecular and cellular biology* **25**, 9920-9935 (2005).

160. Wang, Y. et al. Muscle A-Kinase Anchoring Protein-α is an Injury-Specific Signaling Scaffold Required for Neurotrophic- and Cyclic Adenosine Monophosphate-Mediated Survival. *EBioMedicine* **2**, 1880-1887 (2015).

161. Lipscombe, D. et al. Imaging of cytosolic Ca2+ transients arising from Ca2+ stores and Ca2+ channels in sympathetic neurons. *Neuron* **1**, 355-365 (1988).

162. Willoughby, D., Wachten, S., Masada, N. & Cooper, D.M. Direct demonstration of discrete Ca2+ microdomains associated with different isoforms of adenylyl cyclase. *Journal of cell science* **123**, 107-117 (2010).

163. Yang, J.H., Polanowska-Grabowska, R.K., Smith, J.S., Shields, C.W.t. & Saucerman, J.J. PKA catalytic subunit compartmentation regulates contractile and hypertrophic responses to beta-adrenergic signaling. *Journal of molecular and cellular cardiology* **66**, 83-93 (2014).

164. Yonaha, M., Chibazakura, T., Kitajima, S. & Yasukochi, Y. Cell cycle-dependent regulation of RNA polymerase II basal transcription activity. *Nucleic acids research* **23**, 4050-4054 (1995).

165. Kleman, A.M., Yuan, J.Y., Aja, S., Ronnett, G.V. & Landree, L.E. Physiological Glucose is Critical for Optimized Neuronal Viability and AMPK Responsiveness In Vitro. *Journal of neuroscience methods* **167**, 292-301 (2008).

166. Longair, M.H., Baker, D.A. & Armstrong, J.D. Simple Neurite Tracer: Open Source software for reconstruction, visualization and analysis of neuronal processes. *Bioinformatics* (2011).

167. Castro, L.R.V., Verde, I., Cooper, D.M.F. & Fischmeister, R. Cyclic Guanosine Monophosphate Compartmentation in Rat Cardiac Myocytes. *Circulation* **113**, 2221-2228 (2006).

168. Fischmeister, R. et al. Compartmentation of cyclic nucleotide signaling in the heart the role of cyclic nucleotide phosphodiesterases. *Circulation research* **99**, 816-828 (2006).

169. Brown, D.A. & London, E. Structure and function of sphingolipid-and cholesterol-rich membrane rafts. *Journal of Biological Chemistry* **275**, 17221-17224 (2000).

170. Pilz, R.B. & Casteel, D.E. Regulation of gene expression by cyclic GMP. *Circulation research* **93**, 1034-1046 (2003).

171. Watson, J. The influence of intracellular levels of cyclic nucleotides on cell proliferation and the induction of antibody synthesis. *The Journal of experimental medicine* **141**, 97-111 (1975).

172. Ignarro, L.J. et al. Role of the arginine-nitric oxide pathway in the regulation of vascular smooth muscle cell proliferation. *Proceedings of the National Academy of Sciences* **98**, 4202-4208 (2001).

173. Jobgen, W.S., Fried, S.K., Fu, W.J., Meininger, C.J. & Wu, G. Regulatory role for the arginine–nitric oxide pathway in metabolism of energy substrates. *The Journal of nutritional biochemistry* **17**, 571-588 (2006).

174. Koch, K.-W. & Stryer, L. Highly cooperative feedback control of retinal rod guanylate cyclase by calcium ions. (1988).

175. Bönigk, W. et al. Rod and cone photoreceptor cells express distinct genes for cGMP-gated channels. *Neuron* **10**, 865-877 (1993).

176. Misono, K.S. et al. Structure, signaling mechanism and regulation of the natriuretic peptide receptor guanylate cyclase. *The FEBS journal* **278**, 1818-1829 (2011).

177. Tinker, J.H. & Michenfelder, J.D. Sodium nitroprusside: pharmacology, toxicology and therapeutics. *Anesthesiology* **45**, 340-354 (1976).

178. Gao, X. & Zhang, J. Spatiotemporal Analysis of Differential Akt Regulation in Plasma Membrane Microdomains. *Molecular biology of the cell* **19**, 4366-4373 (2008).

179. Szczesna-Skorupa, E., Chen, C.-D., Rogers, S. & Kemper, B. Mobility of cytochrome P450 in the endoplasmic reticulum membrane. *Proceedings of the National Academy of Sciences* **95**, 14793-14798 (1998).

Appendix

Developing a peptide based LKB1 inhibitor

Introduction

The Liver Kinase B1 (LKB1) is a heterotrimeric protein consisting of LKB1 and cofactors STRAD-α and MO-25[179]. LKB1, a *bonafide* tumor suppressor, is a master kinase of 13 kinases of the AMPK subfamily including BRSK1/2, AMPK, NUAK, SIK, and MARK[180-182]. LKB1 is activated by cofactor binding and recruitment out of the nucleus[183]. It is considered to be constitutively active; any endogenous agonists or antagonists that directly bind to LKB1 have yet to be identified. However, regulation by posttranslational modifications have been described. For instance, PKA phosphorylation of Ser431 on LKB1's C-terminal tail increases LKB1 dependent phosphorylation of the AMP-activated protein kinase (AMPK)[184], however this point of LKB1 regulation is controversial[185]. LKB1's role in cell polarity has been well documented in cortical neurons *in vitro*[94] and *in vivo*[31] and drosophila epithelium. Loss of LKB1 activity by mutating Ser431 or transgenic knockout prevents axon initiation and neuronal polarization in cortical neurons[93]. Currently, there is only one way to pharmacologically inhibit LKB1 function. Developed by Mellman et al., an analogue sensitive kinase allele by mutating the "gatekeeper" Met 129 to Gly makes LKB1 sensitive to inhibition by the small molecule 1-NM-PP1[186]. Despite this development, studying LKB1 activity dynamics has been a challenge due to a lack of tools to perturb LKB1 function. Given that LKB1 is a critical player in axon initiation, it is important to understand LKB1 dynamics in living cells. To this end, we have been developing a genetically encoded LKB1 substrate peptide to use as a competitive inhibitor in living cells.

This approach was successfully demonstrated for AMPK by Miyamoto et al. who successfully constructed an AMPK substrate based inhibitor peptide called AMPK inhibitor peptide (AIP)[187]. LKB1 kinase activity assays demonstrated the highest

phosphorylation efficiency for SIK, NUAK, BRSK1/2, and AMPK[180]. For our first attempt, we have utilized the AMPK T-loop phosphorylated by LKB1 to generate an LKB1 inhibitor peptide (LIP). For LKB1 studies, HeLa cells are an appropriate choice as they do not express LKB1 endogenously and are a natural control for LKB1 overexpression experiments[179, 188].

Results

Our assay for LKB1 activity consists of the coexpressing the AMPK and BRSK activity reporter (ABKAR)[189] (Fig. 4a) with either LKB1 or LKB1 and a fusion protein consisting of mCherry, FKBP, and LIP (mChF-LIP) in HeLa cells (Fig. 4.1a). The mCherry is a fluorescent protein tag and allows us to detect expression, while the FKBP increases the versatility of the tool for future applications involving FRB-FKBP chemically induced dimerization[187]. In this assay, we are using AMPK activity and the ABKAR FRET response as a proxy for LKB1 activity. If LKB1 activity is high, we should see a relatively high FRET ratio in cells expressing LKB1 compared to those not expressing LKB1. When mChF-LIP is coexpressed with ABKAR and LKB1, we would expect a lower FRET ratio as LKB1 phosphorylation of the reporter would be competitively inhibited by mChF-LIP.

We first observed the ABKAR starting ratio (SR) to assess basal activity of AMPK and therefore LKB1. Cells expressing ABKAR alone had an average SR of 0.98±0.032% (mean±S.E.M, n=14) (Fig. 4.1b). The SR of cells co-expressing ABKAR and LKB1 was 0.93±0.022% (mean±S.E.M, n=11) and was not significantly different than ABKAR-only expressing cells. Interestingly, the SR of cells co-expressing ABKAR, LKB1, and mChF-LIP was significantly lower than ABKAR + LKB1 at 0.87±0.0061% (mean±S.E.M, n=19). This test did not prove reliable as the control condition with LKB1 did not increase the SR

of ABKAR. Therefore, we cannot conclude that mChF-LIP decreased the basal activity of LKB1.

Next, we observed the normalized emission ratio changes under stimulated conditions. 2-deoxyglucose (2-DG) inhibits glucose metabolism and lowers ATP concentrations inside of the cell[190]. AMPK activity depends on phosphorylation of the T172 residue in the T-loop by LKB1 or CAMKK and increases in the AMP:ATP ratio. Stimulation of HeLa cells expressing ABKAR with 20 mM 2-DG increased the FRET ratio by only 2.60±1.18% (mean±S.E.M, n=14) (Fig. 4.1b,c). Cells expressing ABKAR + LKB1 responded with a significantly greater FRET ratio increase of 23.91±2.70% (mean±S.E.M, n=11). Coexpression with mChF-LIP decreased the FRET response to 18.06±1.99% (mean±S.E.M, n=19). However, this diminished FRET response was not statistically significant.

Finally, we tested mChF-LIP inhibition of LKB1 activity using western blot for p-AMPK T172, the amino acid residue phosphorylated by LKB1. An analysis of normalized relative density of p-AMPK to total AMPK revealed an ~50% decrease in AMPK phosphorylation (Fig. 4.1e,f).

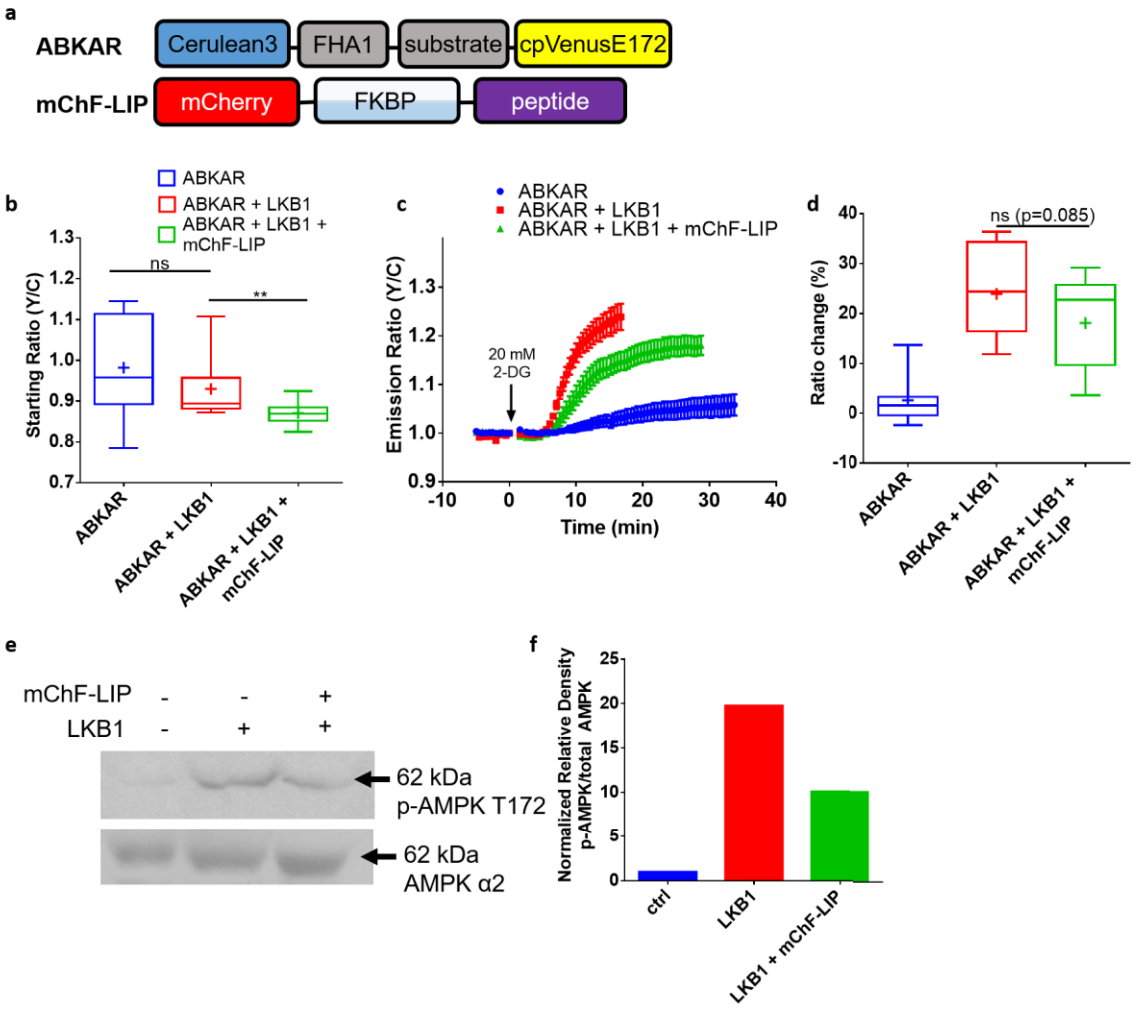

Figure 4.1 Preliminary testing of the LKB1 inhibitor peptide in HeLa cells
(a) Design of ABKAR and mChF-LIP. The ABKAR reporting unit consists of Cerulean3 as the FRET donor and cpVenusE172 as the FRET acceptor. The kinase substrate and the phosphoaminoacid binding domain FHA1 make up the sensing unit. The ABKAR substrate is an AMPK phosphorylation consensus sequence that can be phosphorylated by both AMPK and BRSK1/2. mChF-LIP is a fusion protein made up of mCherry acting as a fluorescent tag, FKBP, and the AMPK T-loop to competitively inhibit LKB1 activity. (b) Average YFP-FRET/CFP starting ratios for HeLa cells expressing ABKAR, ABKAR + LKB1, and ABKAR + LKB1 + mChF-LIP. (c) Average YFP-FRET/CFP emission ratio curves for HeLa cells expressing ABKAR, ABKAR + LKB1, and ABKAR + LKB1 + mChF-LIP. (d) Average ratio changes from curves in c. (e) Western blot of whole cell lysate from HeLa cells expressing LKB1 alone LKB1 co-expressed with mChF-LIP. AMPKα2 has a MW of 62 kDa. Lysate was probed with antibodies for p-AMPKα2 T172 and total AMPKα2. (f) Relative band density of pAMPK T172 normalized to band density of total AMPK. Data in b and c shown as box-and-whisker plots, with the box showing the median, 25% quartile, and 75% quartile, and the whiskers designating the 5th and 95th

percentiles; a "+" indicates the mean. * = $p<0.05$, ns, not significant according to Student's t-test.

These preliminary analyses indicate that mChF-LIP may indeed be competitively inhibiting LKB1 activity. More imaging and biochemical studies need to be done to further confirm this inhibitory effect. The dual phosphorylation of AMPK T172 by LKB1 and CAMKK complicates this approach in a similar way to the development of the AMPK activity reporter[189]. Future studies will require confirmation that LKB1 inhibition by mChF-LIP is independent of inhibitory activity on CAMKK.

To see if mChF-LKB1 was able to perturb any biological functions, we turned to the established role of LKB1 in initiating axon outgrowth in cortical neurons within the developing brain. PKA phosphorylation of LKB1 at Ser431 was shown to be critical for axon initiation in *in vivo* mouse studies[94]. To test if mChF-LIP could prevent axons from growing out of migrating cortical neurons, we *in utero* electroporated the following constructs into E15.5 embryos, pCAG-LSL-GFP (2ug/ul), pCAG-Cre (2ng/ul), and pCAG-LSL-mChF or pCAG-LSL-mChFLIP (1ug/ul)[191]. This technique allows us to target the DNA constructs to specific brain regions, while Cre-dependent recombination and a low concentration of Cre DNA allows for clear identification of individual cells. We harvested the embryos at E18.5, took 250 μm sections of the brains and immunostained with the following primary antibodies: chicken anti-GFP (AVES) 1:1000, rabbit anti-DsRed (Living Colors) 1:1000, and mouse anti-Tau1 (Chemicon) 1:1000; and the following secondary antibodies DAPI 1:3000 (molecular probes), goat anti-chicken Alexa488 (molecular probes) 1:1000, goat anti-rabbit Alexa555 (molecular probes) 1:1000, and goat anti-mouse Alexa647 (molecular probes) 1:1000.

A preliminary analysis of axon outgrowth revealed that brain slices expressing mChF-LIP (Fig. 4.2b-d) had more cells without axons (13.2±4.4, n=5 brains) than those expressing mChF (5.00±2.19, n= 5 brains) (Fig. 4.2a,c,d). This observation is consistent with the previous data indicating mChF-LIP can inhibit LKB1 activity and produce biologically relevant effects. However, brain slices expressing mChF-LIP also contained more cells with axons. To normalize these values, we calculated an axon outgrowth index (AOI) by dividing the total number of cells with axons by the total number of cells without axons. A larger AOI index indicates more axon outgrowth. mChF produced an AOI of 4.73 compared to mChF-LIP, which had an AOI of 2.46. This data suggests mChF-LIP does indeed inhibit LKB1's ability to initiate axon outgrowth from cortical neurons in the developing brain.

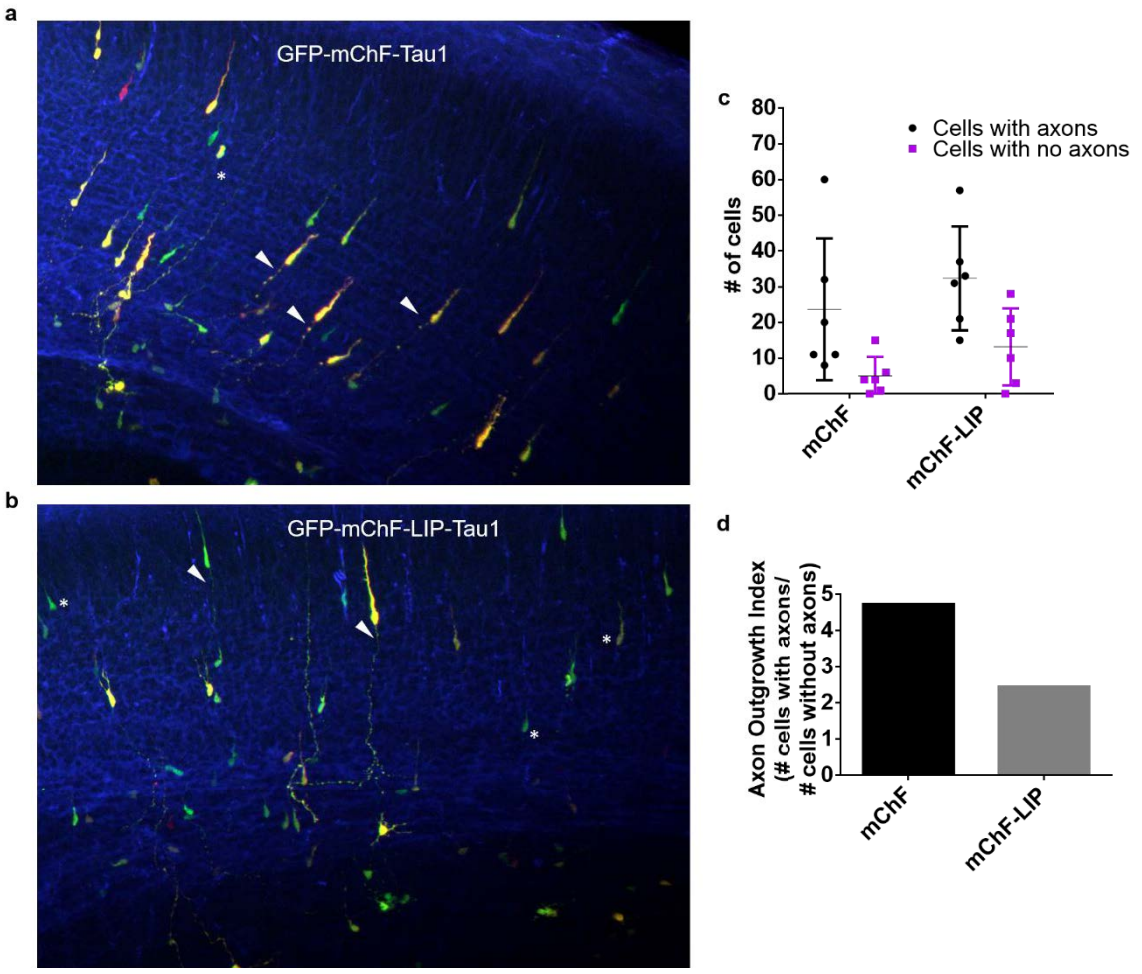

Figure 4.2 mChF inhibits axon polarization in mouse cortical neurons *in vivo.* Confocal images of a coronally sectioned E18.5 mouse somatosensory cortex. Brain hemisphere was electroporated with GFP and mChF (a) or mChF-LIP (b) and fluorescent signal was immunoenhanced with antibodies against GFP and mCherry. Cells are migrating towards the dorsal surface of the brain and extending axons (white arrowheads) at the trailing end. Examples of cells without axons indicating with asterisks. (c) Average number of cells with and without axons per brain slice for mChF and mChF-LIP. (d) Axon outgrowth index calculated by dividing the total number of cells with axons by the total number of cells without axons in all brains slices.

Appendix References

1. Hawley, S. et al. Complexes between the LKB1 tumor suppressor, STRADalpha/beta and MO25alpha/beta are upstream kinases in the AMP-activated protein kinase cascade. *Journal of Biology* **2**, 28 (2003).

2. Lizcano, J.M. et al. LKB1 is a master kinase that activates 13 kinases of the AMPK subfamily, including MARK/PAR-1. *EMBO J* **23**, 833-843 (2004).

3. Shaw, R.J. et al. The LKB1 tumor suppressor negatively regulates mTOR signaling. *Cancer Cell* **6**, 91-99 (2004).

4. Bright, N.J., Carling, D. & Thornton, C. Investigating the regulation of brain-specific kinases 1 and 2 by phosphorylation. *The Journal of biological chemistry* **283**, 14946-14954 (2008).

5. Boudeau, J. et al. Analysis of the LKB1-STRAD-MO25 complex. *Journal of cell science* **117**, 6365-6375 (2004).

6. Sapkota, G.P. et al. Phosphorylation of the protein kinase mutated in Peutz-Jeghers cancer syndrome, LKB1/STK11, at Ser431 by p90(RSK) and cAMP-dependent protein kinase, but not its farnesylation at Cys(433), is essential for LKB1 to suppress cell vrowth. *The Journal of biological chemistry* **276**, 19469-19482 (2001).

7. Fogarty, S. & Hardie, D.G. C-terminal phosphorylation of LKB1 is not required for regulation of AMP-activated protein kinase, BRSK1, BRSK2, or cell cycle arrest. *The Journal of biological chemistry* **284**, 77-84 (2009).

8. Barnes, A.P. et al. LKB1 and SAD Kinases Define a Pathway Required for the Polarization of Cortical Neurons. *Cell* **129**, 549-563 (2007).

9. Shelly, M., Cancedda, L., Heilshorn, S., Sumbre, G. & Poo, M.-m. LKB1/STRAD Promotes Axon Initiation During Neuronal Polarization. *Cell* **129**, 565-577 (2007).

10. Shelly, M. & Poo, M.-M. Role of LKB1-SAD/MARK pathway in neuronal polarization. *Developmental Neurobiology* **71**, 508-527 (2011).

11. Lo, B. et al. Lkb1 regulates organogenesis and early oncogenesis along AMPK-dependent and -independent pathways. *The Journal of cell biology* **199**, 1117-1130 (2012).

12. Miyamoto, T. et al. Compartmentalized AMPK signaling illuminated by genetically encoded molecular sensors and actuators. *Cell reports* **11**, 657-670 (2015).

13. Woods, A. et al. Ca 2+/calmodulin-dependent protein kinase kinase-β acts upstream of AMP-activated protein kinase in mammalian cells. *Cell metabolism* **2**, 21-33 (2005).

14. Sample, V., Ramamurthy, S., Gorshkov, K., Ronnett, G.V. & Zhang, J. Polarized Activities of AMPK and BRSK in Primary Hippocampal Neurons. *Molecular biology of the cell* (2015).

15. Kern, K.A. & Norton, J.A. Inhibition of established rat fibrosarcoma growth by the glucose antagonist 2-deoxy-D-glucose. *Surgery* **102**, 380-385 (1987).

16. Hand, R.A., Khalid, S., Tam, E. & Kolodkin, A.L. Axon Dynamics during Neocortical Laminar Innervation. *Cell reports* **12**, 172-182 (2015).

Curriculum Vitae

Kirill Gorshkov

4400 East-West Highway
Apartment 207
Bethesda, MD 20814
(713)444-5317

Kgorshkov89@gmail.com

EDUCATION

The Johns Hopkins University School of Medicine*, Baltimore, MD.* PhD Candidate, Department of Pharmacology and Molecular Sciences, 2011-present. PhD expected September 2016

The University of Texas at Austin*, MD.* GPA 3.53/4.0, B.S. Biology, December 2010.

AREAS OF EXPERTISE

Molecular Biology - Engineering FRET biosensors, genotyping, primer design, PCR, mutagenesis
Cell Culture - Primary neuronal culture, cell line maintenance, growth assays
Histology – microtome, cryotome, brain dissection and sectioning, spinal cord sectioning, organotypic brain slice culture
Biochemistry – Immunocytochemistry, immunohistochemistry, western blot
Microscopy - Confocal and epifluorescence imaging, live-cell FRET imaging, image analysis and quantification of FRET data

RESEARCH EXPERIENCE

Industry internship research: Dr. Alexander Efanov, Eli Lilly Company, Indianpolis, IN, July – August 2015

- Characterized the signaling pathway of an orphan GPCR related to diabetes pathology using luciferase based reporters of signal transduction
- Used high-throughput biology equipment
- Gained experience using luciferase based assays in 96-well format
- Conducted qPCR studies for orphan GPCR expression in cell lines

Graduate student research: Dr. Jin Zhang Lab, The Johns Hopkins Medical School, Baltimore, MD. July 2012 - Present.

- Project involved the development and usage of genetically encodable biosensors to detect cAMP/PKA and cGMP signaling dynamics in living cells using fluorescent and bioluminescent proteins
- Conducted live cell fluorescence imaging of cAMP/PKA spatiotemporal dynamics in primary hippocampal cells *in vitro* as a model for neuronal differentiation
- Implemented an analog-sensitive kinase allele of LKB1 to acutely perturb function in cells
- Cloned and characterized 5 targeted versions of the cGMP biosensor
- Cloned and characterized 4 targeted FRET biosensors for calcineurin activity
- Studied AMPK substrates using a human proteome microarray in collaboration with Dr. Heng Zhu

Graduate rotation student research: Dr. Ronald L. Schnaar, The Johns Hopkins School of Public Health, Baltimore, MD. December - April 2012.

- Analyzed spinal cord and brain tissue from spinal cord injury mouse model for axonal regeneration
- Analyzed behavioral data from mouse model of spinal cord injury
- Analyzed expression of 5-HT in injured spinal cord
- Developed an in vitro model for axonal regeneration using primary rat cerebellar granule neurons

Graduate rotation student research: Dr. Christopher Ross, Division of Neurobiology at The Johns Hopkins University School of Medicine, Baltimore, MD. August – December 2012

- Tested the effects of protease inhibition in Huntington's disease using primary mouse cortical neurons
- Generated mutant versions of LRRK2, a protein involved in Parkinson's disease

Undergraduate research: Dr. Richard Morrisett, The University of Texas at Austin, Baltimore, MD. July 2009 – December 2010.
Investigated the effect of alcohol on the action of CARTp in the PC12 cell line.

- Maintained the PC 12 cell line for the project, isolated and analyzed m-RNA from cells using RT-PCR and gel electrophoresis
- Conducted western blot analysis of ethanol induced enhancement of the activation of p-ERK
- Conducted cryosectioning of rodent brain samples in preparation for c-Fos staining

Undergraduate research: Dr. Wesley Thompson, The University of Texas at Austin, Baltimore, MD. May – June 2009.
Investigated the effect of alcohol on the action of CARTp in the PC12 cell line.

- Assisted with DNA isolation and gel electrophoresis for genotyping of transgenic mice with muscular disorders
- Observed: in-vivo fluorescence imaging of neuromuscular junctions, perfusions, dissections, and creation of a montage of T.E.M. images of a neuromuscular junction to be recreated into a 3D digital image
- Participated in weekly journal club meetings

TEACHING/MENTORING EXPERIENCE

Graduate student mentor: June 2009 - present, Dr. Jin Zhang's Lab, The Johns Hopkins Medical School, Baltimore, MD.

- Mentor of one graduate student that rotated through the lab

GRADUATE COURSEWORK

- **Core Graduate Courses:** Biochemical and Biophysical Principles, Macromolecular Structure and Analysis, Cell Structure and Dynamics, Molecular Biology and Genomics, Organic Mechanisms in Biology, Mechanisms in

Biorganic Chemistry, Pathways and Regulation, Bioinformatics, Organ Physiology

- **Discussion/Seminar Courses:** Core Discussion, Ethics and Career Issues in Science, Topics in Pharmacology
- **Elective Courses:** Neuropharmacology, Neural Differentiation I and II, Trends in the Neurobiology of Aging

PUBLICATIONS

Gorshkov K, Mehta S, Ramamurthy S, Ronnett GV, Zhou F, Zhang J. AKAP-mediated feedback control of cAMP gradients in developing hippocampal neurons. Nature Chemical Biology. (in revision).

Head S, Wei S, Zhao L, **Gorshkov K,** Pasunooti K, Chen Y, Deng Z, Li R, Shim J, Hartung T, Zhang J, Zhao Y, Colombini M, Liu JO. (2015) The antifungal drug itraconazole targets VDAC1 to modulate the AMPK/mTOR signaling axis in endothelial cells. PNAS. 112(52):E7276-85.

Miyamoto T, Rho E, Sample V, Akano H, Magari M, Ueno T, **Gorshkov K**, Chen M, Tokumitsu H, Zhang J, Inoue T. (2015) Compartmentalized AMPK Signaling Illuminated by Genetically Encoded Molecular Sensors and Actuators. Cell Reports. 11(4):657-70.

Sample V, Ramamurthy S, **Gorshkov K,** Ronnett GV, Zhang J. (2015). Polarized Activities of AMPK and BRSK in Primary Hippocampal Neurons. Molecular Biology of the Cell. 26(10):1935-46.

Gorshkov K, Zhang J, (2014) Monitoring Cyclic Nucleotides Using Genetically Encoded Fluorescent Reporter. In Cyclic Nucleotide Signaling. Taylor Francis Group

Gorshkov K, Zhang J, (2014) Dynamics of cyclic nucleotide signaling in neurons. Frontiers in Cellular Neuroscience. 4;8:395**.**

Mehta S, Aye-Han NN, Ganesan A, Oldach L, **Gorshkov K,** and Zhang J. (2014). Calmodulin-controlled spatial decoding of oscillatory Ca^{2+} signals by calcineurin. eLife. 23;3:e03765.

Hua, Y., **Gorshkov, K**., Yang, Y., Wang, W., Zhang, N., and Hughes, D.P. (2012). Slow down to stay alive: HER4 protects against cellular stress and confers chemoresistance in neuroblastoma. Cancer. 118(20):5140-54.

ABSTRACTS

Gorshkov, K., Mehta, S., Ramamurthy, S., Ronnett, G.V., Zhou, F., Zhang J. Spatiotemporal Dynamics and Regulation of cAMP and PKA in Early Stage Hippocampal Neurons. Poster presentation, Department of Pharmacology, UCSD, San Diego, CA, April 2016

Gorshkov, K., Mehta, S., Ramamurthy, S., Ronnett, G.V., Zhou, F., Zhang J. Spatiotemporal Dynamics and Regulation of cAMP and PKA in Early Stage Hippocampal Neurons. Poster presented at the Annual Society of Biochemistry and Molecular Biology Meeting, San Diego, CA, April 2016

Gorshkov, K., Ramamurthy, S., Zhang J. cAMP/PKA signaling in early neuronal development. Oral Presentation, The Department of Pharmacology and Molecular Sciences, Baltimore, MD, March 2015

Gorshkov, K., Ramamurthy, S., Zhang J. Signaling Control of Neuronal Polarization. Oral Presentation, The Department of Pharmacology and Molecular Sciences, Baltimore, MD, February 2014

Gorshkov, K., Ramamurthy, S., Zhang J. Live-cell imaging of neuronal polarization signals. Poster presentation, The Department of Pharmacology and Molecular Sciences, Baltimore, MD, October 2013

Gorshkov, K. Sustainability in Medical Research. Guest lecture, Intersession Sustainability Course Instructed by Dr. Davis Bookhart. Baltimore, MD. January 2013

Gorshkov, K., Yoo, S., Schnaar, R.L. Axon regeneration *in vitro* and *in vivo*. Poster presentation, The Department of Pharmacology and Molecular Sciences, Baltimore, MD, April 2012

Gorshkov, K., Arbez, N., Ross, C.H. The effect of caspase-6 inhibition on Huntingtin toxicity. Oral presentation, The Department of Pharmacology and Molecular Sciences, Baltimore, MD, December 2011

Gorshkov, K., Rodriguez, J., Salinas, A. Characterizing CART expression in undifferentiated and differentiated PC12 cells. Poster presentation, Roads to Research at UT Austin, Austin, TX, December April 2010

HONORS AND AWARDS

- Poster Award, May 2016, UC San Diego Department of Pharmacology
- Scheinberg Travel Award, November 2015, Johns Hopkins University School of Medicine Pharmacology
- Biomedical Scholars Association Milestone Nominee, April 2015, Johns Hopkins University School of Medicine
- National Science Foundation Graduate Research Fellowship, April 2013-present, Johns Hopkins School of Medicine
- Undergraduate Research Fellowship, November 2009-December 2010, The University of Texas at Austin

PROFESSIONAL DEVELOPMENT

GapSummit 2017, November 2015 – Present, Global Biotech Revolution
Position Held: Vice President

- Organizing a global life sciences conference for young leaders in 2017
- Raising funds by partnering with global biotech and pharmaceutical companies
- Networking with influential leaders across the world in the life sciences industry

Leaders of Tomorrow Summit, March 31, 2015, MedImmune, Gaithersburg, MD

Position Held: Vice President

- Helped to plan the first cross-generational leadership summit for the life sciences in the Mid-Atlantic region
- Duties include defining themes and discussion topics for the panel, working with panelists on discussion points, choosing attendees, speaking to the press, and uploading content to the LinkedIn page.

Leadership Initiative for the Environment, Fall 2011 – July 2015, Johns Hopkins School of Medicine, Baltimore, MD

Position Held: President

- Duties included coordinating sustainability events across two Hopkins' campuses by working directly with the Office of Sustainability and Facilities Management, submitting annual budget proposals, developing a yearly schedule of events, coordinating volunteers for green events around Baltimore city, and managing an online presence via social networking sites.
- Main goals are developing sustainable practices at Hopkins and acting as a conduit between facility operations and students, faculty, and staff

OTHER

- Pharmacology program representative for the GSA, August 2013 to August 2015
- Safety Officer for the GSA, August 2013 to August 2015
- Biosafety Officer for the Zhang lab, August 2013 to August 2015
- Fluent in Russian

REFERENCES

Jin Zhang, Professor of Pharmacology
The University of California, San Diego, CA
410-502-0173
jzhang32@ucsd.edu

Dr. Ronald L. Schnaar, Professor of Pharmacology and Molecular Sciences
The Johns Hopkins University School of Medicine
410-955-8392
schnaar@jhu.edu

Dr. Jun Liu, Professor of Pharmacology
The Johns Hopkins University School of Medicine
410-955-4520
joliu@jhu.edu

Dr. Santosh Ramamurthy, Senior Manager
Cote Orphan Consulting
Sramam1@gmail.com